universität wien

DISSERTATION

Titel der Dissertation

The Identification of Potential Factors Involved in the Transcriptional Regulation of the Phloem-Specific Gene *ALTERED PHLOEM DEVELOPMENT* (*APL*) and the Analysis of its Role during Embryogenesis in *Arabidopsis thaliana*

Verfasserin

Mag. Katrin Ollram

angestrebter akademischer Grad

Doktorin der Naturwissenschaften (Dr. rer. nat.)

Studienkennzahl lt. Studienblatt:	A091 490
Dissertationsgebiet lt. Studienblatt:	Dr.-Studium der Naturwissenschaften: Molekulare Biologie
Betreuer:	Dr. Thomas Greb

Wien, September 2011

Acknowledgements

This work has been carried out at the GMI- Gregor Mendel Institute of Molecular Plant Biology in Vienna, Austria.
I would like to thank Thomas Greb for giving me the opportunity to perform my PhD thesis in his group and for his support and scientific advice throughout my thesis.
I would also like to acknowledge my PhD committee, Daniel Schubert and Tobias Sieberer, for discussions and providing helpful suggestions for my project.

Many thanks to all former and current Greb lab members, for providing a great working atmosphere as well as for friendships beyond work! I have always enjoyed our chats about work and life! A special thank you goes to Julia Riefler who helped me to finally increase the screening throughput a lot.

I want to thank all my colleagues and friends from other labs at the institute, making it a really pleasant place to do research - additional thanks to Lilian Nehlin for her introduction into embryo manipulation and Gudrun Böhmdorfer for advice in several issues. I would also like to acknowledge Pawel Pasierbek from the Biooptics facility, always prepared to solve microscopic troubles, and Thomas Lendl for support in creating the 3D image.

A very big THANK YOU goes to my family, especially to my parents who enabled to do my studies and who always supported me in all decisions I made and encouraged me whenever needed!

Table of contents

Abbreviations

AG	AGAMOUS
amiRNA	artificial micro RNA
AP	APETALA
APL	ALTERED PHLOEM DEVELOPMENT
ARF	AUXIN RESPONSE FACTOR
ATP	adenosine-5'-triphosphate
BBR	BARLEY B RECOMBINANT
BDL	BODENLOS
bHLH	basic helix-loop-helix
bp	basepair
BPC	BASIC PENTACYSTEINE
CaMV	cauliflower mosaic virus
CC	companion cells
cDNA	complementary DNA
CUC	CUP-SHAPED COTYLEDON
dCAPS	derived cleaved amplified polymorphic sequences
DEPC	diethylpyrocarbonate
dH_2O	distilled water
DIC	differential interference contrast
DNA	deoxyribonucleic acid
dNTPs	deoxy-nucleotides
DOF	DNA-binding with one finger
EDTA	ethylenediaminetetraacetic acid
EIF	eukaryotic translation initiation factor
EMS	ethyl methanesulfonate
ERF	ETHYLENE RESPONSE FACTOR
ESTs	expressed sequence tags
EtOH	ethanol
fig.	figure

GARP	glutamic acid-rich protein
GFP	green fluorescent protein
GUS	β-glucuronidase
HB	HOMEOBOX
HCl	hydrochloric acid
HD-ZIP	homeodomain-leucine zipper
H_2SO_4	sulfuric acid
HTH	helix-turn-helix
IAA	indol acetic acid
KAN	KANADI
kb	kilobases
KCl	potassium chloride
KNOX	KNOTTED1-like homeobox
LINC	LITTLE NUCLEI
LRR	leucine-rich repeat
LUC	LUCIFERASE
MADS	MCM1 AGAMOUS DEFICIENS SRF (serum response factor)
MAPK	mitogen-activated protein kinase
$MgCl_2$	magnesium chloride
$MgSO_4$	magnesium sulfate
MP	MONOPTEROS
MYB	myeloblastosis
NAC	NAM ATAF1/2 CUC2
NaCl	sodium chloride
NAM	NO APICAL MERISTEM
NaOH	sodium hydroxide
NaH_2PO_4	sodium dihydrogen phosphate
Na_2HPO_4	disodium hydrogen phosphate
NST	NAC SECONDARY WALL THICKENING PROMOTING FACTOR
nt	nucleotide

OC	organizing center
ORF	open reading frame
PBS	phosphate buffered saline
PCR	polymerase chain reaction
PIN	PINFORMED
PD marker	PHLOEM DIFFERENTIATION marker
PHD	plant homeodomain
PP	protophloem
qRT-PCR	quantitative real time PCR
RT	room temperature
RT-PCR	reverse transcriptase PCR
RAM	root apical meristem
ref.	reference
RNA	ribonucleic acid
SAM	shoot apical meristem
SDS	sodium dodecyl sulfate
SE	sieve tube element
tab.	Table
TF	transcription factor
TILLING	Targeting Induced Local Lesions IN Genomes
TRIS	tris(hydroxymethyl)aminomethane
TUB	tubulin
UTR	untranslated region
WOX	WUS-related homeobox
wt	wild-type
WUS	WUSCHEL
Y1H	yeast one-hybrid (screen)

Standard abbreviations are used for units of measurements.

1. Abstract

The vascular bundles, consisting of xylem and phloem, form an interconnected network throughout the whole plant body which is essential for development and growth by mediating long-distance transport and providing mechanical stability. The xylem is responsible for the transport of water and nutrients, while the phloem transports sugars, proteins, RNA, and other signalling molecules. Differentiation into these highly specialized cell types needs to be tightly coordinated in a spatial and temporal manner. Despite several studies, the MYB-like transcription factor ALTERED PHLOEM DEVELOPMENT (APL), is still the only one known required for phloem specification.

Here, I aimed for the identification of novel phloem regulators by looking for factors upstream of *APL*. Testing *APL* promoter fragments for their ability to regulate reporter gene activity and to complement the previously described seedling-lethal *apl-1* mutant, promoter regions harboring essential and vascular-specific regulatory elements were identified. Taking advantage of this information, a yeast one-hybrid screen was performed to identify direct regulators of *APL* transcription. Among the candidates obtained, members of the BASIC PENTACYSTEINE (BPC) transcription factor family were identified as the first candidates for having a direct regulatory effect on *APL*.

In addition, the analysis of a novel *APL* mutant allele, *apl-2*, was used to characterize the function of APL itself in more detail. Surprisingly, *apl-2/+* plants were embryo-lethal, displaying aberrant cell division planes as early as in the octant stage. Considering the defects described for the *apl-1* mutant in connection with the asymmetric cell divisions during phloem differentiation, one might speculate about a general role of APL in orienting cell division planes. Being in line with a described link between cell plane orientation and the PIN/auxin machinery, I observed mislocalization of PIN1 in *apl-2* embryos from globular stage on.

Taken together, candidates for *APL* upstream regulators were identified opening novel avenues to understand the establishment of phloem identity in plants. In addition, I hypothesize that *APL* might have a function during early embryogenesis which is distinct to phloem-specification.

Kurzfassung

Die Gefäßbündel von Pflanzen, bestehend aus Xylem und Phloem, formen ein zusammenhängendes System, welches die gesamte Pflanze durchzieht und essentiell für deren Entwicklung und Wachstum ist. Es ist verantwortlich für den Langstreckentransport und verleiht mechanische Stabilität. Xylem ist zuständig für den Transport von Wasser und Nährstoffen, Phloem transportiert Kohlehydrate, Proteine, RNA und andere Signalmoleküle. Die Differenzierung in diese hoch spezialisierten Zelltypen ist streng reguliert, sowie zeitlich und räumlich koordiniert. Trotz zahlreicher Studien ist der MYB-ähnliche Transkriptionsfaktor ALTERED PHLOEM DEVLOPMENT (APL) nach wie vor der einzig bekannte Faktor, der für die Spezifikation von Phloem essentiell ist.

Das Ziel dieser Arbeit war durch die Identifizierung von Faktoren, die der *APL* Funktion vorgeschaltet sind, neue, für die Phloementwicklung spezifische Regulatoren zu identifizieren. Zu diesem Zweck wurden *APL* Promoter Fragmente in Hinsicht auf ihre Fähigkeit getestet, einerseits Reportergene zu aktivieren, sowie den bereits beschriebenen Phänotyp der keimling-letalen *apl-1* Mutante zu komplementieren. Dadurch konnten Promoterregionen identifiziert werden, die essentielle und gefäßspezifische regulatorische Elemente enthalten. Diese Information wurde für die Durchführung eines Yeast One-Hybrid Screens genutzt, mit dem Ziel, Faktoren mit direktem transkriptionellen Einfluss auf *APL* zu identifizieren. Unter den erhaltenen Kandidaten konnten Mitglieder der Familie der BASIC PENTACYSTEINE (BPC) Transkriptionsfaktoren als erste potentiell direkte Regulatoren von *APL* identifiziert werden.

Weiters wurde ein bisher unbeschriebenes mutantes *APL* Allel, *apl-2*, analysiert, um die Funktion von APL selbst näher zu charakterisieren. Überraschenderweise waren *apl-2/+* Pflanzen embryoletal und entwickelten sich bereits im Oktantstadium abnormal. Im Hinblick auf die beschriebenen Defekte der *apl-1* Mutante im Zusammenhang mit den asymmetrischen Teilungen während der Phloemdifferenzierung, kann man über eine generelle Rolle von APL in der Orientierung von Zellteilungsebenen spekulieren. In Übereinstimmung mit der beschriebenen Verbindung zwischen der Orientierung von

Zellteilungsebenen und der PIN/Auxin – Maschinerie, beobachtete ich eine Mislokalisation von PIN1 in *apl-2* Embryos vom globulären Stadium an.

Zusammenfassend identifizierte ich Faktoren, die möglicherweise an der transkriptionellen Regulation von *APL* beteiligt sind und neue Perspektiven in unserem Verständnis eröffnen, wie Phloemidentität festgelegt wird. Ein weiteres Ergebnis ist die Indentifizierung einer möglichen Rolle von *APL* während der frühen Embryogenese, welche unabhängig von der Spezifikation des Phloemgewebes ist.

2. Introduction

2.1 The vascular system

The vascular system forms an interconnected network throughout the whole plant body which is essential for development and growth by mediating long-distance transport of water, nutrients, and small molecules and provides mechanical stability. The main conducting tissue types are the phloem and xylem tissues (Fig. 2.1) Postembryonically, these tissues derive directly or indirectly from meristems located at the shoot and root tip of the adult plant, the shoot apical meristem (SAM) and root apical meristem (RAM), respectively. These give rise to procambial cells which are further specified to phloem and xylem cells. SAM and RAM are already established during embryogenesis providing the sources for all cells during subsequent development. Most angiosperms and most dicotyledonous plants also establish a cambium, a lateral meristem, important for secondary (thickening) growth of stems and roots by the production of secondary phloem and xylem (Baucher et al., 2007; Cano-Delgado et al., 2010; Peris et al., 2010; Sieburth and Deyholos, 2006).

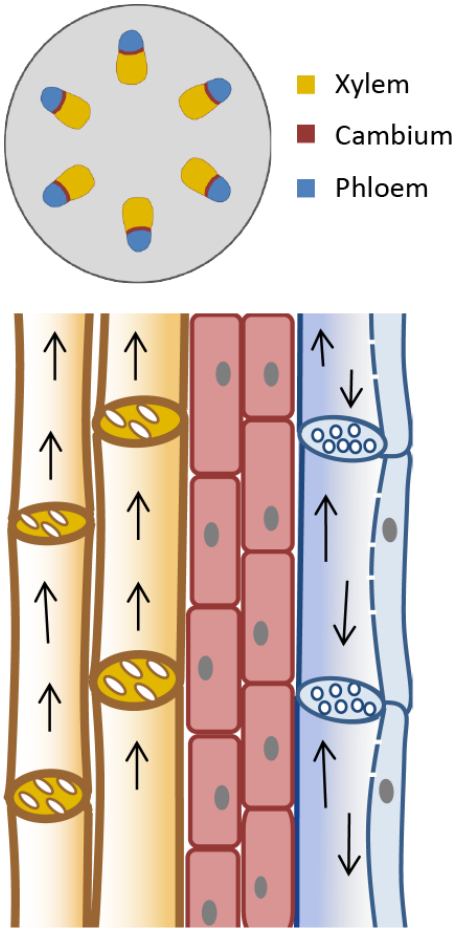

Fig. 2.1: The main conducting tissue types. In the scheme of a stem cross section a typical arrangement of collateral vascular bundles corresponding to *Arabidopsis* is shown. The cambium is located in between phloem pointing towards the outside and xylem facing the inside. Below a scheme of a longitudinal section through a vascular bundle is depicted. In a continuous process, tracheary elements of the xylem and sieve tube elements and smaller companion cells of the phloem differentiate from the cambium.

2.1.1 The conducting tissue types

Xylem precursor cells differentiate into tracheary elements, xylem parenchyma and xylem fibers, which together form the xylem tissue. At maturity, tracheary elements undergo programmed cell death, during which all cell contents, including the nucleus, are degraded resulting in hollow tubes, connected by pores at the basal and

apical ends. Xylem vessels are specialized for the transport of water and nutrients also due to their characteristic thickened secondary cell walls. They add strength and rigidity to the vessels to resist the high pressure that is exerted on fluid uptake (Fukuda, 2004).

Phloem transports carbohydrates, amino acids, fatty acids, RNA, and other signaling molecules. It consists of cells specialized for transport as well as phloem parenchyma and, in some species, phloem fibers. The sieve cells are the primary conducting units and comprise sieve tube elements (SE) and smaller companion cells (CC) which derive from the same precursor cells. SEs enucleate in the course of differentiation and maturation. Furthermore, most organelles degenerate, including nucleus, vacuoles, rough endoplasmic reticulum (ER), and Golgi. In addition, pores are formed within the cell wall of the SEs, the sieve plate at the apical and basal side of the sieve element and sieve areas for lateral transport. Both structures are formed at sites of plasmodesmata, a process which involves the deposition of callose in the wall around the plasmodesmata. In contrast, CCs keep their nuclei and, thereby, serve as important regulators of the SEs (Le Hir et al., 2008; Oparka and Turgeon, 1999; Ruiz-Medrano et al., 2001; Sjolund, 1997; Xie et al., 2011).

2.1.2 Specification and differentiation

The specification and differentiation into these highly specialized vascular tissue types underlies a well–defined and predictable differentiation program integrating positional information and developmental signals. Still, it remains a flexible system responding to endogenous and environmental stimuli to adapt the vascular network to the current requirements.

Differentiation into different cell types often implies asymmetric cell division, by which one or both daughter cells will develop in a different way than their mother cell. As plant cells are immobile due to the cell wall, the correct orientation of division has to be ensured to generate the overall cellular pattern of the plant. Asymmetric division is regulated by segregation of intrinsic determinants during division and/or extrinsic factors for subsequent determination of the cell fate (Ten Hove and Heidstra, 2008).

Thus, vascular differentiation depends on and must be regulated by local cell-cell communication between developing vascular cells as well as signals from neighboring cells not committed to become vascular tissue (Fukuda, 2004; Ohashi-Ito and Fukuda, 2010; Ten Hove and Heidstra, 2008). In any case, the execution of the desired response depends on regulated gene expression for which the establishment of a specific transcription factor (TF) profile plays a pivotal role. The knowledge of factors involved in phloem specification and differentiation is very limited. To date, only the MYB-like TF ALTERED PHLOEM DEVELOPMENT (APL) has been shown to be necessary for phloem specification and maintenance (Bonke et al., 2003) (see **2.4**). During the last years, microscopic techniques improved (Bauby et al., 2007; Truernit et al., 2008) providing further details about early phloem differentiation and revealing novel early phloem markers (Bauby et al., 2007). Transcript profiling has been mainly done on whole phloem tissues, phloem-enriched tissues or phloem sap leaving out information about transcripts present in immature phloem (Le Hir et al., 2008). Furthermore, transcript profiling has been done in combination with fluorescent cell sorting for various developmental stages of the root tissue (Birnbaum et al., 2003; Brady et al., 2007; Cano-Delgado et al., 2010; Lee et al., 2006; Zhang et al., 2008). Still, the identification of key phloem regulators remains an important task for further investigations.

2.2 Transcription factors – a crucial component to regulate gene expression

The establishment of specific tissues in multicellular organisms requires spatially and temporally coordinated gene expression.

Gene expression can be regulated at several levels, transcriptionally and post-transcriptionally (Mallory and Vaucheret, 2010; Riechmann, 2002; Seo et al., 2011) (Fig. 2.2). Thus, although there is a multitude of possible modulating actions, TFs play a central role in establishing particular transcriptional profiles. TFs exert their function by definition by binding directly to the promoters of target genes in a sequence-specific manner thereby activating or repressing the transcription of the downstream target genes (Qu and Zhu, 2006; Riechmann, 2002; Riechmann et al., 2000). In *Arabidopsis* more than 2,000 genes have been annotated as TFs on the ATH1 array (Lee et al., 2006), about 7.7 % of the total number of ~26,000 genes. TFs are usually grouped into different

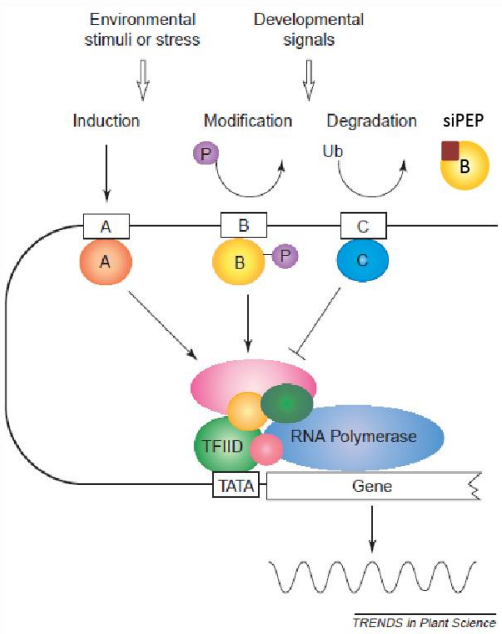

Fig. 2.2: Scheme of transcriptional regulatory networks. Environmental stimuli and developmental signals activate or repress transcription factors (TF) which regulate the transcriptional initiation complex. TF activatory/inhibitory properties and abundance are further regulated by modifications, degradation, and interaction with other components and small interfering peptides (siPEP). Rectangular boxes represent *cis*-regulatory elements (labeled A, B, C), ellipses TFs (labeled A, B, C) and the small brown box a siPEP. The TATA box represents the core promoter for assembly of the transcriptional initiation complex (including factor TFIID) activating the RNA polymerase. Ub, ubiquitin. Modified from ref. (Yamaguchi-Shinozaki and Shinozaki, 2005).

families according to their DNA binding domains (Luscombe et al., 2000). They can interact with several additional proteins involved in transcriptional regulation: the basic transcriptional machinery (e.g. RNA polymerases, general transcription factors), large multi-subunit co-activators and other cofactors as well as chromatin-related proteins (e.g. histones, chromatin remodeling complexes) (Riechmann, 2002).

In *Arabidopsis* large TF families comprise the types of e.g. MYB (myeloblastosis), MADS (MCM1 AGAMOUS DEFICIENS SRF), basic helix-loop-helix (bHLH), NAC (NAM ATAF1/2 CUC2), APETALA2 (AP2)/ETHYLENE RESPONSE FACTOR (ERF) and HOMEOBOX (HB) containing TFs subdivided in further classes based on combinations with other domains (e.g. leucine zipper, START (steroidogenic acute regulatory protein related lipid transfer) domain, PHD (plant homeodomain) finger) (Qu and Zhu, 2006; Riechmann, 2002).

2.2.1 Regulatory DNA sequences

In plants, upstream regulatory sequences of genes usually span regions of about 1 to 2 kilobases (kb) of DNA which is much less than in animals in which more than 10 kb can be required to confer all temporal and spatial input for gene expression (Riechmann, 2002). Still, regulatory elements can also be located downstream of the transcriptional start site, in the 5' untranslated region (5'UTR), in introns, or in 3' regions. As examples, bindings sites for the AP2-type TF WRINKLED1 are present in the 5'UTR of its target gene *Pl-PKbeta1*, a subunit of a pyruvate kinase involved in fatty acid synthesis (Maeo et al.,

2009), or elements located in introns are required for normal expression of the homeotic MADS box gene *AGAMOUS* (*AG*) (Sieburth and Meyerowitz, 1997).

Eukaryotic transcription factor binding sites are usually about 5 to 10 basepairs (bp) long which are recognized by TFs in a combinatorial fashion to selectively control expression of distinct genes. By this mode, multiple inputs (endogenous signals, environmental cues) can be converged and gene transcription can be adjusted to and coordinated with the current requirements (Riechmann, 2002). These *cis*-acting modules can act synergistically exerting a different regulatory feature than each in isolation. This was first dissected in more detail in the plant field for the cauliflower mosaic virus (CaMV) 35S promoter whose different promoter subdomains confer specific expression in various tissues (Benfey and Chua, 1990; Benfey et al., 1990). Photosynthesis-related promoters provide other examples in *Arabidopsis* which integrate different light and developmental inputs by combinations of several light-responsive-elements (LREs) (Chattopadhyay et al., 1998; Puente et al., 1996).

2.2.2 Regulation by TF interactions

The regulatory complexity is increased by the possibility for combinations of *trans*-acting factors, the TFs themselves. In addition to DNA-binding domains, TF often have motifs for protein-protein interactions (Riechmann, 2002), like leucine-zipper or PHD motifs (Mason and Arndt, 2004; Sanchez and Zhou, 2011). Direct interaction between TFs of the same or another family creates a large pool of possible regulatory actions with a need for a specific distribution of regulatory promoter elements (Riechmann, 2002). Dimeric complexes of the same family often bind (pseudo-)palindromic sequences e.g. the floral identity TF LEAFY (LFY) or HD-ZIP (homeodomain-leucine zipper) class I factors (Hames et al., 2008; Johannesson et al., 2001). Even higher order regulatory protein complexes can be formed exerting different functions dependent on the protein composition. One example is the composition of complexes containing members of MYB-bHLH transcription factors in association with WD40-repeat proteins which determine epidermal cell fate to root hairs, trichomes, or stomata (Ramsay and Glover, 2005).

2.2.3 Redundant and overlapping functions

Related TFs frequently exert overlapping and/or redundant functions as found within different groups as e.g. MADS-box, HD-ZIP III or KANADI (KAN) TFs. For instance, partial redundancy for MADS-box genes *AP1*, *CAULIFLOWER* (*CAL*), and *FRUITFULL* (*FUL*) in specifying floral meristem identity has been reported (Bowman et al., 1993; Ferrandiz et al., 2000; Kempin et al., 1995). Another example are *KAN1* and *KAN2* which act redundantly in the establishment of abaxial cell fates in lateral organs and which are involved in vascular patterning and development (Eshed et al., 2001). This is similar to the *HD-ZIP III* genes *PHABULOSA* (*PHB*), *PHAVOLUTA* (*PHV*) and *REVOLUTA* (*REV*) involved in adaxial fate determination (Emery et al., 2003) (see also **2.6**). Thus, to determine the necessity of an individual factor within a process often requires the knockout of several factors. In addition, redundancy between non-related factors can hardly be predicted by sequence analysis (Riechmann, 2002).

2.3 *Arabidopsis* embryogenesis – general issues and meristem formation

During the first developmental stages, *Arabidopsis* embryogenesis follows a very predictable scheme of cell divisions allowing the study of clonal relationships in the course of tissue patterning and specification (Fig. 2.3). In this respect, the plant hormone auxin plays an important role (Capron et al., 2009; De Smet et al., 2010; Gao et al., 2008; Jenik et al., 2007; Laux et al., 2004; Moller and Weijers, 2009; Peris et al., 2010). During embryogenesis, the transmembrane auxin efflux transporters PINFORMED 1 (PIN1), PIN4, and PIN7 are differentially expressed up to the globular stage. Regulation of the direction of auxin flux and, in turn, the establishment of auxin gradients is required to elicit specific cellular and developmental processes (Benkova et al., 2003; Friml et al., 2003).

2.3.1 Formation of the apical-basal axis

After fertilization, the zygote elongates which is followed by an asymmetric cell division giving rise to a small apical cell with dense cytoplasm and a larger basal cell highly vacuolated. Thereby, the apical-basal axis is already specified. The apical cell undergoes

two rounds of longitudinal divisions, followed by a third transverse division, giving rise to eight cells which is designated as the octant stage embryo (Fig. 2.3 and Fig. 2.4). The basal cell and its descendants divide solely transversely, forming the extra-embryonic filamentous suspensor which connects the embryo with the maternal tissue. Only the uppermost suspensor cell, the hypophysis, is incorporated into the embryo proper later on.

At the octant stage, four different domains can be distinguished along the apical-basal axis: 1) an upper tier of four cells of the embryo proper (apical embryo domain) which will form the shoot meristem and most of the cotyledons, 2) a lower tier of four cells of the embryo proper (central embryo domain), which will give rise to the hypocotyl and root, and part of the cotyledons and root meristem, 3) the hypophysis (basal embryo domain) which will generate distal parts of the root meristem, the quiescent center, and the stem cells of the central root cap, and 4) the extraembryonic suspensor (Laux et al., 2004; Peris et al., 2010).

For the first divisions, a MAPK (mitogen-activated protein kinase) cascade involving the MAPK kinase kinase YODA (Jeong et al., 2011; Lukowitz et al., 2004) and auxin signaling

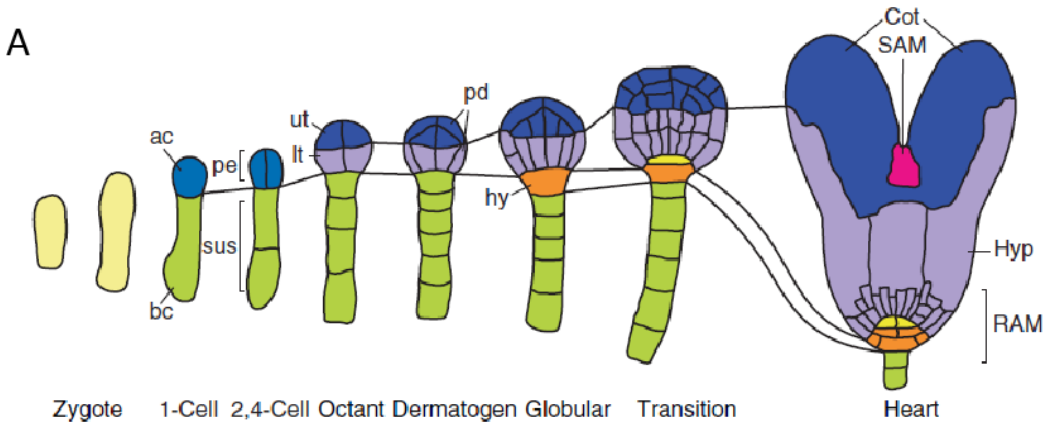

Fig. 2.3: *Arabidopsis* embryogenesis and lineage relationships. A) *Arabidopsis* embryogenesis follows a predictable patterning enabling to follow distinct cell lineages during the first stages. Cell lineages are highlighted in individual colors and lineage relationships by the lines in between different stages. Embryo stages are written below. The devel--opment throughout the distinct stages is described in the text. The yellow color marks the lens-shaped cell generated by asymmetric division of the hypophysis. Abbreviations: ac, apical cell; bc, basal cell; Cot, cotyledons; hy, hypophysis; Hyp, hypocotyl; lt, lower tier; pd, protoderm; pe, proembryo; RAM, root apical meristem; SAM, shoot apical meristem; sus, suspensor; ut, upper tier. **B)** Magnification of the central zone at transition stage. g, ground tissue; p, pericycle; v, vascular stem cells (procambium). Modified from ref. (Peris et al., 2010).

(e.g. PIN transporters, auxin response factor (ARF) TF family, etc.) are essential. After the first division of the zygote, PIN7 is polarly localized to the apical membrane of the basal cell creating an auxin maximum in the apical cell, as visualized by the activity of the auxin responsive *DR5* reporter. PIN7 localization remains there until globular stage (Fig. 2.4) (Peris et al., 2010). The different domains up to the octant stage are marked by differential expression of members of the *WOX* (WUS-related homeobox) transcription factor family (*WOX2, WOX8*, and *WOX9*) which are also involved in determining the apical and basal cell fates (Breuninger et al., 2008; De Smet et al., 2010; Haecker et al., 2004; Ueda et al., 2011). The WOX activity is further required for the expression of PIN1 and the establishment of auxin maxima in the hypophysis and cotelydonary tips of the embryo later on (see below) (Breuninger et al., 2008).

2.3.2 Establishment of radial symmetry

At the dermatogen stage, tangential divisions give rise to the protoderm, the founder cells of the future epidermis, and eight inner cells, which are the precursors of ground and vascular tissues. Thus, at the dermatogen stage radial symmetry of the embryo is established (Fig. 2.3 and Fig. 2.4).

There is hardly any knowledge of how embryonic cells sense their outside position and how they are specified to become the protoderm. One hypothesis is that cell wall components are maintained from the zygote at the outside of cells after division and

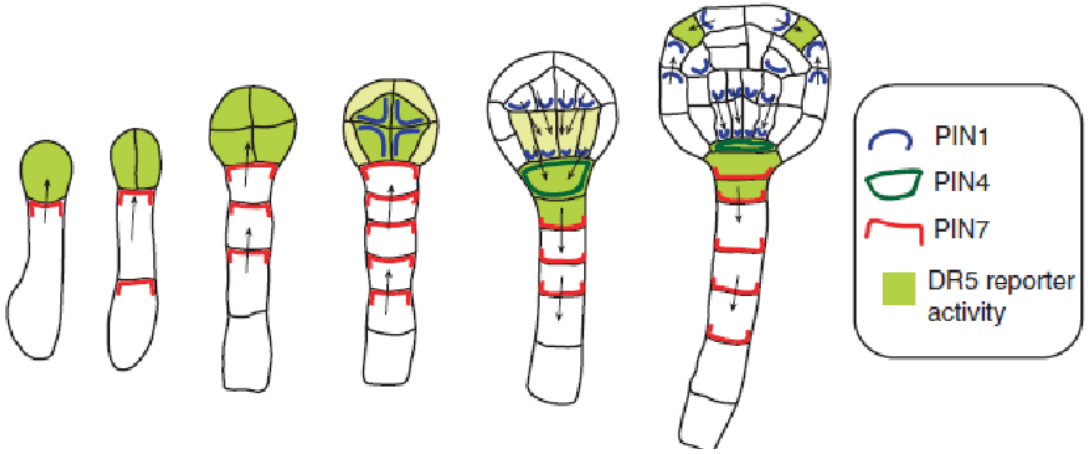

Fig. 2.4: Polar auxin transport during embryogenesis. Differential expression and localization of PIN1, PIN4, and PIN7 create distinct auxin flows and maxima as visualized by *DR5* reporter gene activity. Embryo stages correspond to Fig. 2.3. See text for details. Fig. derived from ref. (Peris et al., 2010).

serve as positional cues to destine epidermal identity (Johnson et al., 2005; Laux et al., 2004). In addition epidermal factors like the HD-ZIP TF *ATML1* and its homolog *PROTODERMAL FACTOR 2* (*PDF2*) get restricted to the protodermal cells, possibly by a complex regulatory feedback loop involving factors in the central domain which inhibit *ATML1* and *PDF2* expression (Abe et al., 2003; Takada and Jurgens, 2007). The inner cells are marked by the presence of transcripts like from the *ARF* gene *MONOPTEROS* (*MP/ARF5*) (Hardtke and Berleth, 1998) or *PIN1* (Friml et al., 2003).

2.3.3 Establishment of vascular precursor cells

At the dermatogen stage, the inner cells undergo one round of vertical divisions (globular stage, Fig. 2.3 and Fig. 2.4). A subsequent horizontal division gives rise to apical cells contributing to the base of the cotyledons and basal descendants forming the precursors of the hypocotyl, embryonic root, and proximal stem cells of the root meristem (Laux et al., 2004).

The terminology of cells giving rise to vascular cells is overlapping and redundant. The term vascular primordium is defined here as cells giving rise to the procambium, to show a time course of ongoing cell divisions. The terms vascular stem cells, procambium, and vascular precursors are used in parallel.

The four central cells in the lower tier form the vascular primordium. Subsequently, the cells of the vascular primordium divide horizontally, then vertically, elongate and form the procambium surrounded by the pericycle cells around transition stage (Fig. 2.3 B). The ground tissue splits into an inner layer of endodermis and an outer layer of cortex cells (Laux et al., 2004; Scheres et al., 1995; Scheres et al., 1994). Sterols seem to be involved in procambium formation as sterol biosynthesis mutants, like *fackel*, show failures in asymmetric cell division and cell elongation of the central embryo domain (among other defects in embryo patterning) (Laux et al., 2004; Schrick et al., 2000; Schrick et al., 2002). Sterols might act as structural cell membrane component also affecting cell polarity and auxin transport or as signaling molecules (Laux et al., 2004).

2.3.4 Establishment of RAM and SAM

Around dermatogen/globular stage, the shoot apical meristem (SAM) is initiated, indicated by the expression of the marker for the organizing center (OC) *WUS* (Laux et al., 2004; Peris et al., 2010). The OC is required for the maintenance of the stem cells in the SAM, similarly to the quiescent center (QC) in the root. Concomitantly, the uppermost cell of the suspensor is specified to become the hypophysis. At the globular stage the hypophysis divides asymmetrically forming an upper lens-shaped cell, the precursor of the QC, and a lower daughter cell giving rise to the columella stem cells (Peris et al., 2010; Scheres et al., 1994). Hypophysis specification depends on the expression of *MP/ARF5* and the auxin response protein from the Aux/Indol Acetic Acid (IAA) family BODENLOS (BDL/IAA12) in the provascular cells directly adjacent to the hypophysis. Thus, they seem to act in a non-cell-autonomous manner (Weijers et al., 2006). The PIN1 protein, which is present in all inner cells membranes until globular stage, is shifted towards the future hypophysis immediately prior to its specification, resulting in a maximum of auxin in the hypophysis. At the same time, PIN7 is relocalized to the basal membranes in the suspensor cells and PIN4 is activated in the hypophysis (Fig. 2.4) (Benkova et al., 2003; Friml et al., 2003; Izhaki and Bowman, 2007). *PIN1* expression and, in turn, polar auxin-transport requires *MP*. As external auxin treatment does not restore root formation in the *mp* mutant, other mobile signal(s) were suggested to act in parallel (Weijers et al., 2006). Indeed, *MP* regulates root formation as well by inducing the bHLH TFs *TARGET OF MONOPTEROS7* (*TMO7*) and *TMO5* which act in a non-cell-autonomous and cell-autonomous way, respectively (Schlereth et al., 2010). Several other factors are involved in RAM establishment like the AP2-related TFs PLETHORA and the GRAS-type TFs SHORTROOT (SHR), SCARECROW (SCR) or the phosphatases POLTERGEIST (POL) and POL-like (PLL1) (Capron et al., 2009; De Smet et al., 2010; Laux et al., 2004).

At the globular stage, a few cells at the flanks of the apical embryo domain are selected to become cotyledons and start proliferating. The correct establishment is controlled by auxin transport, biosynthesis, perception, and response which affect cotyledon patterning in case of alterations (Moller and Weijers, 2009). In contrast to the inner

provascular cells of the embryo, PIN1 localized in the protoderm faces the cotyledon initiation sites to establish the auxin maxima in the incipient cotyledon primordia (Benkova et al., 2003; Steinmann et al., 1999).

With the initiation of the cotyledons, the embryo establishes its bilateral symmetry. The specification of cotyledons coincides with SAM formation, involving the KNOTTED1-like homeobox (KNOX) factor SHOOT MERISTEMLESS (STM) (Aida et al., 1999; Long et al., 1996; Vroemen et al., 2003) and NAC (NAM ATAF1,2 CUP-SHAPED COTYLEDON)-domain TFs CUC1-3 (Aida et al., 1997; Aida et al., 1999). Although the processes are linked, they do not depend on each other as deduced from mutant phenotypes (e.g. *stm* or *wus* lack a SAM but contain cotyledons)(Barton and Poethig, 1993; De Smet et al., 2010; Laux et al., 1996).

With the establishment of all meristematic tissues, the embryo is equipped with cells required for post-embryonic growth. During subsequent stages of embryogenesis (heart, torpedo, walking stick, bent-cotyledon, mature) the embryo grows further and gets prepared for dormancy at the mature stage (Peris et al., 2010).

2.4 Phloem specification and differentiation

As described above (see **2.3**), a continuous network of vascular precursors is established in the embryo. In *Arabidopsis*, the first phloem- and xylem-related divisions take place already during embryogenesis but the cells get fully differentiated only after germination. How procambial cells are selected to become phloem or xylem remains unclear (Bauby et al., 2007; Busse and Evert, 1999; Cano-Delgado et al., 2010; Scheres et al., 1995). Fig. 2.5 shows a scheme of sequential stages of phloem patterning and specification (Bauby et al., 2007).

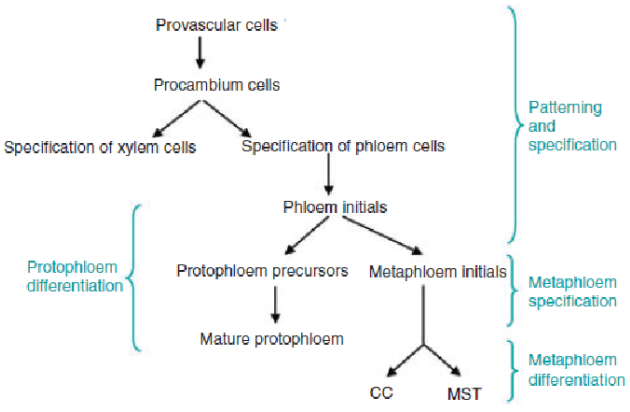

Fig. 2.5: Scheme of early phloem development in *Arabidopsis*. CC, companion cells; MST, metaphloem sieve tubes. Model derived from ref. (Bauby et al., 2007).

So far, only one gene has been identified to be essential for

phloem specification, namely *ALTERED PHLOEM DEVELOPMENT* (*APL*), a single MYB-repeat protein (Bonke et al., 2003) (see **2.4.1**). The MYB-domain is the conserved DNA-binding domain named after the mammalian TF c-MYB (c-myeloblastosis) (Jin and Martin, 1999). The MYB-domain consists of up to four imperfect amino acid sequence repeats (R) of about 52 amino acids with three alpha-helices each, forming a helix-helix-turn-helix (H-HTH) structure. According to c-MYB, the repeats are referred to as R1, R2, and R3. R2 and R3 were shown both to be necessary for DNA-binding; R3 interacts with the core of the recognition sequence, whereas R2 is involved in interactions with nucleotides peripheral to the core (Dubos et al., 2010; Jin and Martin, 1999). Thus, MYB proteins with a single (or a partial) MYB repeat were suggested to bind DNA in a different manner similar to homeodomain proteins, which also have a HTH motif (Nishikawa et al., 1998), or as homo- or hetero-dimers (Jin and Martin, 1999).

As visualized using reporter genes fused to the promoter of *APL*, the first phloem-specific asymmetric divisions (Fig. 2.6) take place during transition from torpedo to bent-cotyledon stage. Thus, phloem development is a quite late process during embryogenesis and starts when the ground tissue has already been specified (Bonke et al., 2003; Scheres et al., 1995). Using high-resolution confocal microscopy, a detailed morphological description of early phloem development in mature embryos and in seedlings was done by Bauby et al. (Bauby et al., 2007). They determined characteristic features for different stages of protophloem (PP) cells (cell elongation, cell wall thickening, loss of the nucleus) which have a characteristic bone-shaped form. In addition, they identified novel early phloem differentiation markers (PD1-5) being expressed during early phloem development. They could show that the timing of PP differentiation is organ dependent and starts earlier in the cotyledons than in the rest of the plant, already during

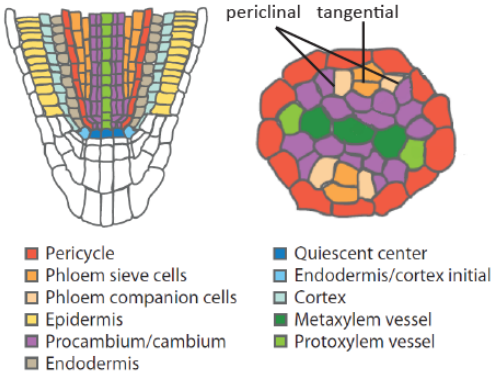

Fig. 2.6: Asymmetric phloem-divisions in a scheme of a post-embryonic root section. Phloem differentiation involves asymmetric divisions generating SEs and CCs. Xylem and phloem poles display a bisymmetric pattern in the root cross section. Several root tissue types are depicted as indicated by the legend. Fig. derived and modified from ref. (Cano-Delgado et al., 2010).

embryogenesis (Bauby et al., 2007). Similarly to protoxylem differentiation (Pyo et al., 2004), PP differentiation is initiated at distinct loci after germination and progresses almost simultaneously along the cotyledons, hypocotyl and root. Thus, xylem and phloem differentiation seem to be tightly linked (Bauby et al., 2007).

The identified PD markers include genes encoding for proteins potentially involved in signaling pathways like glycosylphosphatidylinositol (GPI)-anchored proteins and phosphoinositide phosphate kinases (PIP-K) (Bauby et al., 2007). One member of this family has been localized in the procambium and might be involved in the regulation of cell proliferation (Elge et al., 2001). PD4 was identified as the TF BREVIS RADIX (BRX) which is required for normal root growth and is involved in auxin signaling (Mouchel et al., 2006; Scacchi et al., 2009).

2.4.1 *APL* expression and the *apl-1* mutant

The MYB-like TF *APL* was identified as vascular identity gene required for phloem-related asymmetric cell divisions and cell differentiation, probably especially for SE and CC differentiation. Ectopic expression of *APL* in the vascular stele under a procambium-specific promoter prevented or delayed xylem differentiation but did not induce ectopic phloem differentiation. Thus, *APL* was suggested to be essential but not sufficient for phloem differentiation, and to inhibit xylem differentiation at phloem positions (Bonke et al., 2003).

As already mentioned, *APL* is expressed specifically in (future) phloem cells from torpedo stage on shortly after the first phloem-related divisions have taken place. The expression pattern was dynamic as shown in the seedling root. Expression takes place first in the immature SE and CC and remains in the CC upon differentiation, mirroring the spatial and temporal developmental pattern of these cell types. Homozygous *apl-1* mutants (which refers to the published '*apl*' in reference (Bonke et al., 2003)) are seedling-lethal and develop only short roots and only occasionally side roots and the first few true leaves; phloem development is severely impaired throughout the whole plant (Bonke et al., 2003). Initially wild-type-like developing strands of PP cell files (Truernit et al., 2008) gain xylem-like characteristics within one to three days after germination (Bonke et al., 2003; Truernit et al., 2008). Early PP PD markers were expressed in the *apl-1* background

(Truernit et al., 2008), in contrast to the PP SE specific marker *J070I* and CC specific marker *SUCROSE TRANSPORTER2* (*SUC2*) (Bonke et al., 2003).

2.4.2 Auxin and cytokinin in vascular patterning

The regulation of auxin concentrations is also important for the differentiation into either xylem or phloem and influence the patterning of vascular tissues (Aloni, 2001; Aloni et al., 2006). Recently, it was shown that auxin interacts with the phytohormone cytokinin in a mutually inhibitory way to define the boundaries of hormonal output in roots. Thereby, high cytokinin signaling in the procambial cells promotes the bisymmetric distribution of PIN proteins, which channel auxin toward a central domain. Subsequently, high auxin promotes transcription of *AHP6* (*ARABIDOPSIS INHIBITORY PSEUDOPHOSPHOTRANSFER PROTEIN 6*), a cytokinin signaling inhibitor, closing the feedback loop. The bisymmetric high auxin signaling domain specifies the differentiation of protoxylem in the bisymmetric pattern, present in roots (Fig. 2.6) (Bishopp et al., 2011a). In this respect, a role for long-distance basipetal (top-down) transport of cytokinin within the phloem was shown in controlling polar auxin transport and maintenance of the vascular pattern in the root meristem (Bishopp et al., 2011b).

A similar mechanism involving auxin/cytokinin was suggested for symmetry breaking in embryos when cotyledons are specified around heart stage and the radial symmetry of the root vascular precursors transits into bisymmetry (Bishopp et al., 2011a). During embryogenesis, auxin and cytokinin signaling seems to have an antagonistic function in the initiation of the root meristem itself. At globular stage, auxin signaling is high in the hypophysis. Upon division, giving rise to the lens-shaped cell and a basal daughter cell, auxin signaling remains high only in the basal cell. Conversely, first cytokinin signaling is high in the suspensor including the hypophysis. Upon asymmetric division, signaling remains high in the lens-shaped cell and the suspensor, but is reduced in the basal cell (Jeong et al., 2011).

2.5 Other vascular-related transcription factors

The screen of phloem cells for TF transcripts in different species revealed *APL* as well as TFs from the DOF (DNA-binding with one finger) and NAM family. These families might include phloem key regulators but differentiating SEs were expected to be under-represented in the tissues used (Le Hir et al., 2008).

DOF proteins are named by their DNA binding domain, DNA-binding with one Zinc finger, and are involved in a variety of plant-specific processes like light, phytohormone or defense responses and seed development and germination (Yanagisawa, 2004). Interestingly, recent studies revealed a direct connection to vascular development. DOF TFs have been shown to be expressed during procambium formation and early vascular development in embryos as well as in later stages (Konishi and Yanagisawa, 2007), also coinciding with the expression of the procambium-specific *HD-ZIPIII* TF *ATHB8* during vein formation in the leaves (Baima et al., 1995; Gardiner et al., 2010), and promoting *REV* expression and, thus, being involved in abaxial-adaxial patterning (see **2.6**) (Kim et al., 2010). Transcript profiling of cell-sorted root tissues revealed one DOF TF being expressed in phloem precursors of the root meristem and a GATA Zinc-finger TF within the protophloem and metaphloem sieve cells from the vascular initials to top (Cano-Delgado et al., 2010; Lee et al., 2006).

The TF NAM, one of the original defining names for the NAC domain (NAM ATAF1,2 CUC2) (Aida et al., 1997), was identified in petunia to be required for SAM and embryo development (Souer et al., 1996). In general, NAC domain proteins are not only implicated in SAM formation (Aida et al., 1997) but also in lateral root formation, defense responses and abiotic stress as well as in vascular development (Olsen et al., 2005; Yamaguchi et al., 2008). The family of *VASCULAR RELATED NAC-DOMAIN* (*VND1* to *7*) genes and *NAC SECONDARY WALL THICKENING PROMOTING FACTOR* (*NST*) genes are involved in xylem differentiation and secondary wall formation of xylem fibers (Kubo et al., 2005; Ohashi-Ito and Fukuda, 2010; Yamaguchi et al., 2008).

2.6 Phloem – xylem – cambium interaction

Differentiation and patterning of phloem versus xylem cells also involves the antagonistic roles of GARP TFs *KAN* and *HD-ZIP III* genes (*REV*, *PHB*, *PHV*, *CORONA* (*CRN*),

ATHB8). *KAN* genes are associated with phloem (abaxial) patterning and *HD-ZIP III* members with xylem (adaxial) patterning of vascular strands in leaves and shoots. Both classes of TF are also implicated in patterning of embryos and establishment of the procambium (Dinneny and Yanofsky, 2004; Izhaki and Bowman, 2007; Ohashi-Ito and Fukuda, 2010).

Although *KAN* genes are preferentially expressed in the phloem tissue (Eshed et al., 2001), analysis of gain- and loss-of-function plants of *KAN* genes suggested that *KAN* may function in the restriction of procambium precursor cells by suppressing *PIN1* expression and reduction of auxin levels (Ilegems et al., 2010; Ohashi-Ito and Fukuda, 2010). Similarly, the members of the HD-ZIP III family were suggested to be involved in a feedback-loop of auxin-flow-MP-PIN1-auxin-flow to restrict procambium precursor cells to continuous and narrow regions (Baima et al., 1995; Carlsbecker et al., 2010; Donner et al., 2009; Ohashi-Ito and Fukuda, 2010).

Analysis of *phb phv rev crn athb8* loss-of-function mutants and of lines with reduced transcript levels of all five members indicated that *HD-ZIP III* genes positively influence xylem specification (Ohashi-Ito and Fukuda, 2010). Moreover, *ATHB8*, specifically expressed in procambium precursors and procambial cells (Baima et al., 1995; Donner et al., 2009), promotes xylem differentiation upon overexpression (Baima et al., 1995). Recently, a sophisticated system of bidirectional signaling between stele and endodermis involving the TF SHORTROOT and miR165/166 was shown to regulate *HD-ZIP III* levels and thereby define the differentiation of xylem subtypes (proto- and metaxylem) (Carlsbecker et al., 2010).

Communication between procambium, phloem, and xylem in the course of differentiation is also shown by another signaling loop. The CLAVATA3/ ENDOSPERM SURROUNDING REGION RELATED (CLE) 41/44 peptides, also called TDIF, for TRACHEARY ELEMENT DIFFERENTIATION INHIBITOR FACTOR, are produced by phloem cells adjacent to (pro)cambial cells. (Pro)cambial cells express the CLE41/44 receptor PXY (PHLOEM INTERCALATED WITH XYLEM), also known as TDR (TDIF RECEPTOR), a member of the leucine-rich repeat (LRR) receptor-like kinase family. Based on the findings from different studies, CLE-peptide signaling is required for the maintenance of (pro)cambial

cells by promoting their proliferation and preventing xylem differentiation as well as by regulating the cell division orientation (Etchells and Turner, 2010; Fisher and Turner, 2007; Hirakawa et al., 2010; Hirakawa et al., 2008). A procambium-specific LRR receptor-like kinase VASCULAR HIGHWAY 1 (VH1)/ BRASSINOSTEROID RECEPTOR LIKE 2 (BRL2) is also required for functional phloem development in the leaf (Clay and Nelson, 2002), and other provascular expressed LRR receptor-like kinases (BR-INSENSITIVE 1, BRL1, BRL3) are also implicated in regulating phloem-xylem ratios (Cano-Delgado et al., 2004).

As shown by the examples mentioned above, (pro)cambial, phloem, and xylem development is linked by partially overlapping intercellular communication during various developmental stages and within different organs. Thus, it is plausible that vascular identity factors like *APL* are part of this regulatory network and its expression is influenced by components of this network (and vice versa) (Cano-Delgado et al., 2010; Dinneny and Yanofsky, 2004).

2.7 Aim of the study

As outlined, the vascular tissue is essential for the plant and its establishment depends on a very coordinated regulatory network and on cell-to-cell communication. The specification and differentiation of the vascular precursors into distinct vascular cell types is thus embedded in a well defined temporal and spatial control system, still flexible to adapt to environmental cues. The integration of all input signals greatly depends on TFs, key components for regulating gene expression and thus for the execution of specific developmental programs.

However, data about phloem regulators and especially early phloem-specific genes are scarce. Even though some markers are available and more phloem-related TFs have been identified, *APL* (Bonke et al., 2003) is still the only phloem-identity gene known to date. Thus, it is an attractive aim to shed more light on the process of phloem specification and differentiation by identifying factors which are involved in this process.

To this end, I aimed for the identification of factors upstream of *APL* thereby revealing novel phloem regulators. As *APL* is expressed already during embryogenesis but still seems to have a major role in differentiation of phloem into SEs and CCs after

germination, regulators up-stream of *APL* have the potential to act at a central point of phloem establishment at different developmental stages.

During my study, I characterized the *APL* promoter by analyzing promoter fragments for their ability to drive reporter gene expression and to complement the *apl-1* mutant phenotype when driving *APL* expression. Additional information about distinct promoter regions was gained by analyzing *APL* expression levels in lines harboring T-DNA insertions at different positions in the *APL* promoter region. Taking advantage of results obtained by these experiments, a yeast one-hybrid screen was performed and potential *APL* regulators were identified.

The same question was addressed by performing a forward mutagenesis screen using a plant line expressing the *LUCIFERASE* gene under the control of the *APL* promoter. Based on alterations of luminescence intensities due to induced mutations within the genome, regulators directly or indirectly affecting *APL* expression should have been revealed. Unexpectedly, no mutant candidates were identified which raised the possibility of an initially underestimated importance of APL during early stages of embryo development. This theory was supported by the subsequent characterization of a novel *APL* mutant allele, *apl-2*. Microscopic analysis of *apl-2/+* plants led to the hypothesis that APL has a function even prior and distinct to the regulation of vascular development during the first embryonic cell divisions.

3. Material and methods

3.1 Enzymes

All enzymes used in this study were purchased from Fermentas or from New England Biolabs (NEB) and were used according to the manufacturer's instructions.

3.2 Vectors

As plasmid backbones the vectors *pGreen0229* (Fig. 3.1) (Hellens et al., 2000), *pGreen0229-AlcA* (Deveaux et al., 2003), and *pGreen0129-pAlcA::GUS* (Deveaux et al., 2003) were used. All vectors contain the *NptI* gene encoding the bacterial enzyme neomycin phosphotransferase conferring resistance to kanamycin (bacterial selection). The bacterial bialaphos resistance gene (*bar*) encodes the enzyme phosphinotricin acetyl transferase (PAT) conferring resistance to glufosinate ammonium (BASTA) in *pGreen0229* and *pGreen0229-AlcA* (plant selection). *pGreen0129-pAlcA::GUS* contains the bacterial *Aph IV* gene encoding an aminoglycoside phosphotransferase which confers resistance to hygromycin B (plant selection).

3.3 Plasmids used and created in this study

All plasmids were cloned according to description in chapter **3.8**. DNA templates, target vectors, primer names, restriction enzymes, and the yielded constructs are listed in Tab. 3.1 (part 1 and 2). Primer sequences are shown in Tab. 3.2 (part 1 and 2). Information concerning cloning strategies and performances is provided below (numbers always refer to the transcriptional start site (+1) in the promoter; '-'upstream; '+'downstream):

The endogenous sequence of the *APL* promoter (*pAPL*) harbors a *SpeI* restriction site (at position -152 to -147) which was used for cloning of *pKO18*, *pKO19*, *pKO20* (Fig.3.1), and *pKO21*.

For creation of *pCK17* (cloned by Claudia Kerzendorfer; Fig.3.2), one primer (APLrev7-B) contained an *XbaI* extension, to gain compatible overhangs to *SpeI* for subsequent cloning into *pGreen0129-pAlcA::GUS*.

Tab.3.1: Plasmids used and created in this study (part 1).

ß-glucurodinase(GUS) - and *luciferase* (*LUC*) reporter constructs						
plasmid	**DNA template**	**target vector**	**primer 1**	**primer 2**	**restriction sites**	**construct**
pKO1	*pTOM13*	*pTOM13*	delAPL for1	APLrev5	*SacI, NcoI*	*-140 pAPL::GUS*
pKO2	*pTOM13*	*pTOM13*	delAPL for2	APLrev5	*SacI, NcoI*	*-755 pAPL::GUS*
pKO3	*pTOM13*	*pTOM13*	delAPL for3	APLrev5	*SacI, NcoI*	*-1761 pAPL::GUS*
pKO4	*pTOM13*	*pTOM13*	delAPL for4	APLrev5	*SacI, NcoI*	*-44 pAPL::GUS*
pKO5	*pTOM13*	*pTOM13*	delAPL for5	APLrev5	*SacI, NcoI*	*+45 pAPL::GUS*
pKO12	*pCBK04*	*pGreen0229*	35S term-rev1	min35S-for1	*PstI, EcoRI*	*pMin::GUS*
pKO13	*pTOM13*	*pTOM13*	delAPL-for6	delAPL-rev1	*SpeI, NcoI*	*Δ-147 to -46 pAPL::GUS*
pKO14	*pTOM13*	*pKO12*	APLmotif150-for1	APLmotif150-rev1	*NotI, NcoI*	*-142 to +8 pAPL:pMin::GUS*
pKO20	genomic wt Col DNA	*pTOM13*	APL5for4	APLrev18	*SacI, SpeI*	*-3086 pAPL::GUS*
pTOM7*	*LUC ORF****	*pTOM4*	LUCforNcoI	LUCrevPstI	*PstI, NcoI*	*-2587 pAPL::LUC*
pTOM13*	*pCBK04*	*pTOM4*	GUSforNcoI	GUSrevPstI	*PstI, NcoI*	*-2587 pAPL::GUS* (Sehr et al., 2010)

APL complementation constructs						
plasmid	**template**	**target vector**	**primer 1**	**primer 2**	**restriction sites**	**construct**
pKO15	genomic wt Col DNA	*pGreen0229*	delAPL for1	APLrev7	*SacI, KpnI*	*-140 pAPL::APL*
pKO16	genomic wt Col DNA	*pGreen0229*	delAPL for4	APLrev7	*SacI, KpnI*	*-26 pAPL::APL*
pKO17	genomic wt Col DNA	*pGreen0229*	delAPL for2	APLrev7	*SacI, KpnI*	*-755 pAPL::APL*
pKO18	genomic wt Col DNA	*pKO17*	APLfor1	APLrev18	*SacI, SpeI*	*-2587 pAPL::APL*
pKO19	genomic wt Col DNA	*pKO17*	APL5for4	APLrev18	*SacI, SpeI*	*-3086 pAPL::APL*
pKO21	*pKO3*	*pKO18*	T3	APLrev18	*SacI, SpeI*	*-1747 pAPL::APL*

Ethanol-inducible system						
plasmid	**template**	**target vector**	**primer 1**	**primer 2**	**restriction sites**	**construct**
pCK17**	*pTOM4*	*pGreen0129-pAlcA::GUS*	APLfor6	APLrev7-B	*NotI, XbaI* (product) *NotI , SpeI* (vector)	*-2587 pAPL::AlcR (nos term)*
pKO26	fragment d	*pGreen0229-AlcA*	oligoA_AatII	oligo-B-EcoRI	*AatII, EcoRI*	*pAlcA::amiRNA αAPL (35S term)*
fragment a	*pRS300*	-	amiRNA_A	amiRNA-APL_2-IV	-	-
fragment b	*pRS300*	-	amiRNA-APL_2-III	amiRNA-APL_2-II	-	-
fragment c	*pRS300*	-	amiRNA-APL_2-I	amiRNA_B	-	-
fragment d	fragments a, b, and c	-	amiRNA_A	amiRNA_B	-	precursor amiRNA*αAPL*

Probes for RNA *in situ* hybridization

plasmid	template	target vector	primer 1	primer 2	construct
pMS6***	cDNA	*pGEM-T* (linear, Promega)	APLfor15	APLrev15	*APL* antisense
pTOM16*	cDNA	*pGEM-T* (linear, Promega)	ATHB8for5	ATHB8rev5	*ATHB8* (AT4g32880) sense (Agusti et al., 2011)
pTOM 17*	cDNA	*pGEM-T* (linear, Promega)	ATHB8for5	ATHB8rev5	*ATHB8* antisense (insert in opposite orientation) (Agusti et al., 2011)

Additional vectors/plasmids

plasmid	construct	source/reference
pCBK04	*pCMV 35S::GUS*	provided by Karel Riha
pGreen0129-pAlcA::GUS	*pAlcA::GUS, -AlcR*	Deveaux et al., 2003
pGreen0229	-	Deveaux et al., 2003
pGreen0229-AlcA	*pAlcA*	Deveaux et al., 2003
pRS300	miR319a precursor in *pBSK 4*	http://wmd3.weigelworld.org
pTOM4*	*-2587 pAPL - 3'UTR APL*	corresponds to *pTOM13* prior to the insertion of the *GUS* ORF (Sehr et al., 2010)

* cloned by Thomas Greb
** cloned by Claudia Kerzendorfer
*** cloned by Martina Schwarz
**** *LUC ORF* corresponds to *pVRN::LUC* (Greb et al., 2007)

Tab.3.1: Plasmids used and created in this study (part 2).

For creation of *pKO12*, the sequence spanning -46 to +1 of the *35S Cauliflower mosaic virus (CaMV)* promoter (here designated as minimal promoter, *pMin*), *GUS* and *NOS terminator* were amplified from *pCBK04* (provided by Karel Riha) and introduced into *pGreen0229* using the *PstI* and *EcoRI* restriction sites. Primer min35S-for1 (see Tab. 3.2) contains the *PstI* and *NcoI* restriction sites; the *NcoI* site, preserved after cleavage with *PstI*, was used to clone region -142 to +8 *pAPL* to *pMin*, creating *pKO14* (Fig. 3.1).

For creation of *pKO13* (Fig. 3.1), a primer (delAPL-for6) was designed harboring a *SpeI* restriction site annealing to region –45 to -15 in *pAPL*. A PCR product was generated in combination with primer delAPL-rev1 (covering the *NcoI* site in *pTOM13*, which was

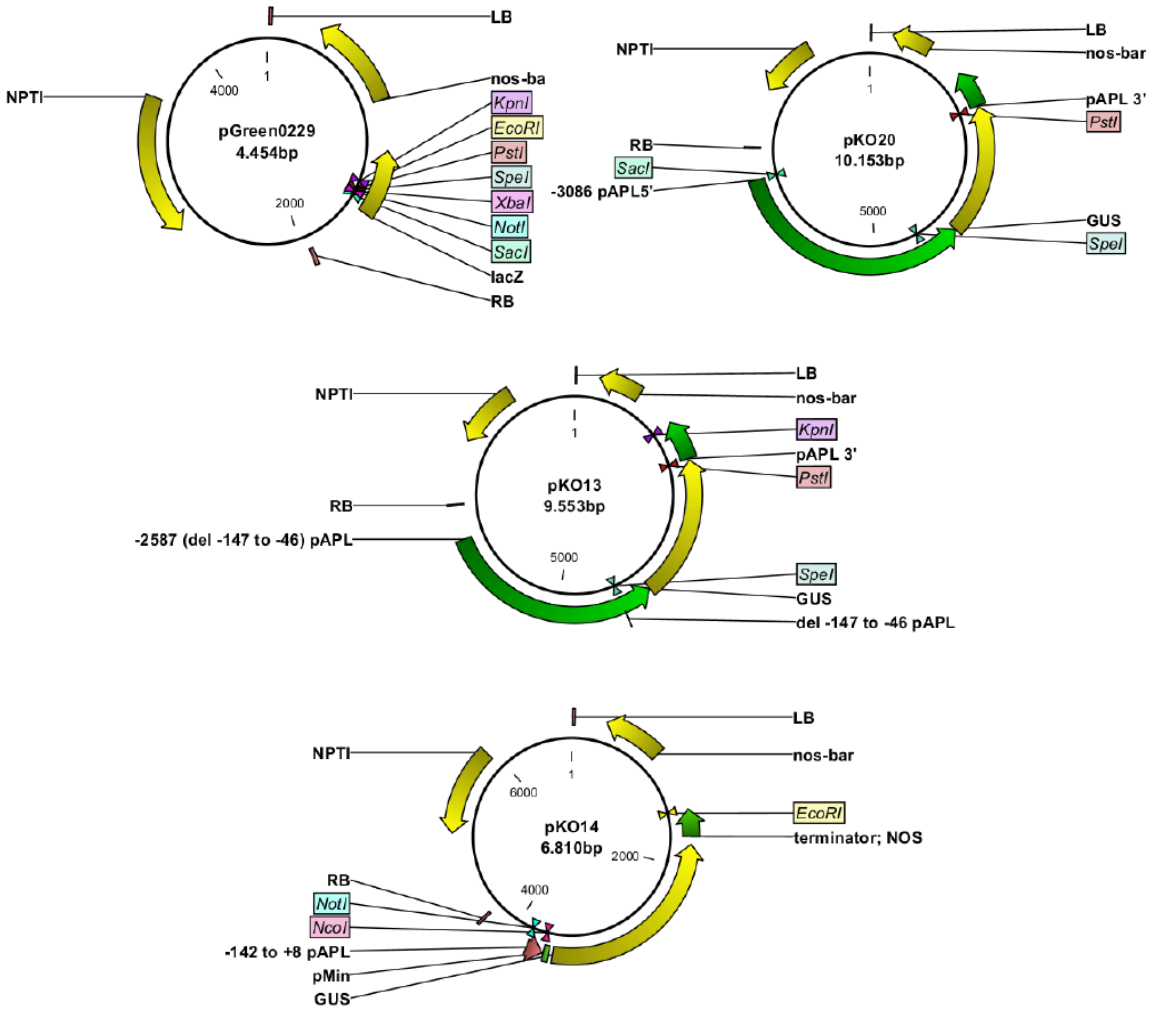

Fig. 3.1: Vector *pGreen0229* and cloned *GUS*-related plasmids.

used previously for cloning *pAPL* to *GUS* (Sehr et al., 2010)). The PCR product was used to replace region -147 to +356 *pAPL* in *pTOM13* using restriction sites *SpeI* and *NcoI*, thereby deleting region -147 to -46 from *pAPL* in *pTOM13*.

pKO15, *pKO16*, *pKO17*, and derived plasmids harbor the genomic *APL* sequence with promoter lengths as described in Tab. 3.1. All plasmids include the 3'UTR of *pAPL* corresponding to the sequence cloned in *pTOM13* (293 bp downstream of the stop codon). Plasmid *pTOM7* contains the *LUC* ORF (corresponding to ref. (Greb et al., 2007)) cloned to the *APL* promoter as in *pTOM13* (see Tab. 3.1).

The sequences for the probes used for RNA *in situ* hybridization (*pMS6*; *pTOM16*, *pTOM17* (Agusti et al., 2011)) was amplified from cDNA and cloned into into the *pGEM-T* vector (Promega) (Tab. 3.1).

For the ethanol-inducible downregulation of *APL*, *pKO26* (Fig. 3.2) encoding the artificial microRNA (amiRNA) construct targeting *APL* mRNA was cloned according to the instructions on the website of the WMD3-Web MicroRNA Designer tool (http://wmd3.weigelworld.org). Briefly, four primers (Tab. 3.1 and Tab. 3.2) were retrieved from the program to engineer the amiRNA precursor, targeting exon 2 in *APL* (At1g79430.2). Three overlapping fragments (a,b,c) were generated from the *pRS300* plasmid (miR319a precursor in *pBSK4*; http://wmd3.weigelworld.org) by site-directed mutagenesis, which were fused in a subsequent reaction to fragment 'd'. Subsequently, fragment 'd' was amplified with primers containing *AatII* and *EcoRI* extensions, respectively, and introduced into the dephosphorylated vector *pGreen0229-AlcA* (see Tab. 3.1). (For dephosphorylation, 1.5 µl Shrimp Alkaline Phosphatase (SAP, Fermentas) was added to the double digested *pGreen0229-AlcA* vector and incubated for 90 min at 37°C. The vector was purified with the QIAGEN QIAquick PCR purification kit prior to ligation.)

3.4 Primers

Primers used in this study were designed either using Vector NTI 10.1.1 (Invitrogen) or the CLC Main Workbench 6.0.1. Primers for cloning *pKO26* and dCAPS marker were generated as mentioned in chapter **3.3** and **3.20.2**, respectively. All primers were purchased at Sigma-Aldrich. See Tab. 3.2 (part 1 and 2).

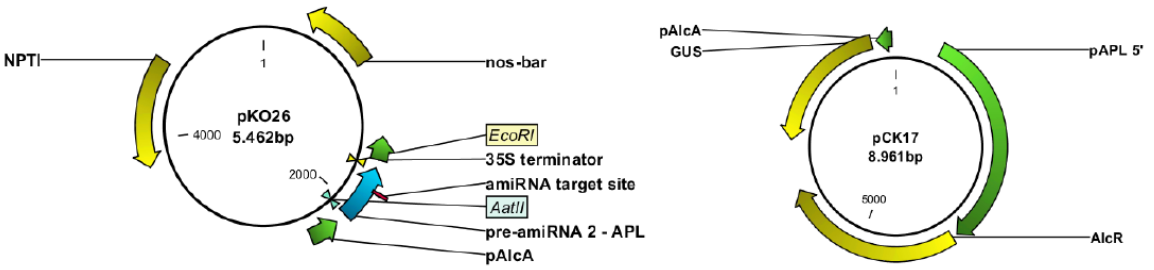

Fig. 3.2: Plasmids used in the ethanol-inducible system.

Cloning	
primer name	**sequence (5'- 3')**
amiRNA_A	CTGCAAGGCGATTAAGTTGGGTAAC
amiRNA_B	GCGGATAACAATTTCACACAGGAAACAG
amiRNA-APL_2-I	GATATAATCGTCTTTGGGGGCGCTCTCTCTTTTGTATTCC
amiRNA-APL_2-II	GAGCGCCCCCAAAGACGATTATATCAAAGAGAATCAATGA
amiRNA-APL_2-III	GAGCACCCCCAAAGAGGATTATTTCACAGGTCGTGATATG
amiRNA-APL_2-IV	GAAATAATCCTCTTTGGGGGTGCTCTACATATATATTCCT
APL5 for4	ACTAGAGCTCTCGGACAATTTTTGCTTTGGATATAC
APLfor6	ACTAGCGGCCGCAGCTCTTAGTTTGCTTCAACAAC
APLfor15	AGCACAAGGAAAGTACATGCAATCT
APLmotif150-for1	ACTAGAGCTCATGCGGCCGCATCTTTAGTTCTCTTCCTTACTAACGATAAAAC
APLmotif150-rev1	ACTACCATGGATTGTGATGCAAAAATGTGAGAGAATACG
APLrev5	ACGTCGACTGCTGCAGATCCATGGTAATCGTCTTTGGGGTCGC
APLrev7	ACTAGGTACCGGCAAACTGTCAAATATGAAAATCG
APLrev7-B	ACTATCTAGATAATCGTCTTTGGGGTCGC
APLrev15	AACACGAGCAAAACTAATCCGGT
APL rev18	TTTCAGACTAGTACACAGAC
ATHB8for5	TCACTCTTCTTGTGAACTCCTCTC
ATHB8rev5	TACCGGAGATAAGGCCTTGA
delAPL for1	TATGAGCTCCTTTAGTTCTCTTCCTTACTAACG
delAPL for2	TATGAGCTCAGAAAATATTTACAAATCTTTGATTAC
delAPL for3	TATGAGCTCAAGAGGTCCCCAACGTTAACTC
delAPL for4	TATGAGCTCCGTCATCTGATCTCTTCAAAAACGC
delAPL for5	TATGAGCTCAGAGAGTCAGAGAGAGAGAGAGAGAG
delAPL-for6	ACTAACTAGTCGTCATCTGATCTCTTCAAAAACGCATCG
delAPL-rev1	TAACGCCATGGTAATCGTCTTTGGGGTC
GUSforNcoI	ACTACCATGGCGTTACGTCCTGTAGAAACCC
GUSrevPstI	ACTACTGCAGTCATTGTTTGCCTCCCTGCTG
LUCforNcoI	ACTACCATGGAAGACGCCAAAAACATAAAG
LUCrevPstI	ACTACTGCAGTTACACGGCGATCTTTCCGCCCTTC
min35S-for1	ACTACTGCAGATCCATGGATGCAAGACCCTTCCTCTATATAAGGAAG
oligoA_AatII	ACTAGACGTCCCCCAAACACACGCTCGG
olig-B-EcoRI	AGGTGAATTCCATGGCGATGCCTTAAATAAAG
35S term-rev1	CTGAGCTGAATTCCCGATCTAGTAAC
T3	AATTAACCCTCACTAAAGGG

Genotyping	
primer name	**sequence (5'- 3')**
apl-F1	GGTTCAGGCTCACATCATGCTA
apl-F2gen	CGATTGGTTTGCGGAAAGATC
APLfor20	AAAGTACATGCAATCTATCTT
apl2-for	ATTTCATTCAATTTTTATAGGTGCAAAGACATCTGCAACTGAGGATTGAAGCACA AGGAAAGTACATGCAATCTATCTTGGAGAGAGCTGGC
apl-R1	GAAGGTTGCATGAACAGCTAGA
APLrev12	CTTTTTGTGATGGTGCTTTG
APLrev21	ATGGGATATATATACTGGTTAAGG
apl-2rev	GCGGCTGCCATGTTCTCACCGGCTAGGGCTT
er105 for	AGCTGACTATACCCGATACTGA
er105 rev	AAGAAGTCATCTAAAGATGTGA
LINC2rev4	TCCAATATTTCCCACTCCTTTTCA
LINC2for4	CGAAGTCTAAAGAAACTGAAGAGGACA
LUCforNcoI	ACTACCATGGAAGACGCCAAAAACATAAAG
SALK_014183-LP	ATGTGTGTTCATACTGTCGGG
SALK_014183-RP	ACTCCAAATCAAGCATGATTAAG
SALK_068444-LP	GTATACGACTCTCCTCGTGCG
SALK_068444-RP	ACAAAACGCTCGTGGAGTTC
SALK_069587-LP	ATTGCATGAGAATTGGAATCG
SALK_069587-RP	TTCTCCTCCACTCGTATCCTTC
SALK_088773-LP	TGCATGATTTGTTGCATGATG
SALK_088773-RP	TTGTGTGTGCATATCAGCCTC
SALK_058157-LP*	ATCCAAAACCGTTAGGTACGG
FLAG_268C11-LP**	TGTGGCTGGCCAAGTTTATAC
SALK_LBa1	TGGTTCACGTAGTGGGCCATCG
T7	GTAATACGACTCACTATAGGGC
*used as LP (left border primer) for SALK_029212	
**used as RP (right border primer) for SALK_029212	

Tab. 3.2: Primers used in this study (part 1).

(q)RT-PCR	
primer name	**sequence (5'- 3')**
APLversion1_for	AGTTTTTGATCATTTCTATTTGC
APLversion2_for	GCCCCGACAAAGCGACCC
aplF4-gen	CCTCAGTTGCAGATGTCTTTG
TUBfor3	TTCGTTCCTCGTGCAGTGCTCA
TUBrev2	AAGGTAAGCATCATGCGATCTGGGT
APLfor22	ACCACCGACCCTAAACCGC
EIF4A1for	ATCCAAGTTGGTGTGTTCTCC
EIF4A1rev	GAGTGTCTCGAGCTTCCACTC
for apl-R1, apl-F2gen see Genotyping	

Probes for Southern blot	
primer name	**sequence (5'- 3')**
GUSfor2	CCGGGAAAAGTGTACGTATCACCG
GUSrev2	CCACGCCGTATTCGGTGATGA

Sequencing the *LUC* ORF in *pAPL::LUC*	
primer name	**sequence (5'- 3')**
APL5for2	TGGTCTACATTTTAACATGTAC
APL5 for3	ATTTACTCCAAATCAAGCATG
APL5rev1	CTGAATCAAAGATATTGCAC
LucAPL3for	GACCAACGCCTTGATTGACAAG
LucAPL5rev	TCTTTATGTTTTTGGCGTCTTCC
Lucfor2	TGAACGTGAATTGCTCAACAG
Lucrev2	AGCCATCCATCCTTGTCAATC
LUCrev3	GGTAATCCGTTTTAGAATCC
Lucrev4	TAGTCTCAGTGAGCCCATATC
for LUCforNcoI, LUCrevPstI, T3 see Cloning; for T7 see Genotyping	

Sequencing of the cloned plasmids	
primer name	**sequence (5'- 3')**
AlcAprom-for	GCATCCCCGCATAGCTGAAC
apl-F1gen	ATTGTATCACCCAAATGGCGAG
APLfor1	ACTAGAGCTCAGCTCTTAGTTTGCTTCAACAAC
APLfor5	CCATGGATCTGCAGCAGTCGACGTGATACAATTTATTAATTTTTATCTATGAGTG
APLfor11	TAATATTGTTGGCGCAATAAG
APLfor12	GTCCGTGTTTATAATATGTATA
APLfor13	GTGTCCATACAAGTAATTTAG
APLfor14	TTCCTTTCTCTATCAAATTAGG
APLfor16	AAGGAAAGGACTATTGATGTG
APLrev10	AAATCTTGGCTGTGAAACGAA
APL rev12	CTTTTTGTGATGGTGCTTTG
APLrev13	ATGGATTGAATATATATTTGTGT
APLrev14	ACTTGAAGGTTTCTTAGCATG
APLrev16	GCTTTCCCTTAATTAATACTTA
APL5 rev1	CTGAATCAAAGATATTGCAC
GUSfor4	ACGGATGGTATGTCCAAAGCG
GUSrev3	ACGAATATCTGCATCGGCGAAC
GUSrev4	ATTACGCTGCGATGGATTCCG
pAPLintern_for1	TTTGTTCCAAAAATATACGGTCTATTAATT
pAPLintern_rev1	CGTTAGTAAGGAAGAGAACT
35Sterm-rev	AAGAACCCTAATTTCCCTTATCGG
for APLrev7, delAPL for1, delAPL for5, T3 see Cloning; for apl-F2gen, apl-R1, T7	
see Genotyping; for GUSfor2, GUSrev2 see Probes for Southern blot	

Tab. 3.2: Primers used in this study (part 2).

3.5 Bacterial strains

For propagation of plasmids *Escherichia coli* strain DH5α was used. For transformation of plants *Agrobacterium tumefaciens* strain C58C1 harboring the helper plasmid *pSoup* (Hellens et al., 2000) was used.

3.6 Plant lines

All plant lines used were *Arabidopsis thaliana* (L.) Heynh. plants of the accession Columbia-0 (Col-0). Additional plant lines were ordered from the Nottingham Arabidopsis Stock Centre (NASC) (Alonso et al., 2003) or donated by the colleagues, as listed in Tab. 3.3.

The allele published as '*apl*' (Bonke et al., 2003) is designated as '*apl-1'* in this thesis for distinguishing it from the second allele analyzed here, named '*apl-2*'.

Plant lines

NASC ID	information	Reference
N9362	Insertion of *mGFP4* into the *PIN1* genomic fragment (*PIN1-GFP*)	Benkova et al., 2003
N90088	TILLING line, point mutation in *APL* (Q168*; *apl-2* in this study), Col-0 background with *erecta-105* mutation; plants wild-type for the *ERECTA* locus were analyzed. The *erecta-105* locus was identified with primer combination er105 for/er105 rev.	Till et al., 2003;Torii et al., 1996; this study
N514183	SALK_014183 (T-DNA insertion: *pAPL -396*)	this study
N529212	SALK_029212 (T-DNA insertion: *pAPL -1816*)	this study
N568444	SALK_068444 (T-DNA insertion: *pAPL -316*)	this study
N569587	SALK_069587 (T-DNA insertion: *pAPL -2784*)	this study
N588773	SALK_088773 (T-DNA insertion: *pAPL -1146*)	this study

donated lines	information	Reference
apl-1	*En1*-transposon insertion in *APL* exon 6 (after nt position +1088, interrupting codon Q160)	Bonke et al., 2003
bpc1246	*bpc1-1 bpc2-1 bpc4-1 bpc6-1* (all single mutants originally derived from SALK lines except for *bpc4* which is a SAIL line)	Monfared et al., 2011
bpc12346	*bpc1-1 bpc2-1 bpc3-1 bpc4-1 bpc6-1* (*bpc3* single mutant is derived from a TILLING line)	Monfared et al., 2011

Abbreviations: *PIN1* , *PINFORMED1* (At1g73590); mGFP, modified Green Fluorescent Protein; TILLING, Targeting Induced Local Lesions IN Genomes; Q, Glutamine; *, stop codon; *pAPL*, promoter of *ALTERED PHLOEM DEVELOPMENT* (At1g79430). For SALK lines (*pAPL*) positions of T-DNA insertions were determined by sequencing. Numbers refer to the position upstream (-) or downstream (+) of the transcriptional start site (+1)(as annotated in TAIR).

Tab. 3.3: Plant lines used in this study.

3.7 Online tools for promoter and protein analysis

3.7.1 *APL* promoter analysis

The *APL* promoter sequence was retrieved as sequence upstream of the annotated transcriptional start site of *APL* (At1g79430) in the The Arabidopsis Information Resource (TAIR) database (www.arabidopsis.org). For *in silico* analysis, the *APL* promoter sequence spanning region -3086 to +356 referring to the transcriptional start site +1 for *APL* (At1g79430) was used for motif search using the Genomatix software MatInspector 7.7.3 (www.genomatix.de, preliminary full access trial version, August 2008; search was done with default settings for Transcription factor binding sites (Weight Matrices), Matrix Family Library Version 7.1, General Core Promoter Elements (0.75 core/Optimized matrix sim), Plants (0.75 core /Optimized matrix sim).

3.7.2 *APL* protein analysis

The amino acid sequence of APL isoform 1 (At1g79430.2) was analyzed (retrieved from the TAIR database). Protein domains were derived from http://www.uniprot.org/uniport/Q9SAK5; Isoform 1 [UniParc]; last modified March 24, 2009. Version 2. Checksum: F92EABC974F8BF9F.

For prediction of the coiled-coil region the program available on http://www.ch.embnet.org/cgi-bin/COILS (Lupas et al., 1991) was used (default settings; NCOILS version 1.0; MTIDK matrix, no weights).

Information about Expressed Sequence tags (ESTs) for *APL* were obtained from TAIR.

3.8 Molecular cloning

All vectors were produced according to the following procedure:

3.8.1 Amplification of the sequence of interest

The sequence of interest was amplified by PCR reaction using primers with extensions for specific restriction sites required for directional cloning. Templates were either genomic DNA or pre-cloned plasmids (see Tab. 3.1). For amplification, either Phusion DNA Polymerase (Finnzymes) or Pfu DNA Polymerase (Fermentas) was used following

the manufacturer's protocols. The PCR product was purified using the QIAGEN QIAquick PCR purification kit following the manufacturer's protocol.

3.8.2 Enzymatic restriction

The PCR product and the target vector (~2 µg) were double digested with the restriction enzymes given by the restriction sites of the primers used. The digested products were purified using the QIAGEN QIAquick PCR purification kit or the QIAquick Gel Extraction Kit following the manufacturer's protocol.

3.8.3 Ligation

The DNA concentrations of the purified PCR product/vector were measured using the NanoDrop Spectrophotometer ND-1000. The amounts of DNA used for ligation was calculated according to the formula: insert (ng) = 6x (insert (bp)/vector (bp)) x vector (ng). Ligation was performed using the T4 DNA ligase (Fermentas) either for 1 h at RT or over night at 16°C following the manufacturer's protocol.

3.8.4 Transformation of competent *E. coli*

About 200 µl of competent *Escherichia coli* (DH5α) were thawed on ice and mixed with 10 µl of the ligation reaction. The suspension was placed on ice for about 20 min followed by a heat shock at 42°C for 90 sec. After addition of 700 µl LB-medium, bacteria were incubated at 180 rpm at 37°C for 60 min. Finally, the bacteria were plated on LB-medium containing the appropriate antibiotic and incubated over night at 37°. About 4 ml selective LB-medium were inoculated with growing colonies for subsequent testing and/or propagation and plasmid preparation. For selection, kanamycin was used at a concentration of 50 µg/ml and ampicillin at 100 µg/ml LB-medium. A cryostock was prepared by pipetting 800 µl of a dense bacterial culture with 200 µl sterile glycerol in a cryovial which was immediately frozen at -80°C.

LB-medium (for plates)

1% Peptone

0.5% Yeast extract

1% NaCl

1.5% Bacto agar

autoclave

3.8.5 Plasmid preparation and analysis

For isolation of the plasmid about 2 ml of a bacterial over night culture were processed using the QIAGEN QIAprep Spin Miniprep Kit following the manufacturer's protocol. A test restriction was performed of the newly generated plasmid and analyzed by agarose gel electrophoresis. Plasmids were sequenced.

3.9 Footprint analysis

Genomic DNA from a pool of 8 *apl-1* homozygous seedlings (~3 weeks old) was extracted (see **3.11.1**). The primer combination AW (apl-R1/apl-F2gen, see Tab. 3.2) was used for amplification of the transposon excision based former *apl-1* locus with either Phusion or homemade Taq DNA polymerase. A 3' overhang was extended to the blunt-ended PCR product produced by the Phusion polymerase; Taq DNA polymerase was added and the samples were incubated for 10 min at 72°C. The PCR product was purified and ligated into the *pGEM-T* vector (linear, Promega) according to the instructions by the supplier (90 min at RT; 10 ng vector). The ligation mix was transformed into competent *E.coli* DH5α (see **3.8.4**). Blue/white selection was performed on LB-Amp plates (100 µg/ml); for blue/white selection, 50 µl of X-Gal [20 ng/ml dimethylformamide] (Fermentas) and 100 µl of Isopropyl β-D-1-thiogalactopyranoside (IPTG) [100 µg/ml] (Fermentas) were distributed on the surface per plate. White colonies were picked and added to a standard PCR reaction mix (Taq) for amplification (see **3.14.1**) of the cloned insert (primer pair AW). The PCR reaction was diluted 1:1 with dH_2O and directly used for sequencing (primer apl-R1).

3.10 Sequencing

Sequencing of PCR products and plasmids were performed by the in-house sequencing facility (IMP/IMBA/GMI), AGOWA GmbH (Germany), or VBC-BIOTECH Service GmbH (Austria). The AB1-files were processed and analyzed using the software CLC Main Workbench 6.0.1.

3.11 DNA extraction

3.11.1 DNA extraction (PCR-grade)

A small leaf was harvested, put into an Eppendorf tube containing 200 µl of extraction buffer and ground manually with a blue drill. Again, 200 µl of extraction buffer were added and tubes were centrifuged for 5 min at maximum speed (14,000 rpm) at room temperature (RT). The supernatant was pipetted into a fresh Eppendorf tube containing 350 µl isopropanol. DNA was precipitated for 10 min at RT and then centrifuged for 5 min at maximum speed. The supernatant was removed, and the pellet was washed with 700 µl 70% EtOH followed by centrifugation for 1 min at maximum speed. The ethanol was removed and the pellets were dried in a vacuum centrifuge (Eppendorf concentrator 5301) for 10 min at 30°C. Subsequently, DNA was resolved in 50 µl dH_2O for 10 min at 65°C (800 rpm) using a thermo mixer (Eppendorf) and stored at -20°C.

DNA extraction buffer
200 mM Tris-Cl, pH 7.5
250 mM NaCl
0.5% SDS
25 mM EDTA
autoclave

3.11.2 CTAB

Fresh plant material was harvested into a 2 ml Eppendorf tube and immediately frozen in liquid nitrogen. Frozen plant material was ground using an overhead stirrer (IKA RW 20.n) (max. speed) or mortar and pestle, intermitted by cooling in liquid nitrogen. Frozen

pulverised plant material was put into an Eppendorf tube containing 1 ml 2x CTAB buffer, vortexed and incubated for 5 min at 65°C. 400 µl chilled phenol:chloroform:isoamyl alcohol (PCI) (25:24:1, AppliChem) were added. Samples were shaken vigorously and centrifuged at maximum speed (14,000 rpm) for 10 min at RT. The aqueous phase (around 900 µl) was transferred into a fresh Eppendorf tube supplied with 800 µl ice-cold isopropanol and shaken vigorously. DNA was precipitated at RT for about 10 min, followed by centrifugation for 20 min at RT (14,000 rpm). The supernatant was decanted and the pellet was washed with 300 µl 70% EtOH. After centrifugation for 5 min, the supernatant was carefully removed. The DNA pellet was dried and resuspended in 100 µl dH_2O. To remove RNA, 1 µl RNase A (10 mg/ml, DNase and protease-free, Fermentas) was added and incubated for 20 min at 37°C. 200 µl PCI were added, mixed and centrifuged for 10 min as before. The aqueous phase was transferred into a fresh tube containing 400 µl EtOH absolute and 20 µl 3 M sodium acetate (pH 5.2) to precipitate DNA. Samples were mixed, incubated for at least 1 hour at -20°C and centrifuged for 10 min. The supernatant was removed and pellets were dried. DNA was resolved in 100 µl dH_2O shaking for 10 min at 65°C. DNA concentration was determined using the NanoDrop Spectrophotometer ND-1000.

2x CTAB buffer

1,4 M NaCl

100 mM Tris-Cl, pH 8

20 mM EDTA

2% CTAB (Cetyltrimethylammonium bromide)

autoclave

3.11.3 DNA extraction of *Arabidopsis* embryos

Siliques were fixed on double-adhesive tape and sliced open along both sides of the replum with needles (Roth, 6183.1) and lancets (Roth, 6181.1). Seeds were transferred into tap water drops to prevent drying. Almost mature embryos (and corresponding aborted ones) were dissected from the ovules and directly transferred into PCR reaction tubes filled with 10 µl 0.25 M NaOH and incubated for 30 sec at 95°C with open lids. 10

µl 0.25 M HCl and 5 µl buffer (0.5 M Tris/HCl (pH 8.0) with 0.25% IGEPAL) were added and tubes were incubated for 2 min 30 sec at 95°C with open lids. About 3 µl of the lysate were used for PCR reactions.

3.12 RNA extraction

Fresh plant material was harvested into a 2 ml Eppendorf tube and immediately frozen in liquid nitrogen. The frozen tissue was ground with a mortar and pestle; about 400 µl of the fine powder was put into a 2 ml Eppendorf tube containing 1 ml of chilled TRIzol reagent (Invitrogen) and shaken vigorously. The samples were incubated for 5 min at RT and subsequently centrifuged at 4°C at maximum speed for 15 min. The supernatant (~900 ml) was transferred into a fresh tube containing 200 µl of chloroform, shaken vigorously and incubation for 5 min at RT. Samples were centrifuged at maximum speed at 4°C for 15 min. The upper aqueous phase (~400 µl) was transferred into tubes supplied with 500 µl chilled isopropanol. RNA was precipitated for at least 1 hour at -20°C (frequently over night). Subsequently, RNA was pelleted by centrifugation for 10 min at maximum speed at 4°C. The supernatant was discarded, pellets were washed with 1 ml 70% EtOH followed by centrifugation for 5 min at 4°C at 10,000 rpm. The supernatant was removed and pellets were dried by air or by incubation in a thermoblock (Eppendorf) at 37°C with open lids, loosely covered with parafilm. RNA was resuspended in 50 µl DEPC water for direct usage or in 90 µl for subsequent DNase treatment (see below) (if required shaking for 10 min at 55°C). RNA was stored at -80°C.
RNA was purified using the RNeasy Micro Kit (QIAGEN) according to the manufacturer's protocol. Prior, DNase digestion was performed following the protocol instructions (Appendix D). RNA was eluted in 15 µl DEPC treated dH_2O and the RNA concentration was determined using the NanoDrop Spectrophotometer ND-1000.

3.13 Complementary DNA (cDNA) production

cDNA was generated using the RevertAid^{TM} H Minus First Strand cDNA Synthesis Kit (Fermentas) by following the manufacturer's protocol (for total RNA, using the oligo $(dT)_{18}$ primer).

3.14 Polymerase chain reaction (PCR)

3.14.1 Standard PCR

The following standard PCR reaction mix with *Thermus aquaticus* (Taq) DNA polymerase was used:

2.5 µl	10x Taq Buffer (homemade)
1.5 µl	25 mM $MgCl_2$ (homemade)
0.25 µl	10 mM dNTP (Fermentas)
0.25 µl	10 µM primer 1
0.25µl	10 µM primer 2
0.04 µl	Taq DNA polymerase (1:10, homemade)
+ template (100 ng DNA or 1 ng plasmid)	
adjusted with dH_2O to a final volume of 25 µl	

For genotyping *apl-1* complemented plants using a mixed reaction of 4 primers, double amounts of dNTPs were added.

The following standard PCR reaction mix with Phusion DNA Polymerase F-530S (Finnzymes) was used:

8 µl	5x Phusion HF reaction buffer F-518 (Finnzymes)
1.2 µl	50 mM $MgCl_2$ F-510 (Finnzymes)
0.8 µl	10 mM dNTP (Fermentas)
0.5 µl	10 µM primer 1
0.5µl	10 µM primer 2
0.2 µl	Phusion DNA Polymerase F-530S (2u/µl, Finnzymes)
+ template (100 ng DNA or 1 ng plasmid)	
adjusted with dH_2O to a final volume of 40 µl	

PCRs were performed in a Bio-Rad iCycler or a Biometra T3000 Thermocycler using the following standard PCR program:

Denaturation: 95/98°C – 3 min

30 cycles: Denaturation: 95/98°C – 20 sec

Annealing: 56-60°C – 20 sec

Extension: 72°C – 90 sec

Final extension: 72°C – 6 min

Hold 20°C

DNA denaturation was performed at 95°C and at 98°C for the Taq and the Phusion DNA polymerase, respectively. Annealing temperatures were calculated for the primer pairs used. Extension times were adjusted for the expected product length (according to the elongation efficiencies: Taq ~1 kb/min; Phusion ~4 kb/min). Numbers of cycles were adjusted if required. PCR products were analyzed with standard gel electrophoresis as described below.

3.14.2 Reverse transcriptase (RT) PCR

For RT-PCR 1 µl of cDNA generated with oligo $(dT)_{18}$ primer was used as DNA template; residual performance followed the standard PCR protocol. The tubulin beta chain 2 (*TUB2*, At5g62690) was used as reference gene to determine relative expression levels for the genes of interest (GOI) (primer combination TUBfor3/TUBrev2, see Tab. 3.2). To prevent saturation of the amplified PCR product, numbers of cycles were adapted for each primer combination. The resulting PCR products were analyzed with standard gel electrophoresis as described below.

3.14.3 Quantitative real-time (qRT) PCR

qRT-PCR was performed as described in (Nolan et al., 2006). As template for qRT-PCR, cDNA prepared from RNA purified with the RNeasy Micro Kit (QIAGEN) was used. The cDNA was diluted 1:5 for subsequent steps.

For each run a calibration curve had to be included. For this, a standard cDNA dilution series was prepared using the originally diluted (1:5) cDNA as starting solution (corresponding to '1:1'), as follows: 1:1, 1:10, 1:100, and 1:1,000. For each primer pair

three technical replicates were prepared using the following master mix (total volume of 15 µl):

7.5 µl	2x SensiMix SYBR (Peqlab)
0.4 µl	10 µM primer 1
0.4 µl	10 µM primer 2
1.7 µl	dH_2O
5 µl	cDNA template

The primer pairs used for qRT-PCR were tested at different temperatures to determine the optimal correct melting temperature and to detect possible primer dimer formations. The IQ^{TM}5 Multicolor Real-time PCR Detection System (Bio-Rad) mounted on an iCycler PCR machine (Bio-Rad) was used with the following protocol:

Denaturation:		95°C – 10 min
35x:	Denaturation:	95°C – 10 sec
	Annealing:	60°C – 30 sec
	Extension:	72°C – 30 sec
Melting:		73°C – 11 sec
		75°C – 11 sec
		77°C – 11 sec
		79°C – 11 sec
Final extension:		72°C – 1 min

After the run, the melting curve chart and the melting peak chart were analyzed with the IQ^{TM}5 Optical System software and the optimal melting temperature was determined.
As internal control, the *Arabidopsis* eukaryotic translation initiation factor 4A1 (*EIF4A1*, At3g13920, see ref. (Metz et al., 1992)) was used. For each sample and gene, qRT-PCR reactions were performed in technical duplicates with the master mix described above following the qRT-PCR protocol.
Ct (cycle threshold) values were determined by the IQ^{TM}5 Optical System software and exported into a MS Excel Workbook for further analysis. Data for *EIF4A1* (primer

combination EIF4A1 for/EIF4A1 rev, Tab. 3.2) were analyzed at 77°C, for *APL* (primer combination APLfor22/apl-F2gen, Tab. 3.2) at 79°C, respectively.

3.15 DNA agarose gel electrophoresis

For electrophoretic separation of DNA on agarose gels, DNA samples mixed with 0.8% loading dye were loaded on 1% agarose gels (peqGOLD universal agarose, Peqlab) together with 2 µl of a DNA marker (Gene Ruler 1kb DNA Ladder, Invitrogen). Gels were run for 30 to 40 min at 70-125 V in 1x TAE buffer. To stain DNA, gels were incubated in an ethidium bromide staining bath (50 µl EtBr [10 mg/ml] in 500 ml 1x TAE buffer) for about 20-30 min. DNA bands were detected by UV light, photographed and analyzed using the Gel Logic 2000 Imaging System (Kodak).

50x TAE

242 g TRIS

100 ml 0.5M EDTA

57.1 ml acetic acid

Fill up to 1 l with water,

adjust pH to 7.6 with acetic acid and autoclave

Loading dye

0.25% xylene cyanole (XC)

0.25% bromophenol blue (BPB)

50% glycerol

10 mM Tris-Cl, pH 8

1 mM EDTA, pH 8

3.16 Non-radioactive RNA *in situ* hybridization (RISH)

RISH was performed according to the protocol of the “Practical course in molecular and biochemical analysis of *Arabidopsis*, non radioactive *in situ* hybridization”, an EMBO

course held in Cologne 1998 at the Max-Planck Institut für Züchtungsforschung (see ref. (Greb et al., 2003)). Main steps and alterations are described.

3.16.1 Sample preparation /fixation

Siliques were harvested, both ends were cut using fine scissors, and immediately transferred into ice-cold 4% PFA/PBS fixative. Samples were vacuum- infiltrated on ice for 1 hour and stored over night at 4°C. PFA was replaced by 50% ice-cold ethanol, incubated for at least 90 min and subsequently replaced by ice-cold 70% ethanol (stored at 4°C until embedding).

4% PFA/PBS

A small pellet of NaOH was dissolved in about 90 ml PBS-buffer (pH 6.5 – 7) increasing the pH to about pH11 and heated in the microwave to 70°C. 4 g Paraformaldehyde (PFA) were added and dissolved by shaking it vigorously. After cooling on ice, the pH was adjusted to 7 with concentrated H_2SO_4. 30 µl of Triton X-100 (Sigma) were added before adjusting the volume to 100 ml.

10x PBS

1.4 M NaCl

27 mM KCl

100 mM Na_2HPO_4

18 mM NaH_2PO_4

adjust pH to 7.3 with HCl and autoclave

3.16.2 Embedding

The fixed plant material was transferred into embedding cassettes (Sanowa) and the cassettes were placed into a tissue processing machine (Tissue-Tek VIP, Vacuum Infiltration Processor, Sanova). Samples were infiltrated with paraffin following a standard embedding protocol over night. The cassettes were transferred to the embedding centre (Tissue-Tek, Sanova) and the samples were manually embedded into moulds (Tissue-Tek). After hardening at the cooling platform, the moulds were removed and the samples were stored at 4°C until sectioning.

3.16.3 Sectioning

For sectioning, the wax blocks were prepared by trimming the excess wax. 7 µm thick sections were produced using a rotary microtome (Microm). To let the sections (wax ribbons) expand, they were transferred to HistoBond adhesion microscope slides (Marienfeld) covered with dH_2O preheated at 42°C. After about 5 min the water was removed with a pipette and the sections were dried on the slides at a heating bank over night at 42°C. The slides were stored at 4°C.

3.16.4 Preparation of probes

Probes for detection (*pMS6*, *APL* antisense; *pTOM17*, *ATHB8* antisense) and control (*pTOM16*, *ATHB8* sense) have been cloned into the *pGEM-T* vector (Promega) vector (see Tab. 3.1). The *ATHB8* sense probe was used as negative control for *APL* as well.

About 8 µg plasmid DNA were digested for at least 4 h using the appropriate restriction enzyme. Linearized plasmid was purified using the QUIAGEN PCR purification kit and about 1 µg of linearized template DNA was used for *in vitro* transcription (incubation for 120 min). Sp6 RNA polymerase (Roche) was used for *pMS6*, and T7 RNA polymerase (Roche) for *pTOM16* and *pTOM17*, respectively. Probes were labeled by incorporation of Digoxigenin-11-dUTP (Dig-UTP; Roche).

To yield an optimum length of *in situ* probe of about 150 bp, the following formula was used to calculate the time of hydrolysis (mild alkaline conditions):

$$t = \frac{Li - Lf}{K \times Li \times Lf}$$

t = time (minutes)
K = rate constant (= 0.11 kb/min)
Li = initial length (kb)
Lf = final length (kb)

Calculated times: *APL* probe, 49 min; *ATHB8* probes, 51 min.

Probes were tested using anti-DIG antibodies (see below) and stored in aliquots at -20°C.

3.16.5 *In situ* hybridization

Tissue pretreatment was performed following a series of steps to increase the accessibility and reduce unspecific binding of the RNA probe. Subsequently, for hybridization 16 µl of probe mix were added to 64 µl of hybridization buffer (80 µl per slide, 24 x 60 mm area). The hybridization mix was distributed on to the slide and covered with coverslips (24 x 60 mm, Menzel) which have been cleaned with acetone and baked to remove RNases. Slides were incubated over night in an oven at 50°C. The next day, slides were washed and treated with RNase A (Fermentas) to remove unspecifically bound single stranded RNA.

3.16.6 Detection

Detection was performed using anti-DIG (Digoxigenin) antibody coupled to alkaline phosphatase (Fab fragments, 150 U, Roche Diagnostics GmbH, Mannheim, Germany) in a concentration 1:3,000. The blocking reagent and detection reagents NBT (Nitroblue tetrazolium chloride) and BCIP (5-Bromo-4-chloro-3-indolyl phosphate) were purchased from Roche. Slides were incubated in detection solution in the dark until a staining reaction was visible under the microscope (maximum of 3 days). Slides were washed in dH_20 and mounted with Dako Ultramount Aqueous Permanent Mounting Medium (Dako). Samples were analyzed by DIC microscopy (ZEISS Axio Imager M1 upright microscope). Pictures were taken using a color camera from Visitron Systems equipped with the SPOT Advanced software version 4.6.

3.17 Surface sterilization of seeds

3.17.1 Vapor-phase sterilization

Seeds were filled in Eppendorf tubes and placed into a desiccator jar together with an 150 ml beaker containing 50 ml of conventional bleach (DanKlorix). 1.5 ml of concentrated HCl were added carefully initiating a chemical reaction to produce chlorine fume. The desiccator was sealed immediately and seeds were incubated for about 4 h or over night.

3.17.2 Liquid-phase sterilization

Seeds were filled into Eppendorf tubes and successively incubated in 70% EtOH for 1 min and 50% conventional bleach (DanKlorix) for 5 min. Subsequently, seeds were washed three times in sterile H_2O for about 3 min each.

3.18 Plant growth conditions

After disseminating seeds on soil (Huminsubstrat N3, Neuhaus, Klasmann-Deilmann GmbH, Germany), seeds were stratified for three days (4°C, 24 h dark) and, subsequently, transferred to plant growth chambers (21°C, 16 h light, 8 h dark, 60% humidity). After three weeks, plantlets were singularised into single pots (6 x 6 cm) filled with a soil-perlite mixture (4:1) (Einheitserde Special ED 63 T, Profi Substrat, Werkverband E.V.; premium perlite 2-6 mm, Gramoflor GmbH, Germany). Every second week a nematode egg solution (*Steinernema feltiae*, ENTONEM, Koppert) was applied to the plants as treatment against the larvae of black flies (*Sciaridae*).

For growth on plates, sterilized seeds were laid out in a little volume of sterile H_2O onto ½ MS plates under sterile conditions (laminar flow). If required, single seeds were placed on the agar in a grid-like pattern to grow seedlings at similar distance (e.g. luciferase-based screen). For selection of drug-resistant plants, the plates were supplemented either with 50 µg/ml kanamycin or 12.5 µg/ml hygromycin. Plates were sealed with parafilm. Seeds were stratified for three days (4°C, 24 h dark) and placed into the plant culture room (21°C, 16 h light, 8 h dark).

½ MS medium (for plates)

2,21 g/l Murashige & Skoog medium including B5 vitamins

10 g Sucrose

6 g Plant agar

fill up to 1 l with water, adjust pH to 5.8 and autoclave

3.19 Crossing of *Arabidopsis thaliana*

Siliques, open flowers, and buds with visible petals or still too young were removed from the inflorescence of the mother plant. About three developed, still closed buds were opened with forceps and all floral organs besides the gynoecium were removed. Open mature flowers from the father plant were used to pollinate the stigmata of the emasculated inflorescence. The siliques were collected after ripening (Weigel and Glazebrook, 2002).

3.20 Genotyping of *Arabidopsis thaliana*

3.20.1 Standard genotyping

DNA of the respective plants was used in PCR reactions (see **3.14.1**) using primers specific for the allele, insertion, or plasmid to be detected (see Tab. 3.2).

Primers for detection of the presence/absence of the T-DNA insertion of plant lines ordered from the seed stock centre (NASC) were obtained on the SIGnAL homepage (SIGnAL T-DNA verification primer design, http://signal.salk.edu/tdnaprimers.2.html). The right border primer (RP) was used in combination with primer SALK_LBa1 (see Tab. 3.2) to detect the insertion. Homozygous plants were propagated. The position of the T-DNA insertion was determined by sequencing (see **3.10**; Tab. 3.2).

3.20.2 Genotyping with dCAPS marker

For the identification of the single point mutation of allele *apl-2*, dCAPS (derived cleaved amplified polymorphic sequences) marker (Konieczny and Ausubel, 1993) were generated using the dCAPS Finder 2.0 program (Neff et al., 2002). The PCR product amplified from the *apl-2* allele with primer combination A2 (apl2-rev/apl-R1, see Tab. 3.2) was digested with restriction enzyme *Bpu1102I* and separated on a 4% agarose gel. The PCR product amplified from the wild-type *APL* allele with primer combination A2c (apl2-for/APLrev21, see Tab. 3.2) was digested with enzyme *MlsI* and separated on a 1% agarose gel. This combination was used for the differentiation between the endogenous and the transformed *APL* sequence in *apl-2/+* plants (for complementation).

3.21 Transformation of *Arabidopsis thaliana*

3.21.1 Transformation of *Agrobacterium tumefaciens*

200 µl of bacterial cell suspension were thawed on ice, 500 ng of the plasmid of interest were added and incubated on ice for 5 min. According to the freeze-thaw method (Hofgen and Willmitzer, 1988), the tube was frozen for 5 min in liquid nitrogen and subsequently incubated at 37°C for another 5 min. 700 µl LB-medium were added followed by an incubation at 28°C for 2-4 h shaking at 180 rpm. About 200 µl of this cell suspension were plated on selective YEB-medium containing 50 µg/ml rifampicin (selection for *Agrobacterium*), 10 µg/ml tetracycline (selects for the helper plasmid *pSoup*) and the specific antibiotic for the plasmid of interest (50 µg/ml kanamycin). The plates were incubated at 28°C up to 3 days. About 4 ml selective YEB-medium (Rif/Tet/Kan) were inoculated with growing colonies and incubated at 28°C for 2 to 3 days shaking at 180 rpm to prepare cryostocks (as described in **3.8.4**) and as preparatory culture for plant transformation (see below).

YEB-medium (for plates)
0.5% Meat extract
0.5% Peptone
0.1% Yeast extract
0.5% NaCl
0.5% Sucrose
2 mM $MgSO_4$
1% Bacto agar
autoclave

3.21.2 Floral dip transformation of *Arabidopsis thaliana*

A preparatory *Agrobacterium* culture was prepared from growing colonies or from cryostocks, as described above. For the floral dip transformation (Clough and Bent, 1998), two 1 l Erlenmeyer flasks each containing 400 ml YEB with 50 µg/ml kanamycin and 10 µg/ml tetracycline were inoculated with 900 µl of the preparatory culture and

incubated over night at 28°C (180 rpm). The bacterial culture was transferred into 500 ml plastic centrifugation tubes and centrifuged for 15 min at 5,000 rpm at RT using an Avanti J-26 XP centrifuge (Beckman Coulter™; JA-10 rotor). The supernatant was removed, the pellets were washed with 5% sucrose solution and resuspended in 500 ml 5% sucrose solution containing 0.02% Silwet L-77 (Lehle Seeds). Inflorescences of plants (16 plants per pot, 5 pots per construct) were dipped into the bacterial solution for about 5 min. The dipped plants were covered with plastic bags until the next day. Seeds of the transformed plants (T1 seeds) were harvested for further analysis.

3.21.3 Selection of transformed plants

T1 seeds of plants transformed with a plasmid conferring hygromycin resistance were laid out on ½ MS-plates (see **3.18**) supplemented with 12.5 mg/l hygromycin and were placed into the plant culture room.

Surviving plantlets were transferred to soil and raised in the growth chamber for further analysis. T1 seeds transformed with a plasmid conferring BASTA resistance were directly laid out on soil. After germination, seedlings were treated every 2^{nd} to 3^{rd} day by spraying with BASTA (40 mg/l water). Again, surviving plantlets were transferred to new pots for further analysis.

3.21.4 Southern hybridization

Southern blots (Southern, 1975) were performed according to Sambrook and Russel (2001) in order to determine the copy number of the foreign plasmid inserted into the genome of the T1 generation of transformed plants. For transfer of DNA fragments from the agarose gels to nylon membranes (Nytran SPC, 0.45 µm, Whatman) the upward capillary transfer method was used. DNA of T1 plants transformed with *GUS*-reporter constructs was extracted by the CTAB protocol (see **3.11.2**) and digested with restriction enzyme *KpnI*. For the production of the DNA probe a PCR product was amplified from plasmid *pTOM13* (Tab. 3.1) (primer combination GUSfor2/GUSrev2, see Tab. 3.2). The DNA probe was labelled by incorporation of [α-^{32} P]–dCTP and used for the identification of single copy plant lines.

3.22 *In vivo* luciferase-based screen

3.22.1 EMS mutagenesis

EMS mutagenesis was performed similarly to published protocols (Greb et al., 2007; Mittelsten Scheid et al., 1998). Twice about 10,000 seeds (~200 mg) homozygous for the *pAPL::LUC* (*pTOM7*) construct were tightly enclosed in a self-made bag of miracloth (Merck). Seeds were incubated in 100 ml of sodium phosphate (100 mM, pH 5) with 0.3% ethylmethane-sulphate (EMS, Sigma) rocking at a platform for 16 hours. Seeds were washed with sodium thiosulphate ($Na_2S_2O_3$, 100 mM, pH5) three times 15 min each, and subsequently with H_2O three times 15 min each. Seeds were dried and stored in a Falcon tube.

The M1 generation was grown on soil and seeds of single plants were harvested for subsequent screening (M2).

3.22.2 Plant growth for screening

EMS-mutagenized seeds of single M2 *pAPL::LUC* families were screened. Seeds were sterilized (see **3.17**) and about 30 - 40 seeds per family were laid out on ½ MS plates (see **3.18**) (one family per 10 cm-petri dish or one family per quarter of a 20-cm petri dish) at equal space with the help of a grid template; seeds were stratified for 3 days at 4°C. As control the non-mutagenized *pAPL::LUC* line was included. Seedlings were grown in a plant culture room for 12 to 16 days (21°C, 16 h light, 8 h dark) until the first leaves had developed and were screened for the luminescence signal, then.

3.22.3 Luminescence detection

Detection was performed similarly to reported *in vivo* luciferase screens (see e.g. (Chinnusamy et al., 2002)). A reagent solution was prepared containing 1 mM D-luciferin* (Duchefa Biochemie bv, Netherlands) as substrate and 2 mM ATP (Applichem) to reduce variations in signal intensities due to different ATP amounts in the plant tissue (final pH of the solution ~4). The solution was kept on ice protected from light. Screening was performed with the VisiLuxx Imager (Visitron Systems) equipped with a cooled charge-couples device (CCD) camera system (Camera SPOT Xplorer 4Mp, Visitron

Systems). The camera was precooled to -40°C and a dark image was taken with the required settings for subsequent substraction of the background signal. Then, seedlings were sprayed with the reagent solution and plates were incubated in the dark for 20 min to ensure proper distribution within the tissue. Plates were placed in the dark chamber and the produced luminescence signals were scanned for 5 min at a resolution of bin4. Integrated signal output over time was depicted as false color image. A light image was taken afterwards (0.7 sec, maximum LED lamps). Pictures were processed with Meta Vue Imaging Version 7.0.

*D-luciferin (stock 10 mM) was dissolved in dH_2O by adding 2-4 drops of 5 N NaOH (aliquots were stored at -80°C).

3.22.4 Candidate evaluation

Seedlings with an altered luminescence signal and sister plants were transferred to soil. The progeny of surviving mutant candidates and/or sister plants were rechecked in the next generation (M3) for the luminescence phenotype. In parallel, DNA was extracted and PCR products amplified from the *LUC* ORF of the transformed *pAPL::LUC* plasmid were subjected to sequencing (for primers see Tab. 3.2).

3.23 GUS staining

For gene expression analysis, samples of marker lines were collected and transferred into a freshly prepared GUS-staining solution. After vacuum infiltration for up to 1 h, samples were incubated at 37°C for 24 to 72 h. Subsequently, the GUS staining solution was replaced by 70% EtOH for clearing several times and left at RT.

For stereomicroscopic (see **3.26.2**) and light microscopic (see **3.26.3**) analysis, GUS-stained leaves and seedlings were shortly washed in 50% glycerol and subsequently mounted on glass slides in 50% glycerol.

GUS staining solution:

GUS staining buffer containing 2 mM X-Glc A (5-bromo-4-chloro-3-indolyl glucuronide, cyclohexylammonium, Duchefa Biochemie; stock 20 mM: 10.4 mg X-Glc A/ ml dimethylformamide) and 1 mM (standard) or 0.5 mM (for experiments of ethanol-

induced *APL* downregulation, see **3.24**) potassium ferricyanide and potassium ferrocyanide (both stocks: 200 mM in dH_2O) each.

GUS staining buffer

100 mM phosphate buffer, pH 7

10 mM EDTA, pH 8

0.1% Triton-X 100

autoclave

3.24 Ethanol induction

Transgenic plant lines carrying ethanol-inducible constructs (Deveaux et al., 2003; Roslan et al., 2001) were grown as described above (**3.18**). Plants were treated with ethanol when already several shoots with siliques and flowers had formed. 1.5 ml Eppendorf tubes filled with 500 µl of 95% ethanol were placed into the soil next to the plants (1 tube for 2 plants). To generate an ethanol atmosphere the plants were covered with a plastic bag. Plant pots were kept in a tray with water and incubated for 16 h. Two days after induction, leaves were harvested for GUS staining (see **3.23**) and material for RNA extraction (see **3.12**), respectively. In order to maintain ethanol induced expression of the amiRNA α *APL* (*pKO26*/*pCK17*) constantly high, the incubation was repeated two days after the induction (for observation of embryo defects).

3.25 Analysis of the embryo abortion rate

For determination of the abortion rate of embryos, siliques were taken at a stage mature enough to clearly differentiate between aborted seeds (white, brown) and normally developed (green) ones. Seeds from 66 siliques of 7 *apl-2/+* and from 49 siliques of 8 sister plants (wild-type for the *APL* locus) were counted. Abortion ratios were calculated as follows: sum of all aborted seeds divided by the total amounts of seeds (the sum of all aborted and normal seeds). Statistical significance was determined by a chi-square test; the critical 5% value of chi-square for an analysis of two independent categories is 3.841 (McKillup, 2006).

3.26 Photography and Microscopy

3.26.1 Digital photography

All photographs were taken using the digital camera Nikon D80 carrying the objectives AF Micro Nikkor 60 mm (1:2.8 D), AF Nikkor 35 mm (1:2 D) or Tamron AF 17 50 mm (1:2.8 IF).

3.26.2 Stereo microscopy

Samples were analyzed using the LEICA MZ16FA binocular and photographed with the attached LEICA DFC300FX color camera. Pictures were processed with the Leica Application Suite. Alternatively, samples were analyzed using the Leica MZ APO stereomicroscope. Pictures were taken with a LEICA DFC 320 camera and imported into Adobe Photoshop CS4.

3.26.3 Light microscopy

GUS-stained samples were analyzed using the ZEISS Axioplan 2 microscope equipped with a LEICA DFC 320 camera and the SPOT Advance software version 4.6. RNA *in situ* sections were analyzed by differential interference contrast settings (DIC) using the ZEISS Axio Imager M1 upright microscope. Pictures were taken using a color camera from Visitron Systems equipped with the SPOT Advanced software version 4.6.

3.26.4 DIC microscopy

Seeds were dissected as described above (**3.11.3**). For DIC (differential interference contrast) microscopy seeds were directly transferred into a drop (~50 µl) of a modified Hoyer's solution (50 g chloralhydrate, 5 g glycerol, 12.5 ml water) (Bougourd et al., 2000) on a glass slide (Menzel). A coverslip (20 x 20 mm, Menzel) was put onto the seeds and fixed with Fixogum (Marabu). The samples were stored at 4°C over night or until DIC microscopy within the next three days. Microscopy was done on a spinning disc confocal microscope (Axiovert 200M, Carl Zeiss AG, Jena Germany) equipped with DIC optics; the system was controlled by the Meta Imaging Series software version 7.0.

3.26.5 Confocal microscopy

For confocal microscopy seeds were directly transferred into a drop of fixative (4% PFA, 5% glycerol in 1x PBS) with dye FM4-64 (5 µg/ml, Invitrogen) as counterstain. Seeds were covered with a coverslip and incubated for five to 15 min. Ovules were cracked by applying gentle pressure with the backside of forceps onto the coverslip thereby releasing the embryos (protocol provided by Dolf Weijers). The coverslip was fixed as described above and pictures were taken at the same day (within ~6 h). Microscopy was performed using a laser scanning confocal microscope (LSM510 Axiovert 200M, Carl Zeiss AG, Jena, Germany) controlled by the software ZEN 2008 SP1.1. Excitation of GFP and FM4-64 was achieved at 488 nm and 561 nm, detection at BP505-550 and LP 650, respectively. Pictures were processed using the Zeiss LSM Imager Examiner. For the construction of the 3D images the software Imaris x64 Version 7.3.0 was used.

3.26.6 Image processing

All pictures were processed using the application software Adobe Photoshop CS4 (or CS5) and Adobe Illustrator CS4 (or CS5).

3.27 Yeast one-hybrid (Y1H) screen

The screen was performed by Hybrigenics (France) using the bait sequences selected in our lab and is summarized briefly. The following *APL* promoter regions were used as DNA baits (numbers refer to the transcriptional start site +1 of *APL*, At1g79430): long bait -2587 to +356; 2943 bp; short bait: twice -140 to -1- fused by the *SmaI* restriction site. DNA baits were cloned into vector *pB301* (similar to Clontech vector system *pAbAi*, integrative vector) and integrated into the yeast genome (yeast strain YM955; selection on uracil lacking medium) upstream of the *Aur1-C* (aureobasidin A) reporter gene. The screen was performed against the random-primed *Arabidopsis thaliana* (Columbia) cDNA library. cDNA was generated from one week old seedlings (grown *in vitro*, 24°C, with light 16h/day) fused to the *Gal4* transcription activation domain (AD) in vector *pP6*. Selection of the mating reaction was performed on medium lacking leucine and uracil,

supplemented with aureobasidin A at a concentration of 150 ng/ml and 100 ng/ml for the long and the short bait, respectively.

For the long bait 68.2 million interactions were analyzed and 84 clones processed, for the short bait 71.8 million and 181 clones. Interactions were classified according to a statistical confidence score, the Predicted Biological Score (PBS®) defined by Hybrigenics, which ranks interacting proteins according to technical parameters such as the number of independent prey fragments. The statistical analysis takes into account additional information derived from all the screens performed for the same organism at Hybrigenics. The PBS (e-value) varies between 0 and 1 and gives the probability for the interaction to be non-specific. Thresholds were set to define 4 confidence categories: A (very high), B (high), C (good) and D (moderate). Interaction candidates are validated by extracting clones and retransformation into a yeast strain with an unrelated bait (p53-binding sequence) (in progress by Hybrigenics).

4. Results

The knowledge about factors which are important for the specification and differentiation of phloem tissue is limited. In fact, the MYB-like transcription factor APL, is still the only one known required for phloem specification and maintenance (Bonke et al., 2003). Thus, I aimed for the identification of novel phloem regulators by analyzing transcriptional regulation of *APL* and looking for its upstream regulators.

In advance, I would like to give a short overview on two gene models available for *APL*, raising the possibility of the presence of two APL isoforms.

4.1 Potential APL protein isoforms

Two gene models are annotated for *APL* (At1g79430.1, isoform 2; At1g79430.2, isoform 1; gene model derived from TAIR (www.arabidopsis.org); definition of isoforms derived from UniProt, www.uni.prot.org). Both isoforms share the same transcriptional start site but differ in their length of the 5'UTR and number of exons due to alternative coding regions for exon 1 created by alternative splicing (intron retention) (www.uniprot.org/uniprot/Q9SAK5) (Fig. 4.1 A). In eukaryotes, alternative splicing of pre-mRNAs creates an additional way for post-transcriptional gene regulation thereby generating more than one mRNA isoform. The subsequent changes of transcript sequence could affect protein sequence and functionality, introduce premature termination codons encoding truncated proteins or leading to degradation of the mRNA isoform by nonsense-mediated RNA decay (NMD) (see e.g. (Simpson et al., 2010)) as well as regulate the abundance of functional transcripts by the mechanism of regulated unproductive splicing and translation (RUST) (Filichkin et al., 2010; Lareau et al., 2007). In plants, about 42% of genes are currently estimated to undergo alternative splicing (Filichkin et al., 2010).

The first ATG of isoform 1 is located at position +72 referring to the transcriptional start site +1 (exon 1: +72 to 246) which is fused to exon 2 (exon 2: +337 to 413) upon splicing; the transcript encodes a final protein of 358 amino acids. In isoform 2 the first ATG starts at position +357 (exon 1: +357 to 413) encoding a final protein of 293 amino acids. In the gene model of isoform 2, the first possible intron is not spliced (intron retention)

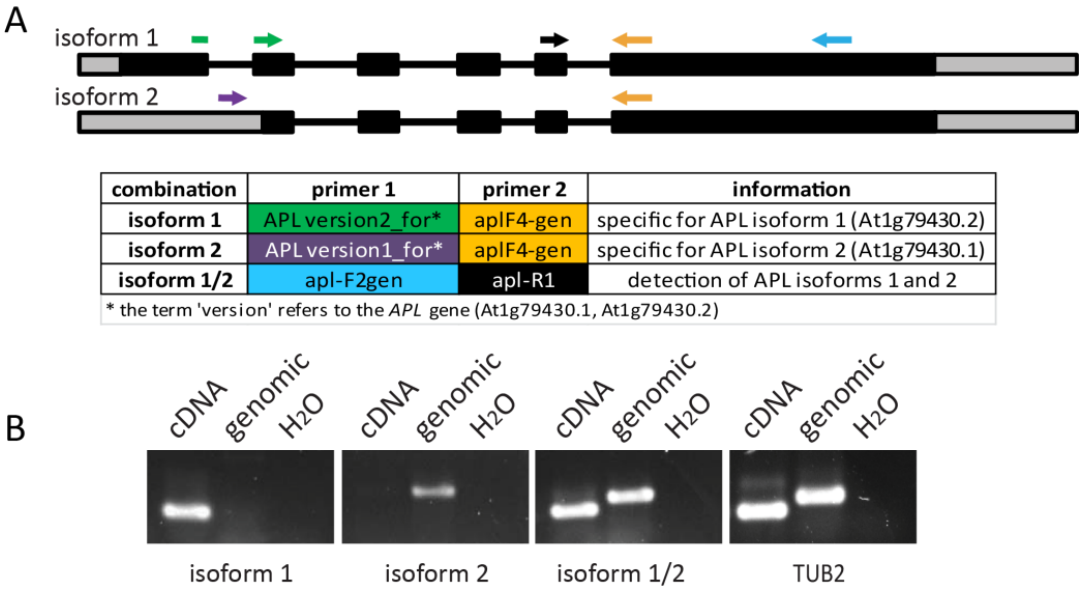

combination	primer 1	primer 2	information
isoform 1	APL version2_for*	aplF4-gen	specific for APL isoform 1 (At1g79430.2)
isoform 2	APL version1_for*	aplF4-gen	specific for APL isoform 2 (At1g79430.1)
isoform 1/2	apl-F2gen	apl-R1	detection of APL isoforms 1 and 2

* the term 'version' refers to the *APL* gene (At1g79430.1, At1g79430.2)

Fig. 4.1: Potential APL isoforms. A) Protein coding gene models (derived from TAIR) are shown for potential APL isoform 1 (At1g79430.2) and isoform 2 (At1g79430.1), respectively. Grey blocks indicate 5'UTR and 3'UTR regions, black boxes exons, and black lines introns. Arrows indicate *APL* isoform-specific primer combinations. The color code corresponds to the different primers in the description. **B)** PCR on cDNA and genomic DNA from wild-type plants using *APL* isoform-specific primer combinations show that *APL* isoform 1 is the predominant form. A transcript specific for isoform 2 was not detectable. A primer combination detecting both isoforms (isoform 1/2) and β-tubulin (TUB2) served as control.

thereby altering the open reading frame (ORF). The first possible exon is 'skipped' as well as 20 bp of exon 2 of isoform 1, and translation starts at the first ATG in frame at position +357. Thus, isoform 2 is predicted to be encoded by 5 exons and isoform 1 by 6 exons, respectively. The missing amino acid residues of isoform 2 (1-65 aa in isoform 1) include part of the predicted helix-turn-helix (HTH) MYB-type domain (31-91 aa in isoform 1) and part of the HTH DNA-binding region (62-87 aa in isoform 1) (see Fig. 4.12) which questions its capacity to act as a transcription factor. The residual features (exons, introns, 3'UTR) are predicted to be identical for both isoforms. Analysis of the APL amino acid sequence of isoform 1 with a program able to predict coiled-coil domains (Lupas et al., 1991) identified a coiled-coiled region of approximate 24 residues present in both isoforms, providing a potential protein interaction site (Bonke et al., 2003) (Fig. 4.12). Annotations of *APL* have already been described by Bonke and co-workers (Bonke et al., 2003).

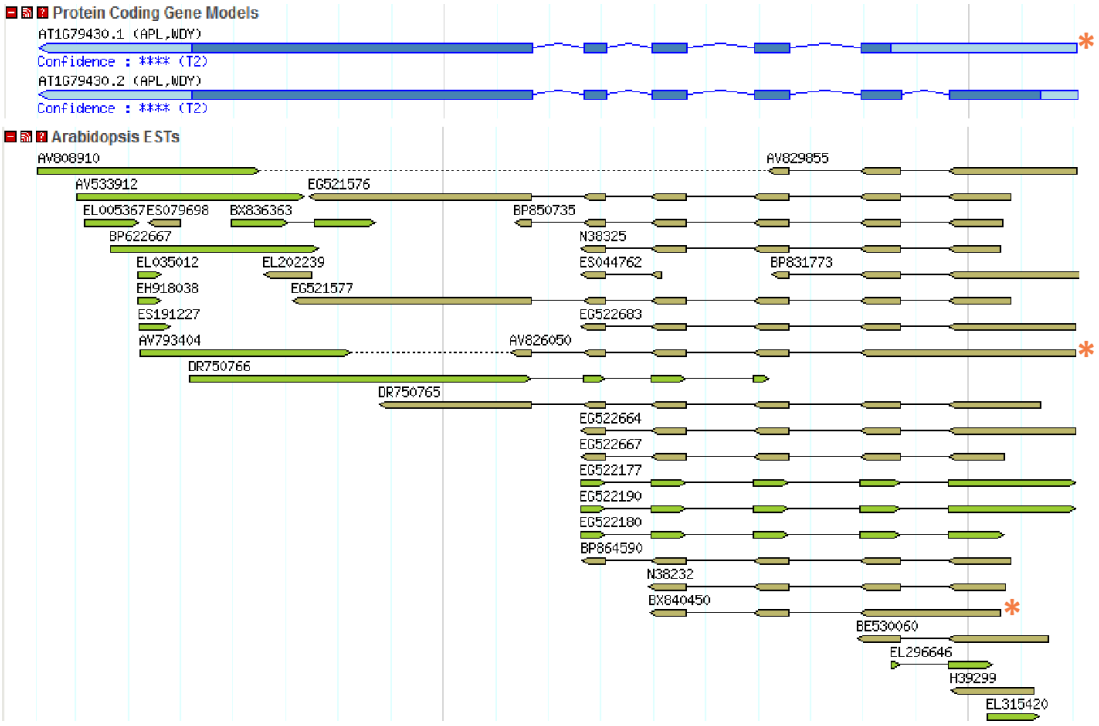

Fig. 4.2: ESTs of potential APL isoforms. Based on ESTs, APL isoform 1 (At1g79430.2) is the predominant form. The protein coding gene model of isoform 2 (At1g79430.1) and the corresponding ESTs are marked with an asterisk. Models are shown with the 5'UTR on the right side. Scheme derived and modified from TAIR; www.arabidopsis.org.

As isoform 2 differs in its N-terminal region affecting the DNA binding motif, a functional difference is possible. The coiled-coil domain would not be affected in isoform 2 and, thus, could alter binding affinities to DNA of potential protein interaction partners (e.g. a hypothetical APL isoform1/2 heterodimer) with impact on transcriptional regulation of their target genes.

The presence of isoform 1 is strongly supported by the collection of ESTs from the *APL* locus presented at TAIR. There are 17 EST-tags corresponding to the spliced mRNA variant encoding isoform 1 and two EST-tags for isoform 2 (Fig. 4.2). RT-PCR using isoform-specific primer combinations on cDNA from wild-type plants showed that isoform 1 is indeed the dominant form (Fig. 4.1 A and B). The PCR reaction using a primer covering the splice-site of isoform 1 only yielded in a PCR product using cDNA as a template but not using genomic DNA, as expected. The primer specific for isoform 2 anneals to the intron, which is spliced in isoform 1. A product specific for isoform 2 was not obtained using cDNA as a template but only when genomic DNA was used. Still, alternative splicing could be regulated in a cell- and tissue-type specific manner

influenced by growth conditions and/or the developmental stage. Thus, individual mRNA isoforms could be under-represented in RNA collected from whole seedlings but still be functionally significant.

4.2 Analysis of the *APL* promoter and the identification of potential phloem regulators

The approach started with the characterization of the *APL* promoter by analyzing different lines harboring T-DNAs inserted into the *APL* promoter. In addition, *APL* promoter fragments were tested for their ability to regulate reporter gene activity and to complement the previously described seedling-lethal *apl-1* mutant (Bonke et al., 2003). Based on the information gained about different promoter regions, a yeast one-hybrid (Y1H) screen was performed to isolate potential *APL*- and, thus, phloem regulators.

4.2.1 Analysis of *APL* promoter T-DNA lines

Four lines carrying individual T-DNAs evenly distributed in the promoter region were available from the SALK-collection (Alonso et al., 2003). The insertions were verified by PCR on genomic DNA, homozygous lines were produced and the exact position of the T-DNA was determined by sequencing. The lines harbored the T-DNA at following positions in basepairs (bp) upstream of the transcriptional start site (+1) of *APL*: -396, -1146, -1816, and -2784 (Fig. 4.3 A).

All lines homozygous for the insertion grew without apparent growth alterations and were completely fertile (Fig. 4.3 B). cDNA from either leaves or seedlings were produced and *APL* mRNA accumulation was analyzed by semi-quantitative RT-PCR (primer combination AW for isoform 1/2, see Fig. 4.1).

APL transcription in lines -1146 and -1816 were strongly reduced indicating that regulatory promoter elements for enhanced expression were affected by the insertions (Fig. 4.3 C). The reduction of *APL* transcription was less pronounced in a line with an insertion further downstream at position -396 suggesting that the promoter elements present within the T-DNA might reactivate transcription (Ulker et al., 2008). As line -

2784 did not show a reduction in *APL* transcript accumulation, I assume that all essential promoter elements are downstream of the insertion site.

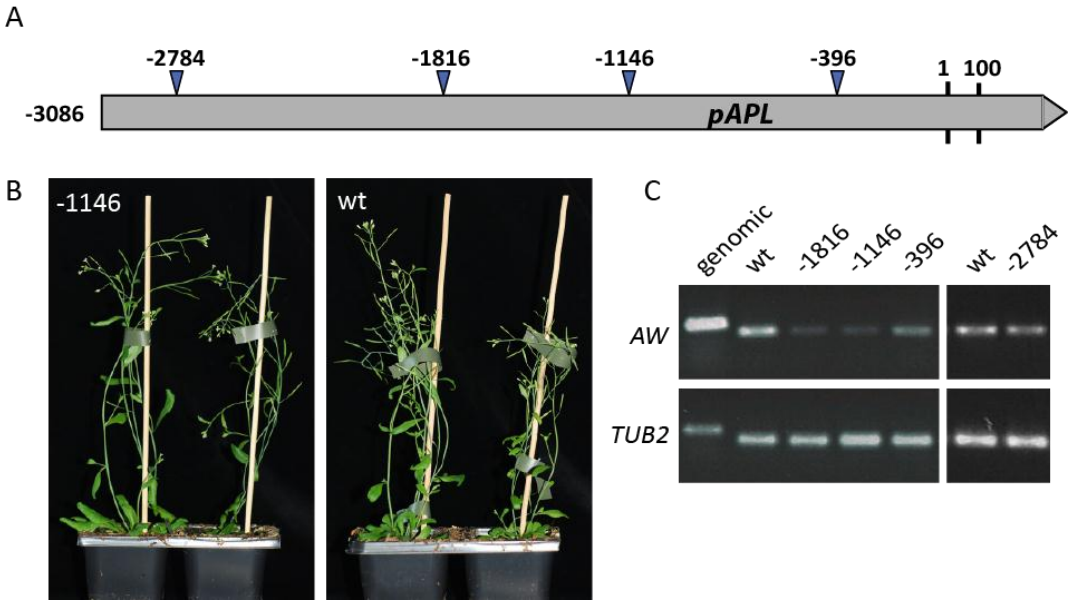

Fig. 4.3: Strong reduction of *APL* expression in T-DNA insertion lines does not cause obvious defects in plant development. A) Schematic view of T-DNA insertion sites in the *APL* promoter upstream of the transcriptional start site which is marked by '1'. **B)** Wild-type-like growth despite reduced *APL* expression; two plants of line -1146 are shown in comparison to wild-type (wt). **C)** Semiquantitative RT-PCR on cDNA from T-DNA insertion lines shows reduced *APL* expression in lines -1816, -1146, and -396 in comparison to wild-type (wt); primer combination AW was designed to detect the wild-type *APL* allele (isoform 1/2); see Fig 4.1). *APL* transcript accumulation in line -2784 is comparable to wt. β-tubulin (*TUB2*) was used as a reference gene; genomic DNA served as size control.

In summary, despite strong reduction of *APL* transcription in some lines, plants developed in a wild-type like manner suggesting that plants are quite robust towards a reduction in *APL* transcript levels.

4.2.2 Analysis of *APL* promoter fragments driving the *GUS* reporter

To further investigate the importance of different promoter regions, a series of *APL* promoter deletion constructs were produced driving the *GUS* reporter gene. The following promoter lengths referring to the transcriptional start site were used: -3086, -2587, -1761, -755, -140, -44, and +45 (Fig. 4.4 A). As the 5'UTR might contain motifs required for gene expression and one cannot exclude the presence of two *APL* isoforms (see **4.1**), the *APL* promoter cloned to drive reporter genes always included the long 5'UTR region of isoform 2 (At1g79430.1; +356). The *APL* 3'UTR region was cloned downstream of the GUS open reading frame (293 bp of the genomic sequence following

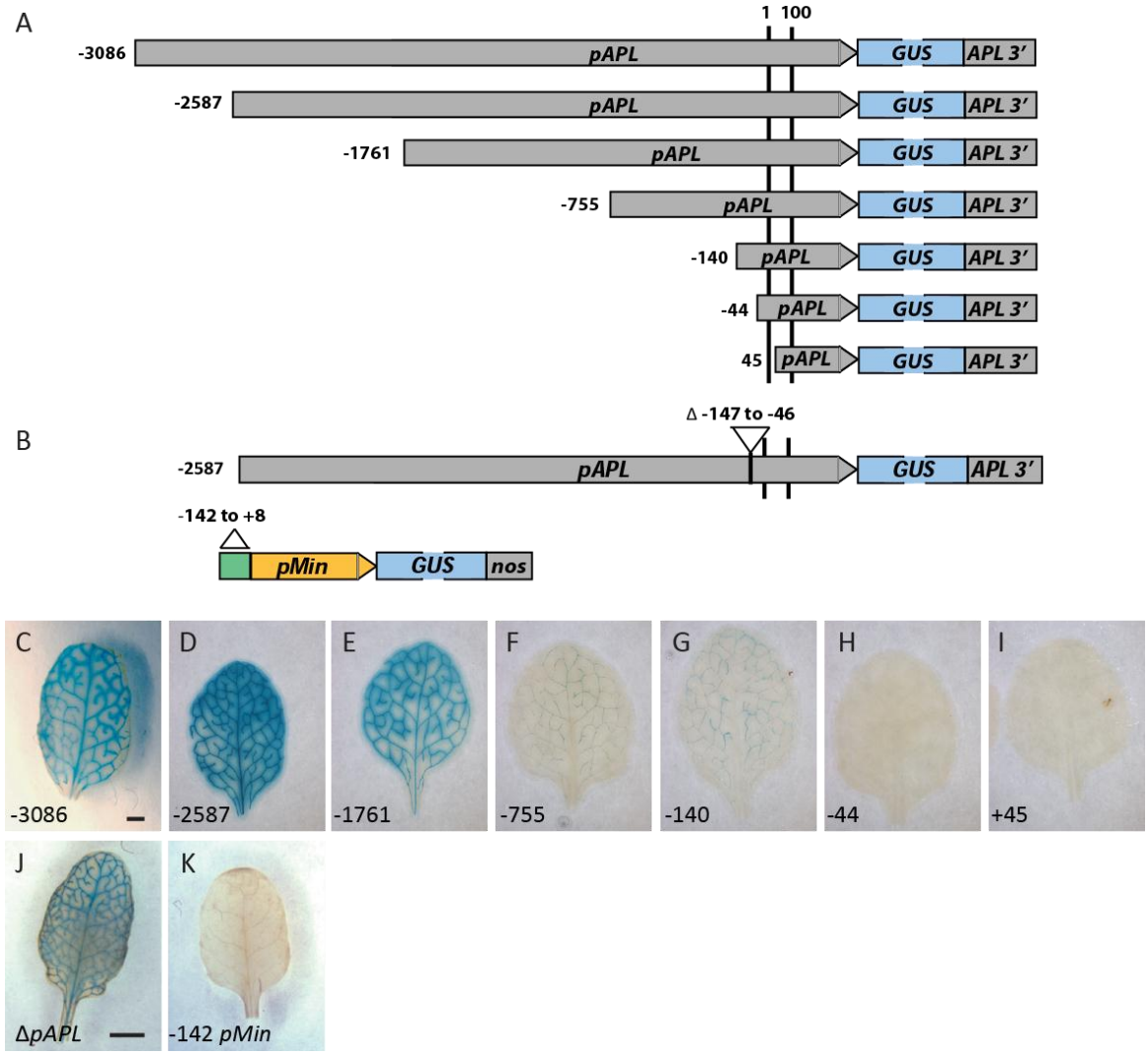

Fig. 4.4: *APL* promoter fragments show different *GUS* activation potential. **A)** Scheme of *APL* promoter fragments (*pAPL*) fused to the *GUS* reporter. Numbers indicate length of the promoter upstream referring to the transcriptional start site marked by '1'. The *APL* 3'UTR (*APL 3'*) was cloned downstream of the GUS open reading frame. **B)** Scheme of the constructs used to test the features of the vascular-specific motif. Region -147 to -46 was deleted from the -2587 construct shown in (A). Region -142 to +8 was cloned upstream of the minimal promoter (*pMin*) derived from the promoter of the Cauliflower mosaic virus transcript 35S which, in this case, drives the GUS reporter gene (*nos*, *nos terminator*). **C-I)** GUS-stained leaves of a representative T1 plant of line -3086 (C) and of homozygous single copy plants for lines -2587 (D), -1761 (E), -755 (F), -140 (G), -44 (H), and +45 (I) are shown. **J-K)** GUS-stained leaves of a representative T1 plant is depicted for construct Δ-147 to -46*pAPL* (J, Δ*pAPL*) and -142 to +8 *pMin* (K, -142 *pMin*), respectively. See text for details. Scale bars: 1mm.

the stop codon). The -3086 construct included 83 bp of the 3'UTR of the next gene upstream of *APL* (At1g79440, *SUCCINIC SEMIALDEHYDE DEHYDROGENASE*). All plasmids were transformed into wild-type plants and, subsequently, reporter gene activity was analyzed.

Homozygous single copy lines were generated and one representative line was selected for each of the promoter fragments, -2587, -1761, -755, -140, -44, and +45, respectively, for further analysis. One representative line -3086, from which no single copy line could

be generated, was analyzed as a heterozygous double copy line in T1, instead of a homozygous single copy line in T2.

Analysis of rosette leaves from adult plants showed comparable staining intensities for

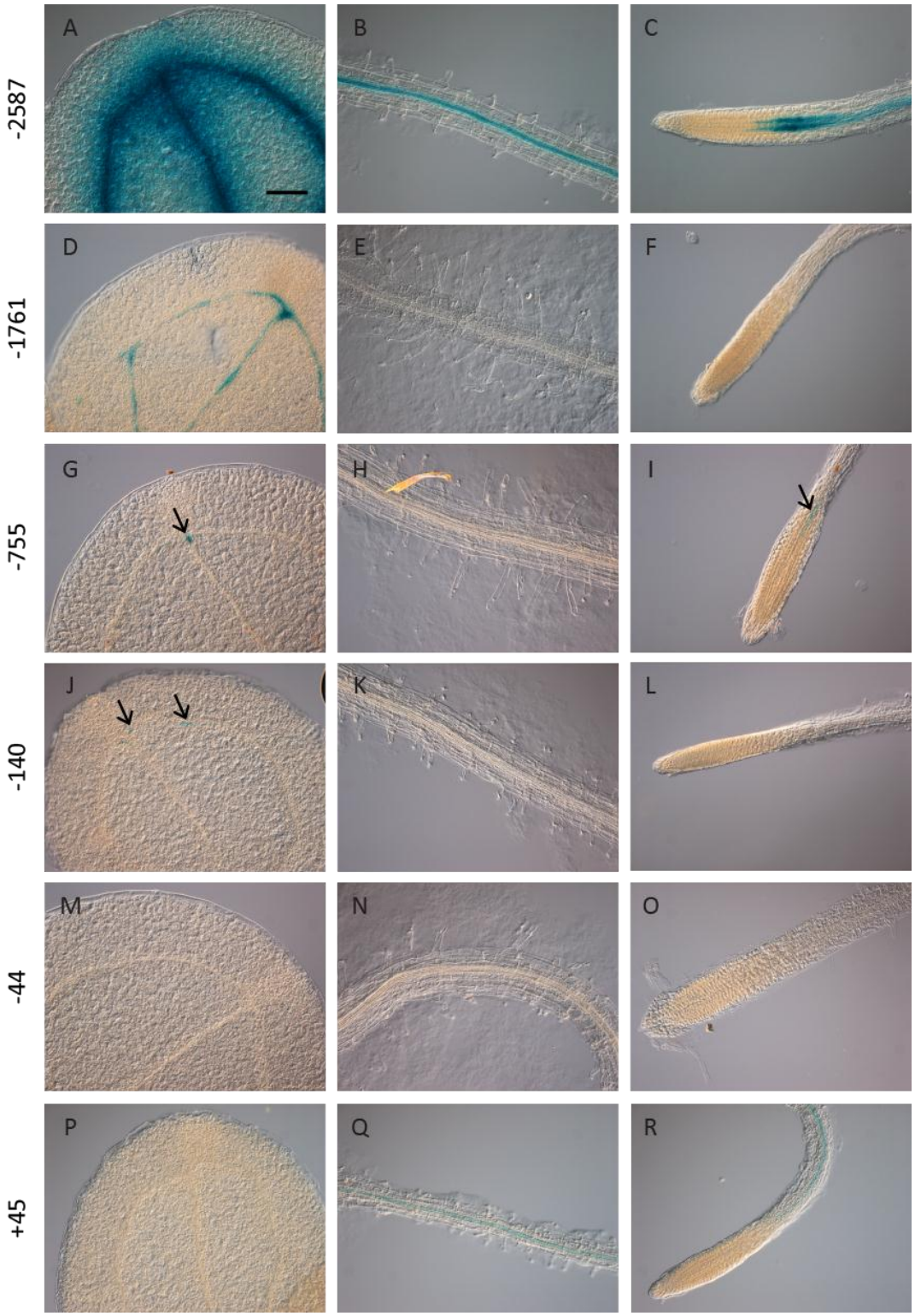

Fig. 4.5: Promoter *APL* fragments show different *GUS* activation potential in seedlings. Seedlings of homozygous single copy lines harboring the distinct *pAPL::GUS* deletion constructs were GUS-stained five days after germination. Cotyledons (A, D, G, J, M, and P), roots (B, E, H, K, N, and Q), and root tips (C, F, I, L, O, and R) are shown for each line. Scale bar: 100 µm.

lines with promoter fragments -3086 and -2587 (Fig. 4.4 C and D). GUS activity in line -1761 was slightly reduced (Fig. 4.4 E) and hardly detectable in lines -755 and -140, although they still displayed a vascular specific activity (Fig. 4.4 F and G). Lines carrying constructs -44 and +45 lacked any specific staining (Fig. 4.4 H and I). In addition, seedlings were stained five days after germination (except for line -3086) confirming the tendency of reduced promoter activities at both developmental stages (Fig. 4.5). Cotyledons showed strongly reduced and partially patchy activity in the vasculature in line -1761 (Fig. 4.5 D). Small patches of GUS activity were observed in veins of cotyledons in lines -755 and -140 (Fig. 4.5 G and J), whereas lines -44 and +45 (Fig. 4.5 M and P) lacked any staining in cotyledons. Reporter activity was rarely detectable within roots of seedlings of lines -1761 and -755 (Fig. 4.5 E, F, H, and I), and not detectable in lines -140 and -44 (Fig. 4.5 K, L, N and O). Only lines -2587 and +45 (Fig. 4.5 B, C, Q to R) displayed GUS staining within mature roots. Due to the intense staining of the vasculature of line -2587 throughout all organs analyzed, the promoter was regarded to activate expression similar to the endogenous *APL* promoter. In case of line +45 one could speculate that expression is reactivated e.g. if a motif inhibiting expression in roots is localized within region -44 and +45.

Taken together, gradual shortening of the *APL* promoter lead to a gradual reduction of GUS reporter gene activity within the vasculature of adult leaves and seedlings. This indicates that several enhancer elements are distributed along the whole promoter region, concentrated within region -2587 to -755. In addition, motifs conferring vascular specific expression are located very close to the transcriptional start site.

4.2.3 Analysis of the minimal promoter region mediating vascular-specific reporter gene activity

To analyze the role of the region close to the transcriptional start site which mediated vascular-specific expression, the region -147 to -46 (102 bp) was deleted from the -2587 construct (Fig. 4.4 B). GUS staining intensities and patterns in leaves of 20 independent T1 (20/20) plants resembled those observed for lines carrying the -2587 construct (Fig. 4.4 J).

The potential of this region to drive vascular-specific *GUS* expression was also tested by cloning the promoter fragment -142 to +8 to a minimal promoter (*pMin*) derived from the promoter of the Cauliflower mosaic virus transcript 35S (Fig. 4.4 B) (Odell et al., 1985). In none of the 20 independent T1 lines the fragment was sufficient to activate GUS expression to detectable levels (Fig. 4.4 K); control lines carrying the *pMin* construct only did not show staining either (not shown).

Both results indicate that enhanced gene expression and vascular specificity are not exclusively mediated by region -140 to +44.

4.2.4 Complementation of the *apl-1* mutant requires *pAPL* promoter fragments with high activity

It was interesting to test to which extent the analyzed promoter regions are able to complement the *apl-1* phenotype when driving the *APL* gene. Thus, constructs were generated comprising the *APL* genomic region (including all introns) plus the upstream sequences of different lengths comparable to the *pAPL::GUS* deletion series, -3086, -2587, -1747, -755, -140, and -26, respectively. All plasmids were transformed into *apl-*

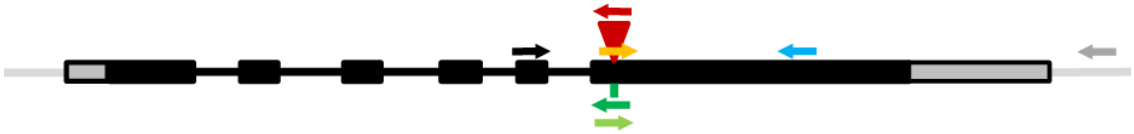

combination	primer 1	primer 2	information
AW	apl-F2gen	apl-R1	detection of *APL* wt allele
A1	apl-F1	apl-R1	detection of *apl-1* allele(Bonke et al. 2003)
A2	apl-2rev	apl-R1	detection of *apl-2* allele (*Bpu1102 I* digest of *apl-2* derived PCR product)
A1c	APLfor20	APLrev21	detection of endogenous wt *APL* locus in *apl-1* complemented plants
A2c	apl2-for	APLrev21	*apl-2* versus *APL* wt in *apl-2* complemented plants (*Mls I* digest of wt *APL* derived PCR product)

Fig. 4.6: Primer combinations for detection of the *APL* alleles. Protein coding gene model according to TAIR for At1g79430.2; grey blocks indicate 5'UTR and 3'UTR regions, black bars exons, black lines introns, and grey lines regions up- and downstream of *APL*. Red triangle marks the *En-1* insertion site and the green line the *apl-2* mutation. Arrows indicate primer combinations to detect and differentiate between *APL* wild-type (wt), *apl-1*, and *apl-2* alleles, respectively (not to scale). The color code corresponds to the different primers in the description.

1/+ plants. T1 plants positively selected for the presence of the constructs, were analyzed for homozygosity of *apl-1*.

One could easily distinguish wild-type and *apl-1* carrying plants by PCR on genomic DNA detecting the *En-1* transposon (primer pair A1, Fig. 4.6) (Fig. 4.7 A). The differentiation between heterozygous and *apl-1* homozygous plants required further analysis. First, a primer was designed which binds the *APL* sequence not present in the transformed plasmids allowing amplification of the endogenous *APL* wild-type sequence only (primer pair A1c, Fig. 4.6). In addition, as PCRs using primer pair A1c on DNA from *apl-1* homozygous seedlings usually gave rise to a (weak) wild-type-like band due to the excision of the *En-1* transposon (see **4.3.5**), an internal control was used to compare PCR product intensities (primer pair LINC: LINC2for4/ LINC2rev4, see Tab. 3.2). In mixed PCR reactions containing both primer pairs wild-type and heterozygous plants gave rise to PCR products of similar intensities. PCR on DNA from homozygous *apl-1* seedlings always produced a stronger LINC-specific band (Fig. 4.7 A).

As a result, only constructs with promoter regions -3086 and -2587 were able to complement the *apl-1* phenotype in ~10% of plants harboring the construct (Fig. 4.7 B).

A

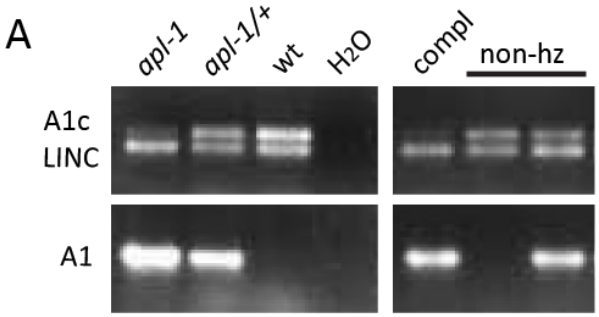

B

pAPL	hz (%)	total
-3086	7 (10)	70
-2587	10 (11)	90
-1747	0	125
-755	0	62
-140	0	30
-26	0	40

Fig. 4.7: 2587 base pairs of the *APL* promoter region are required to rescue *apl-1* seedlings. A) Example of the genotype analysis of potentially complemented *apl-1* plants. A mixed PCR reaction was performed using primer combinations for amplification of the endogenous *APL* locus (A1c) and for the *LITTLE NUCLEI 2* (LINC) locus as a reference, respectively. In combination with a PCR reaction detecting the *apl-1* allele (A1), a clear differentiation between all genotypes (*apl-1*, *apl-1/+*, wild-type wt) was possible. DNA for the respective genotypes served as controls; complemented *apl-1* plant (compl), non-homozygous sister plants (non-hz). **B)** Complementation of *apl-1* seedlings was achieved by -3086 and -2587 *APL* promoter (*pAPL*) regions fused to the *APL* genomic sequence, respectively. A region of -1747 or shorter was not sufficient, indicating the presence of essential elements between -2587 and -1747 nucleotides upstream of the transcriptional start site. Length of *APL* promoter fragments, total number of tested seedlings per construct (total), and numbers of identified *apl-1* homozygous seedlings (hz) are indicated; percentage of *apl-1* homozygous plants in brackets.

As a mixture of wild-type and *apl-1/+* plants (1:2 ratio) were transformed, ~16.7% of *apl-1* homozygous plants were expected in case of complementation (2/3 x 1/4 = 1/6 ~0.167). Thus, the yielded complementation value is lower than expected. Possibly, selection for the presence of the construct did not allow the growth of *apl-1* seedlings with lower *APL* expression efficiency. Interestingly, the promoter regions sufficient for complementation were the ones of comparable size conferring strong GUS activity in the *pAPL::GUS* deletion series (see **4.2.2**). A region of -1747 or shorter was not sufficient for complementation indicating the presence of essential promoter elements between -2587 and -1747 nucleotides upstream of the transcriptional start site.

Thus, essential promoter elements are present within region -2587 and -1747 upstream of the transcriptional start site, possibly regulating features like onset, timing, and/or efficiency of *APL* expression required for complementation.

4.2.5 Identification of potential transcriptional regulators upstream of *APL*

Based on the information about the *APL* promoter a Y1H screen was performed in order to identify direct upstream regulators of *APL* transcription. In this approach, a cDNA library encoding for candidate proteins fused to a transcriptional activation domain (AD) is expressed in a yeast strain, representing the prey. A different strain contains the DNA bait, the sequence of interest fused to a reporter gene (e.g. a nutritional marker allowing growth on media lacking an essential amino acid). Expression is activated upon interaction between DNA and prey proteins allowing the selection of interacting candidates (Deplancke et al., 2004).

4.2.5.1 Design of bait sequences and performance of the Y1H screen

Two different sequences were chosen to be used as baits, a long and a short one, respectively. The long promoter region (-2587 to +356; 2943 bp) should contain all essential motifs required for wild-type like *APL* expression (see **4.2.4**). Sequences of comparable lengths have been used successfully before in Y1H screens (Brady et al., 2011; Deplancke et al., 2004). To select for potential regulators more specifically, a

second bait was designed consisting of two repeats of the region identified to contain the minimal elements mediating vascular specificity (region -140 to -1; see **4.2.2**).

The subsequent steps (e.g. cloning of the bait and prey, selection, etc.) were performed by the company Hybrigenics. The screen was performed against a random-primed cDNA library of *Arabidopsis thaliana* seedlings (1 week old). 68.2 million and 71.8 million interactions were analyzed and 94 and 181 clones processed after the selection for the long and the short bait, respectively. Some of the candidate interaction proteins were represented by more that one clone. Interaction candidates were ranked according to a statistical confidence score, the Predicted Biological Score (PBS) as defined by Hybrigenics, which is computed as e-value (0 to 1). Thresholds were attributed to the e-values and four categories of confidence in the interaction were defined (A, very high; B, high; C, good; D, moderate) (see also **3.27**). Upon receiving the list of interaction candidates I continued with a first evaluation.

4.2.5.2 Evaluation of potential *APL* regulators

The long bait resulted in three candidates (15.8%) for category A, one (5.3%) for B, and one (5.3%) for C; the short bait resulted in one candidate (3.2%) for category A, four (12.9%) for B, and one (3.2%) for C. Category D contained a mixture of false-positive candidates as well as candidates with a reduced chance for effective binding due to either low representation of the mRNA in the library, prey folding, or prey toxicity in yeast - all of which will negatively influence the confidence score. However, true *APL* regulators might still be among those candidates. The majority of interactions fall into category D (25 candidates (80.6%) with the short bait; 14 (73.7%) with the long bait). Only candidates with a predicted localization within the nucleus (four candidates) were considered to be most interesting with the highest chance to function as transcriptional regulator. In total, 13 candidates were selected for further validation, three identified with both baits, and five with the long or the short bait only (Tab. 4.1). One clone per interaction candidate will be extracted and retransformed into a yeast strain with an unrelated bait (p53- binding sequence) to determine unspecific binding properties (performed by Hybrigenics; in progress).

Among all candidates, the members of the BASIC PENTACYSTEINE (BPC) family of transcription factors appeared to be most interesting as they were found more often, namely in categories A (BPC1), B (BPC2), and C (BPC4), respectively. Especially BPC1 was represented by several clones, both with the long (5 clones) and short (8 clones) bait (Tab. 4.1). The BPC factors belong to the family of *BARLEY B RECOMBINANT / BASIC PENTACYSTEINE* (*BBR/BPC*) present throughout land plants. BPC proteins from different species were shown to bind specifically to GA-repeat elements (Meister et al., 2004; Sangwan and O'Brian, 2002; Santi et al., 2003). Thus, I analyzed the *APL* promoter for potential *BPC* binding sites and performed also a search for *cis*-binding elements for the other candidates.

		Y1H category/number of clones	
	GO molecular function/biological process (TAIR)	long bait	short bait
BPC1, At2g01930	specific transcriptional repressor activity, transcription factor activity	A/5	A/8
unknown, At3g57420	unknown	A/6	B/6
unknown, At4g29780	unknown	A/9	n
ABCG25, At1g71960	ATPase activity, abscisic acid transport	D/1	B/7
IPCS1, At3g54020	sphingolipid biosynthetic process	B/3	n
BPC2, At1g14685	transcription factor activity	n	B/3
IPCS2, At2g37940	sphingolipid biosynthetic process	n	B/2
HB-1, At1g28420	transcription factor activity	C/2	n
BPC4, At2g21240	transcription factor activity	n	C/2
ERF5, At5g47230	transcription activator activity, transcription factor activity	D/1	n
NTF2, At3g25150	nucleocytoplasmic transport	D/1	n
GRL, At2g35110	transcription activator activity	n	D/1
KU70, At1g16970	DNA repair, response to heat, telomere maintenance	n	D/1

Tab. 4.1: Potential *APL* regulators. Potential *pAPL* interacting proteins obtained for the long and the short bait are listed according to their occurence in confidence categories A to D (A, very high; B, high; C, good; D, moderate) including the number of clones per bait. For category D only proteins with predicted abundance in the nucleus or nucleic acid binding functions were included. n, not obtained with the respective bait. Orange, obtained with both baits; yellow, with the long bait only; green, with the short bait only. Abbreviations: BPC, basic pentacysteine; ABCG25, ATP-binding cassette family G25; IPCS, inositol phosphorylceramide synthase 1; HB-1, homeobox-1; ERF5, ethylene responsive element binding factor 5; NTF2, nuclear transport factor 2; GRL, gnarled. GO, gene ontologies (GO) functions and biological processes were retrieved from TAIR and partially shortened.

4.2.6 Potential transcription factor binding sites in the *APL* promoter

Transcription factors exert their functions on target genes by binding specific DNA sequences with their distinct DNA binding domains. Several databases have been generated providing information on transcription factors and *cis*-regulatory motifs (see e.g. (Qu and Zhu, 2006; Riechmann, 2002)). To reveal if there is a correlation between the motifs distributed on the *APL* promoter and the observations made in the analysis of the *APL* promoter also in context of the potential *APL* regulators, the *APL* promoter sequence was analyzed *in silico*.

	pAPL (3442 bp) up to ATG of At1g79430.1	*apl-1* complementation	Y1H short bait	5'UTR (for At1g79430.2)	up to ATG At1g79430.1
Family	**-3086 to +356**	**-2587 to -1747**	**-140 to -1**	**+1 to +71**	**+72 to +356**
O$INRE	3	1			
O$MTEN	2				2
O$PTBP	10				1
O$TF2D	1				
O$VTBP	44	9	2		1
P$AHBP	43	15	1		1
P$AREF	1				
P$BRRE	1				
P$CAAT	5	1			1
P$CCAF	4	2			
P$CDC5	3				3
P$CE1F	3				1
P$CGCG	1				1
P$CNAC	7	2			
P$DOFF	25	9	2		
P$DREB	2				1
P$EINL	3				
P$EREF	1				
P$GAGA	17 (12 P$BPC.01)		3 (2 P$BPC.01)	13 (9 P$BPC.01)	
P$GAPB	4	2			
P$GBOX	4	1	1		
P$GTBX	27	8	1		
P$HEAT	1			1	
P$HMGF	7	2			
P$IBOX	12	3	2		
P$IDDF	1				
P$L1BX	23	8			2
P$LEGB	6	1			
P$LREM	9	2			
P$MADS	24	6			3
P$MIIG	2				1
P$MSAE	3				
P$MYBL	22	5	3		1
P$MYBS	16	3			
P$MYCL	4	1			
P$NACF	2				1
P$NCS1	12	4			1
P$NCS2	2				
P$OCSE	8	2	1		
P$OPAQ	6	1			
P$PREM	1				1
P$PSRE	2	1			1
P$ROOT	1				1
P$SALT	1				
P$SBPD	1	1			
P$SEF4	2	1			
P$SPF1	5	1			
P$STKM	4	1			
P$SUCB	12	8			
P$TCPF	3	1			1
P$TEFB	2				
P$TELO	3		1		
P$WBXF	4	1			

P$AHBP	Arabidopsis homeobox protein
P$EREF	Ethylene response element factor
P$GAGA	GAGA elements; matrix: P$BPC.01, Basic pentacysteine proteins
p$MYBL	MYB-like proteins
P$MYBS	MYB proteins with single DNA binding repeat

Tab. 4.2: Promoter motifs present in a region between -3086 to +356 at the *APL* locus referring to the transcriptional start site. List of all elements in the most left column and elements within indicated regions are shown. Element families conferring potential binding sites for candidates obtained from the yeast one-hybrid screen (HB-1, green; BPC factors, yellow; ERF-5, blue) and for APL itself (orange) are highlighted. Match Summary of motif families as retrieved with the Genomatix MatInspector software. O$, general core promoter elements; P$, plant specific elements. Descriptions of Genomatix motif families highlighted are described below (shortened from Genomatix); information concerning residual motif families and matrices can be obtained upon request (not publically accessible).

For *in silico* analysis the *APL* promoter sequence spanning region -3086 to +356 was used for motif search using the Genomatix software MatInspector (www.genomatix.de). Tab. 4.2 shows a summary of all motif families found within the promoter sequence as well as the motifs present within the promoter regions used for different experiments.

As expected, potential motifs were densely distributed all over the promoter creating multiple possibilities for various transcription factors to bind to them. Which of these motifs play a role in regulating the target gene *in vivo* is influenced by the kind and quantity of transcription factors and other regulatory factors or RNAs present in different cells as well as enzymes altering transcription factor activities (e.g. protein modifications) or the chromatin state (see e.g. (Riechmann, 2002)). Concentrating on the motifs related to the isolated candidates (based on the description of the matrices used for the retrieval by the Genomatix software), most striking was the clustering of GA-repeat elements, the binding sites for the BPC factor family, within the 5'UTR (region +1 to +71) (GA repeat inverted in region +35 to +70: $(GA)_4AA(GA)_3TC(GA)_9$) (Tab. 4.2). In *Arabidopsis*, BPC factors bind to $(GA)_6$ and $(GA)_9$ repeats (Meister et al., 2004), and BPC1 in particular binds a purine-rich consensus sequence (RGARAGRRA) (Kooiker et al., 2005). It was shown that the soybean Class I BPC protein (GBP) binds to a GA-repeat in the 5'UTR of the soybean glutamine semialdehyde reductase (*GSA*) gene (Meister et al., 2004; Sangwan and O'Brian, 2002).

Thus, BPC factors might be indeed involved in the regulation of *APL*. In context of the vascular-specific element used for the Y1H screen (short bait, region -140 to -1) and for its potential to activate GUS expression cloned to the minimal promoter (region -142 to +8), it is interesting to mention that the 5'UTR was (largely) excluded. The short bait was still able to retrieve three BPC proteins with the presence of a short stretch of GA-repeats (region -66 to -53: $GA\text{-}C\text{-}(GA)_5$). Thus, additional GA-repeats within the 5'UTR might enable binding of additional, maybe other, BPC factors. Still, as construct -44 *pAPL::GUS* including the 5'UTR was not able to activate GUS expression to detectable levels the additional 5'UTR GA-repeats do not seem to have strong activating potential by themselves. At position -1500 to -1506 a $(GA)_3$ repeat is present as well. As the consensus sequence for BPC1 was not included in the matrix of Genomatix, a manual search located a BPC1 consensus sequence at -2604 to -2591, thus upstream of the construct successfully used for complementation of *apl-1* (*-2587 pAPL::APL*), and

therefore likely not being essential. Other BPC1 consensus sites overlapped with general BPC binding sites within the promoter.

Concerning other *APL* regulatory candidates with transcription factor activity, no clear correlations were obvious. There are several potential homeobox binding motifs (P$AHBP) conferring potential binding sites for HOMEOBOX-1 (HB-1) as well as one element specific for ETHYLENE RESPONSIVE FACTORS (ERF) factors (P$EREF; position -2694). In addition, potential MYB-binding elements (P$MYBL, P$MYBS) are widely distributed.

Taken together, the prevalence of several BPC binding sites especially in the 5'UTR of the *APL* promoter further supports a role of BPC factors in regulating *APL* transcription.

4.2.7 BPC transcription factors might be involved in *APL* regulation

In *Arabidopsis*, there are seven *BPC* genes (*BPC1-7*) (Meister et al., 2004) with *BPC5* being likely a pseudogene due to an in-frame stop codon (Meister et al., 2004; Monfared et al., 2011). The BPC proteins were classified into three groups with class I comprising BPC1, BPC2 and BPC3, class II BPC4, BPC5 and BPC6, and class III with the sole member BPC7 (Meister et al., 2004). Most *BPC* genes show a widespread expression pattern in the plant (including the vasculature) indicating a high level of redundancy (Meister et al., 2004; Monfared et al., 2011). Analysis of multiple *bpc* mutants suggested the BPC factors to be important for several processes that support normal growth and development being involved e.g. in patterning processes and regulation of cell growth (Monfared et al., 2011).

As different BPC factors (BPC1, BPC2, BPC4) were isolated in the Y1H screen I was interested to further elucidate the influence of the BPC factors on *APL* expression. As single mutants were known not to display obvious growth alterations (Monfared et al., 2011), I analyzed the *APL* transcript levels in the recently published higher order mutants, *bpc1-1 bpc2-1 bpc4-1 bpc6-1* (*bpc1246*) and *bpc1-1 bpc2-1 bpc3-1 bpc4-1 bpc6-1* (*bpc12346*), respectively (Monfared et al., 2011). Note that these mutants harbor mutations in the isolated BPC factors. The phenotypic appearance of the *bpc* mutants

corresponded to the description published. The quadruple *bpc 1246* mutant exhibited pleiotropic effects on vegetative and reproductive growth and had e.g. a bushy growth, reduced height, curled leaves, was largely infertile, and showed a delayed senescence. The additional loss of *BPC3* function ameliorated defects of the quadruple mutant like the strongly reduced fertility and it restored plant height (Fig. 4.8 A). *BPC3* was suggested to have, at least partially, antagonistic function to the other *BPC* genes (Monfared et al., 2011).

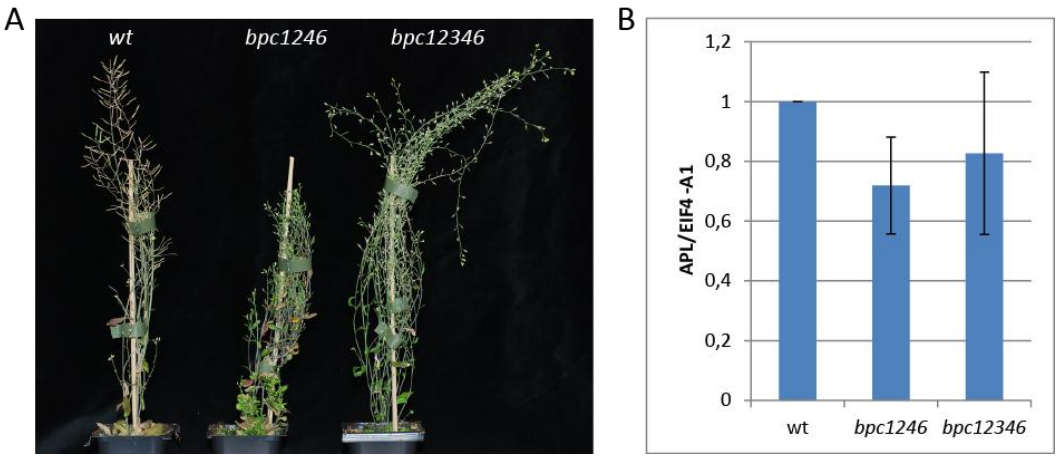

Fig. 4.8: *APL* expression in multiple *bpc* mutant background. A) *bpc1246* shows a more severe phenotype than *bpc 12346* (Monfared et al., 2011), both growing in a bushier way in comparison to wild-type (wt) plants and being severely affected in seed production. Two months old plants are shown. **B)** *APL* transcript levels are reduced in *bpc1246***.** *APL* transcript abundance of two biological replicates with four and two technical replicates each, respectively, were determined by qRT-PCR and normalized to the *Arabidopsis* eukaryotic translation initiation factor *EIF4-A1*. Mean relative expression levels are blotted against wild-type plants which were set to 1.

The cDNA of a mixture of leaves and SAMs of *bpc1246* and *bpc12346* in comparison to wild-type plants (about one month old) were prepared and the relative abundance of *APL* transcripts was determined by qRT-PCR. *APL* transcript levels of *bpc1246* plants were reduced to about 70% in comparison to wild-type. Despite the high standard deviation, there was also a tendency of reduced *APL* transcript levels in *bpc12346*, however, less pronounced than in *bpc1246* (Fig. 4.8 B). The rather slight reduction of *APL* transcript levels is in line with the lack of major defects in vascular patterning and structure of *bpc1246* inflorescence stems (Monfared et al., 2011). Phloem (vascular) defects might be observable in other organs or at higher resolution.

In summary, the BPC proteins are the first candidates for being direct regulators of *APL* expression. It was suggested that BPC factors act on a variety of genes in otherwise

unrelated processes, partially redundantly, and also in concert with other regulatory factors (Meister et al., 2004; Monfared et al., 2011). Based on the qRT-PCR results, *APL* could be among those target genes and being fine tuned by BPC factors. Lack of some of the BPC factors seems to result in rather small defects connected to vascular development, getting maybe more pronounced under specific growth conditions or developmental stages.

4.3 The *in vivo* luciferase-based mutagenesis screen and the analysis of the novel *apl-2* allele

4.3.1 *In vivo* luciferase-based screen for factors involved in vascular development

In order to identify novel key regulators involved in vascular development, with an emphasis on phloem differentiation and *APL* upstream regulators, a reporter gene-based mutagenesis screen was performed. Wild-type plants homozygous for the reporter gene *LUCIFERASE* (*LUC*) driven by the promoter of *APL* (*pAPL::LUC*) were mutagenized by EMS, introducing randomly distributed single point mutations throughout the genome (Kim et al., 2006). It was envisaged that each time a gene crucial for vascular development is affected, it will either directly or indirectly change *LUC*

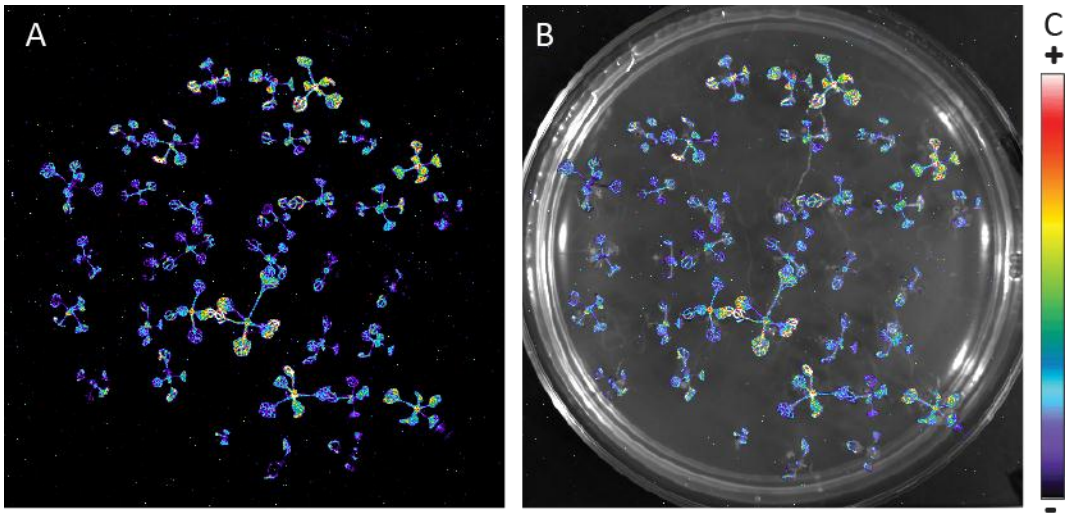

Fig. 4.9: Luminescence signal in *pAPL::LUC* homozygous wild-type plants. A-B) Detection of luminescence upon treatment with luciferin shows signal variations within homozygous *pAPL::LUC* plants; (A) shows the false color image and (B) the overlay with the bright field image. **C)** False color bar indicates signal intensities ranging from high (white) to low (black).

expression levels and consequently the LUC signal intensity. Similarly, it was reasoned that mutations in the promoter of the reporter construct will alter the signal intensity and allows the identification of important *APL* promoter elements.

As it was expected that mutations in regulators of vascular development cause seedling lethality, the progenies of single M1 plants were screened separately, to enable the identification of the mutation within the surviving sister plants.

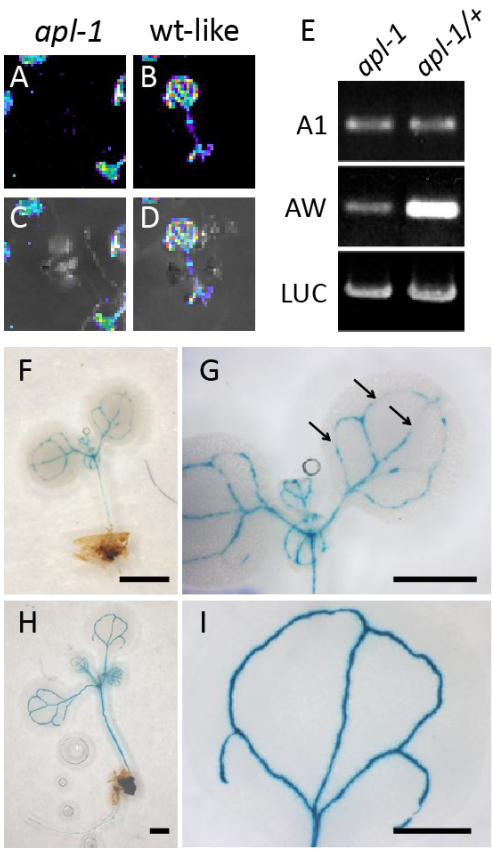

Fig. 4.10: Activities of reporters in *apl-1* background. A-D) *apl-1* homozygous plants (A) lack a detectable luciferase signal in comparison to wild-type (wt)-like plants (B); false color images (A, B) and overlay with bright field images (C, D) are shown. **E)** Genotyping of a phenotypic *apl-1* homozygous and an *apl-1/+* seedling; detection of the *apl-1 En-1* transposon (primer combination A1), wild-type *APL* gene (primer combination AW), and the *pAPL::LUC* construct (LUC). Primer combination AW gives rise to a background PCR product in *apl-1* homozygous plants likely due to *En-1* transposon excision events (see **4.3.5**). **F-I)** GUS-stainings of *pAPL::GUS apl-1* homozygous seedlings (F, G) show a patchy vein pattern (arrows in G) in contrast to wild-type –like plants (H, I); higher magnification of picture F and H are shown in G and I, respectively; scale bars: 1 mm in F and H; 0.5 mm in G and I.

4.3.2 Potential of the screen

Initially, wild-type seedlings carrying the reporter construct were tested for the general signal quality. Due to signal variations within homozygous *pAPL::LUC* populations (Fig. 4.9) the screen concentrated on isolating mutants with gross changes in signal intensities to avoid a high content of false positives among candidates.

Thus, I expected to isolate crucial factors with major impact on vascular development at early time points. In addition, plants with normal appearance and altered signal intensities were expected in case of mutations within crucial *cis*-regulatory elements in the *pAPL::LUC* reporter.

To further proof the potential of isolating vascular mutants, the *pAPL::LUC* reporter was introduced into the *apl-1/+* line by crossing. Plants homozygous for *pAPL::LUC* and displaying the *apl-1* phenotype showed

severely reduced signal intensities in comparison to sister plants, suggesting that respective mutants can be isolated by the chosen screening strategy (Fig. 4.10 A to D). The presence of the *pAPL::LUC* construct was confirmed by PCR on genomic DNA (primer combination LUCforNcoI and T7, Tab. 3.2) (Fig. 4.10 E; for primer combinations see also Fig. 4.6). GUS-stainings of *apl-1* mutants carrying the *-2587 pAPL::GUS* reporter (see **4.2.2**) showed a slightly patchy staining pattern likely due to the disturbed vascularization. In addition, in comparison to leaves of wild-type-like plants, GUS intensity was reduced but not absent suggesting a higher sensitivity of the *pAPL::GUS* reporter in comparison to the *pAPL::LUC* reporter (Fig. 4.10 F to I). This indicated that the *pAPL::LUC* reporter is an appropriate tool for the detection of vascular mutants.

4.3.3 Isolated mutants harbor mutations in the *LUC* reporter gene

After screening of 1,024 single M1 families (~35,000 plants) four families with reduced or abolished LUC activity were isolated (Fig. 4.11). Reduced signal intensity was confirmed by rescreening leaves at later stages, as these mutants developed normally. Sequencing of the reporter showed that in all four mutants a missense mutation resulted in an amino acid substitution altering either the charge (#54 and #85), functional side chain (#48), or the size of the side chain (#4096) at the indicated position within the LUC protein, likely interfering with its function. Except for #48 showing a C to G transversion, mutations were EMS-typical C/G to T/A transitions (Kim et al., 2006). Other lines with reduced LUC activity or lines with enhanced LUC activity were not identified. As overexpression of *APL* in vascular cells was reported to inhibit or delay xylem cell differentiation (Bonke et al., 2003) truly up-regulated *APL* expression could cause plant lethality prior the screening time point. Even though no line without a

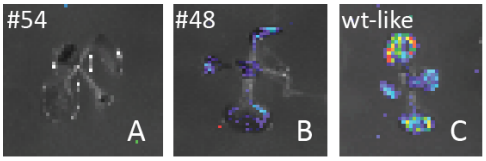

mutant	signal	LUC ORF mutation
#48	reduced	S456C
#54	no	G254E
#85	no	G200E
#4096	reduced	A22V

Fig. 4.11: Selected mutant candidates. Mutant candidates with abolished (A) and reduced (B) luminescence signals are depicted in comparison to a wild-type (wt)-like plant (C) (overlay with brightfield image). Sequencing revealed missense mutations in the *LUCIFERASE* (*LUC*) open reading frame (*ORF*) resulting in substitutions of amino acid residues; codons for the respective amino acid residues are shown: serine (S), cysteine (C), glycine (G), glutamate (E), alanine (A), valine (V).

mutation in the reporter was identified, these results demonstrated that the screen had the potential to isolate mutants with alterations in reporter activity.

Strikingly, *apl* mutants were also not isolated, although, as mentioned above, *apl-1* seedlings carrying the *pAPL::LUC* reporter clearly showed a reduced signal and therefore should have been identified. As mutants carrying mutations in the *LUC* ORF were isolated several times and assuming that the frequency of mutations will occur with approximately the same rate throughout the genome, every essential regulator of *APL* activity should have had a reasonable chance to be identified.
These results raised the possibility that mutants with severely affected *APL* activity do not reach the developmental stage in which plants were analyzed.

4.3.4 *apl-2/+* plants show an embryo-lethal phenotype

Another *APL* mutant allele, designated as *apl-2* in this thesis, was available at the stock center (see **3.6**). *apl-2* was generated by EMS mutagenesis and identified in a tilling approach (Till et al., 2003). *apl-2* harbors a single point mutation in exon 6 (C-to-T) of the *APL* gene (At1g79430.2) 23 bp downstream of the *En-1* insertion site in *apl-1* and creates an in-frame stop codon (Q168*; Asn > stop) (Fig. 4.12). The stop codon is located close to a predicted coiled-coil region (Bonke et al., 2003) (see also results **4.1**). Thus, the protein function could be severely impaired.

In order to remove background mutations generated by the tilling approach, *apl-2/+* plants were backcrossed five times to wild-type Columbia, thereby statistically exchanging ~97% of the EMS-mutated genomic background. *apl-2/+* plants grew indistinguishable from wild-type (Fig. 4.13 A). Seedlings segregating for *apl-2* were genotyped using a dCAPS marker (Fig. 4.14 A; primer combination A2, see Fig. 4.6). Interestingly, no seedlings homozygous for *apl-2* were identified. Growing seedlings showed a 2:1 ratio of *apl-2/+* versus wild-type, indicating that *apl-2* might be a recessive, embryo-lethal allele (Fig. 4.14 B).
For checking the putative lethality of *apl-2* homozygous plants prior to germination, siliques of *apl-2/+* plants were dissected. I observed that part of the seeds was aborted.

Aborted seeds were usually white and of similar size as wild-type plants, an appearance which was not observed among seeds from wild-type plants (Fig. 4.13 C and B). At later

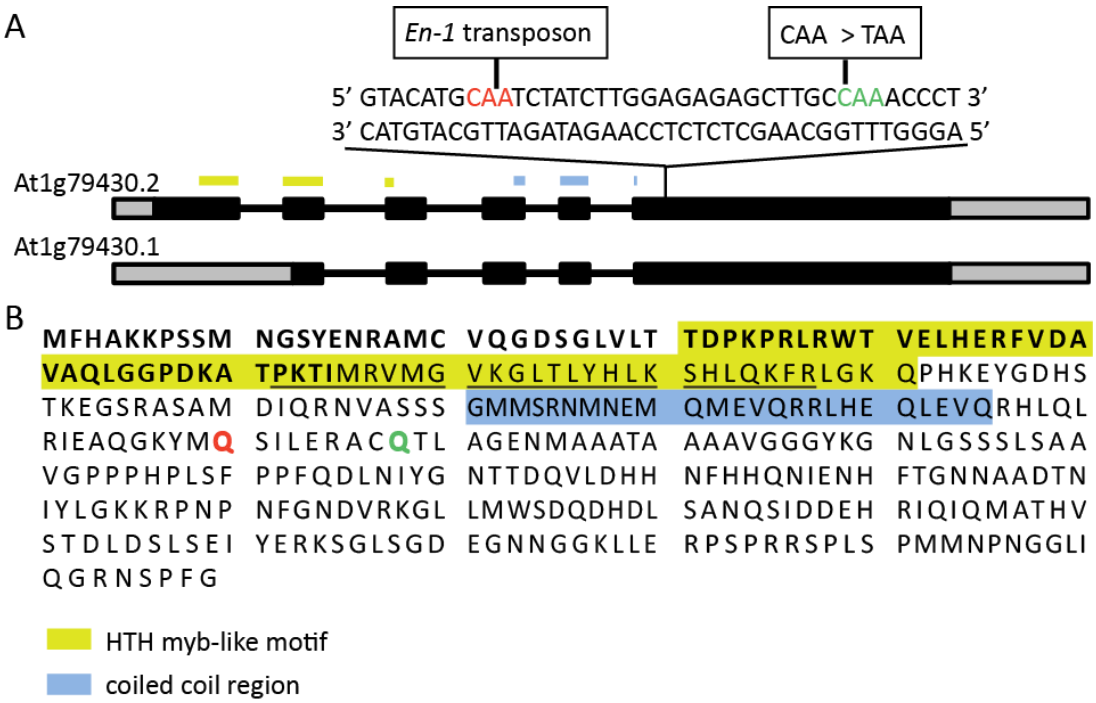

Fig. 4.12: *apl-1* and *apl-2* mutations. A) Protein coding gene models (derived from TAIR) are shown for potential APL isoforms 1 (At1g79430.2) and 2 (At1g79430.1), respectively. Grey blocks indicate 5'UTR and 3'UTR regions, black boxes exons, and black lines introns. Close-up of the sequence shows positions of the *En-1* transposon of *apl-1* (red) and the single point mutation of *apl-2* (green). **B)** The amino acid (aa) sequence for APL isoform 1 (358 aa) is shown including predicted protein motifs (see **4.1**). The HTH (helix-turn-helix) myb-type domain is highlighted in yellow (aa 31-91) including the HTH-DNA-binding motif (underlined; aa 62-87). The *En-1* transposon of *apl-1* is placed within a codon for aa residue Q position 160 (red). The aa residue mutated in *apl-2* is highlighted in green (Q168*). Both mutations, *apl-1* and *apl-2*, are close to each other and next to a predicted coiled-coil region highlighted in blue (approximate site aa 122-145). Bold letters refer to aa residues lacking in isoform 2 (aa 1-65). The HTH- annotations are not valid for APL isoform 2.

stages, white seeds turned brownish and collapsed (not shown). Embryos dissected from aborted seeds were roundish and white when normally developed embryos of the same silique had reached an almost mature stage (Fig. 4.13 D and E). Based on the shape of the embryos, I assumed that abortion takes place before embryos start to develop cotyledons during the transition from the globular to the transition stage.

PCR on DNA from aborted embryos resulted frequently in a gel pattern expected for an *apl-2/apl-2* genotype. Well developed mature embryos never gave rise to a gel pattern expected for *apl-2* homozygous plants (Fig. 4.15 A). Not all of the aborted embryos could be identified as *apl-2/apl-2*, likely due to a contamination of collected material by the

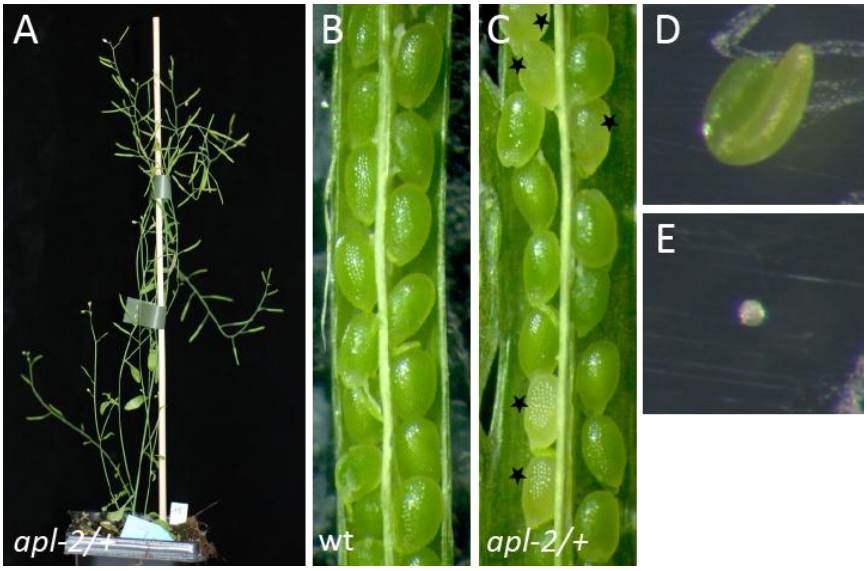

Fig. 4.13: Aborted embryos in *apl-2/+* plants. A-C) Siliques of *apl-2/+* plants (A) harbor aborted big white seeds (C, marked with asterisks) not found in wild-type plants (B). **D-E)** Dissected embryos of green and white seeds derived from the same *apl-2/+* silique are shown in D and E (same magnification), respectively.

seed coat. Sequencing of the PCR products confirmed the presence of *apl-2/apl-2* embryos among the aborted ones (Fig. 4.15.B).

Counting aborted versus normally developed seeds in siliques from *apl-2/+* plants resulted in an abortion ratio of about 26%, almost matching the expected 25% for a lethal mutation with recessive inheritance (Fig. 4.15 C).

These findings were in line with the possibility that *APL* fulfills an essential role during early embryogenesis.

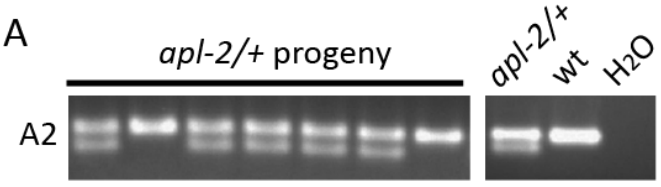

B

	no of plants	%
apl-2/+	80	66,1
wt	41	33,9
total	121	100

Fig. 4.14: No growing *apl-2* homozygous plants among *apl-2/+* progeny. A) The progeny of *apl-2/+* plants was genotyped using a dCAPs marker (A2). The PCR product amplified from the *apl-2* allele can be cut by *Bpu1102 I*. An example of a typical gel pattern showing heterozygous and wild-type genotypes is depicted. DNA from *apl-2/+* and from wild-type plants were used as positive and negative controls, respectively. **B)** *apl-2/+* plants gave rise to *apl-2/+* and wild-type plants in a ratio of 2:1 indicating *apl-2* to be a lethal allele with recessive inheritance.

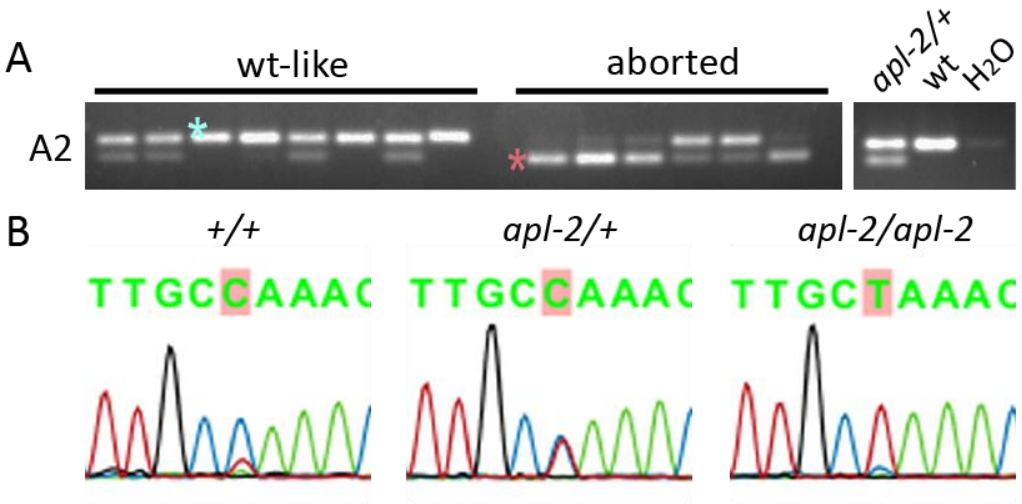

C

	no of plants	no of siliques	seeds total	abort total	ratio (%)
apl-2/+	7	66	3262	842	26
+/+ (tilling)	8	49	2516	20	1

Fig. 4.15: Identification of *apl-2* homozygous embryos among the aborted ones. **A)** Dissected embryos were genotyped using a dCAPs marker (A2). The PCR product amplified from the *apl-2* allele can be cut by *Bpu1102I*. An example of a typical gel pattern is depicted (*APL* wild-type, blue asterisk; *apl-2/apl-2,* red asterisk; *apl-2/+*, no label). DNA from *apl-2/+* and from wild-type plants was used as positive and negative controls, respectively. **B)** Sequencing confirmed the presence of *apl-2* homozygous embryos. Examples of sequencing results aligned to the *APL* genomic sequence are shown (software CLC Main Workbench 6.0.1); *APL* wild-type: *+/+*, single peak for C; *apl-2/+*: overlapping C and T peaks (interpreted as C by CLC Main Workbench 6.0.1); *apl-2/apl-2*: single peak for T. **C)** Abortion ratio of embryos. Numbers (no) of plants, siliques, total amounts of seeds, total amount of aborted seeds and calculated abortion ratios are shown for *apl-2/+* and wild-type segregating from the tilling line. The abortion rate of *apl-2/+* plants meets the expected value of about 25% (Chi square test: 1.148; below the critical 5% value of 3.841).

4.3.5 Footprints and wild-type *APL* sequence are detectable at the *En-1* insertion site in *apl-1* seedlings

This surprising finding also lead to the question why *apl-1* homozygous seedlings develop until the seedling stage. The difference between the severity of *apl-1* and *apl-2* might reside in the nature of these different alleles. Whereas *apl-2* is a stable single point mutation, *apl-1* harbors an *En-1* transposon reported to be frequently excised in somatic and germline cells (Cardon et al., 1993; Schwarz-Sommer et al., 1985). Excision of transposable elements might restore the original sequence (Baran et al., 1992; Rinehart et al., 1997; Scott et al., 1996) or leave footprints in the genome, typically small deletions and insertions at the site of the former transposon (Cardon et al., 1993; Haring et al., 1991; Rinehart et al., 1997; Schwarz-Sommer et al., 1985; Wessler, 1988).

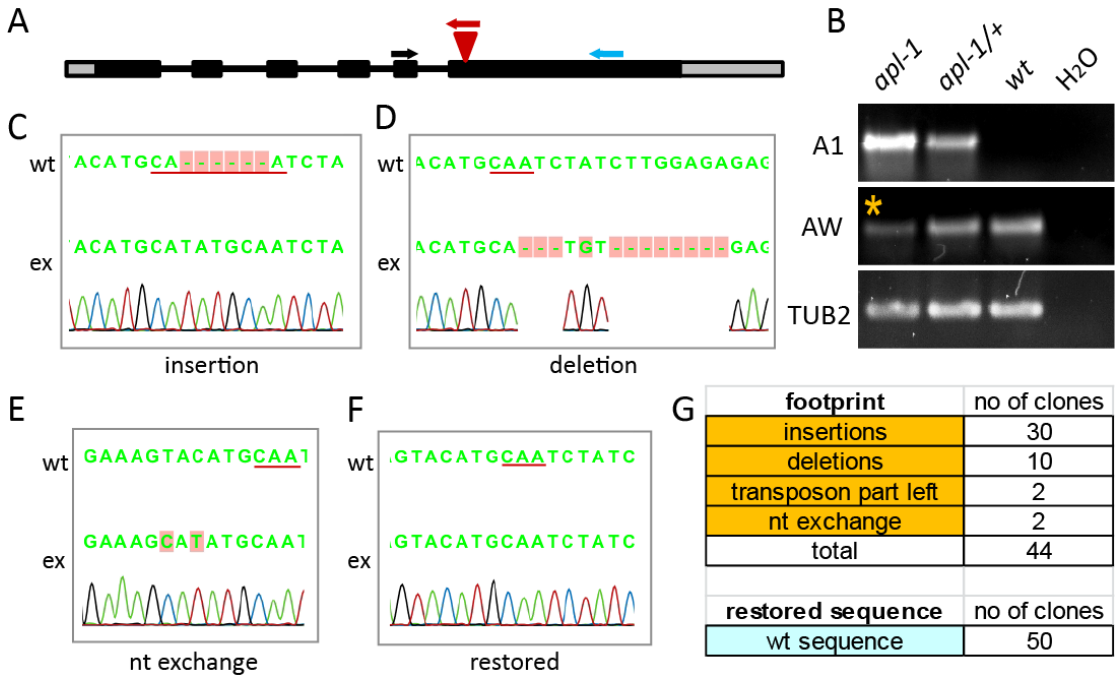

Fig. 4.16: The *En-1* transposon at the *apl-1* locus is frequently excised. A) APL protein coding gene model according to TAIR for At1g79430.2; grey blocks indicate 5'UTR and 3'UTR regions, black bars exons, and black lines introns. Red triangle marks the *En-1* insertion site; arrows indicate primer combinations to detect the *apl-1* (black-red, A1) and the wild-type (black-blue, AW) allele, respectively (not to scale). **B)** Primer combination AW on DNA of *apl-1* seedlings results in a background PCR product (orange asterisk). Control PCRs on DNA of *apl-1/+* and wild-type (wt) plants using primer combination A1 and for β-tubulin (TUB2) are depicted, respectively. **C-F)** Excision of the transposon (ex) leaves footprints or restores the *APL* sequence. Examples for footprints- insertion (C), deletion (D), and nucleotide (nt) exchange (E) - as well as a restored sequence (F) are shown. Alignments of sequencing results to the *APL* genomic sequence (wt) as illustrated by the software CLC Main Workbench 6.0.1. The *En-1* transposon insertion site is underlined. **G)** Numbers of clones obtained for different types of footprints and the restored wt sequence.

Thus, I wanted to test whether transposon excisions are detectable in *apl-1* plants. As already observed during standard genotyping, PCR on DNA from *apl-1* homozygous plants (phenotypic selection) with a primer combination specific for the *APL* wild-type allele frequently gave rise to a PCR product of the same size as obtained by PCR on DNA from wild-type plants (Fig. 4.16 A and B). The *apl-1*-derived PCR product was purified from the gel, cloned into the *pGEM-T* vector and individual clones were sequenced (Fig. 4.16 C to F). Different types of footprints were found, predominantly insertions and deletions of a few nucleotides at the site of transposon insertion, but also residual transposon sequence and nucleotide exchanges. Out of 94 clones tested, 44 contained footprints and 50 restored the wild-type *APL* sequence, representing almost a 1:1 ratio (Fig. 4.16 G).

Taken together, excision of the transposon at the *apl-1* locus takes place and partially restores the *APL* sequence. Thus, one can speculate that if an excision event restores the

APL sequence early enough during development/embryogenesis in cells expressing *APL*, APL might be produced in enough cells to enable growth of seedlings to a certain stage.

4.3.6 *apl-1* seedlings do not recover

As somatic excisions occur during ongoing growth (Cardon et al., 1993), I tested *apl-1* seedlings for their potential of late recovery. 64 *apl-1* homozygous plants identified by the phenotype and randomly chosen sister plants were kept on plates for almost four months (114 days). In between, seedlings were transferred twice (at day 29 and day 65 after germination) to fresh plates to guarantee constant supply with nutrients and enough space for growing.

Although *apl-1* seedlings were usually arrested after development of the first few true leaves (Bonke et al., 2003) (Fig. 4.17 B and C; wild-type like seedling in A) and do not survive on soil for more than about one month, *apl-1* seedlings can be kept on plates for a longer period (Fig. 4.17 G and H). *apl-1* seedlings stayed small constantly developing small leaves. At day 54, 35 out of 64 *apl-1* seedlings were analyzed for restored root growth but none of them showed signs of recovery (Fig. 4.17 E and F, in comparison to a sister plant in D), neither did residual *apl-1* seedlings after 65 or even 114 days (Fig. 4.17 G and H). Nevertheless, plants were obviously able to survive on the medium likely because of a sufficient uptake of nutrients from the medium. Thus, *apl-1* homozygous seedlings

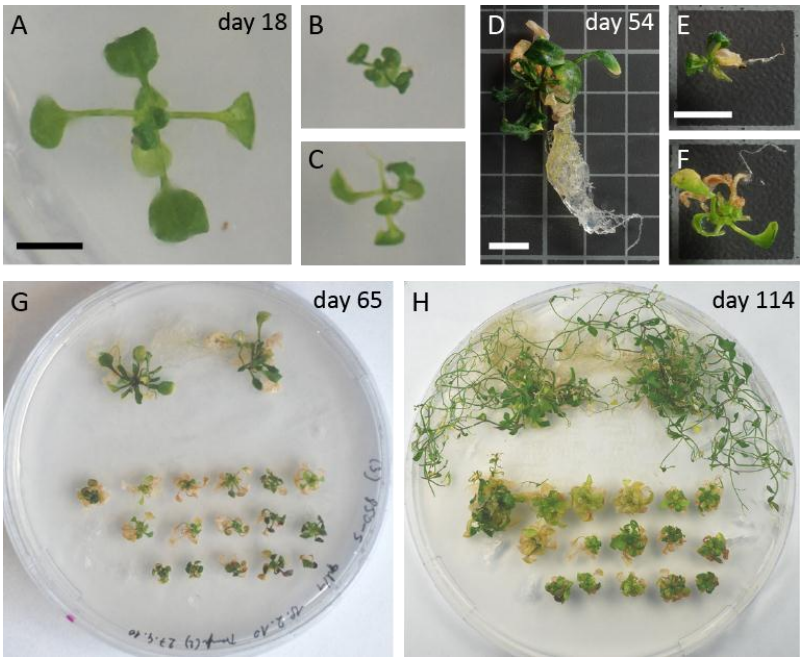

Fig. 4.17: No *apl-1* revertants after a prolonged growth period. A-H) Development of *apl-1* (B, C, E, F, and wild-type (wt)-like seedlings (A, D) is shown 18 (A to C), 54 (D to F), 65 (G), and 114 (H) days, respectively, after germination on plates. The same plate is shown after 65 days and 114 days; two wild-type-like plants are growing above three rows of *apl-1* seedlings. Plants were transferred to fresh plates at day 29 and 65. Scale bars: 0.5 cm; scale bar in A corresponds to B and C; scale bar in E corresponds to F.

presumably die due to impaired root growth and vascular defects hampering uptake of nutrients. Disturbed long-distance transport and distribution of nutrients within the plant might limit expansion of leaves and further growth on plates as well. The reason why no recovery was observed could be that vascular (phloem) defects are too severe to be rescued by single *APL* restoration events.

4.3.7 Allele *apl-2* is allelic to *apl-1*

To reveal whether *apl-2* is as stronger allele than *apl-1* and to see whether both mutations are allelic, plants heterozygous for either allele were crossed and the F1 generation was analyzed 14 days after germination. Segregation will yield in one population of plants containing at least one wild-type allele or in *apl-1/apl-2* plants.

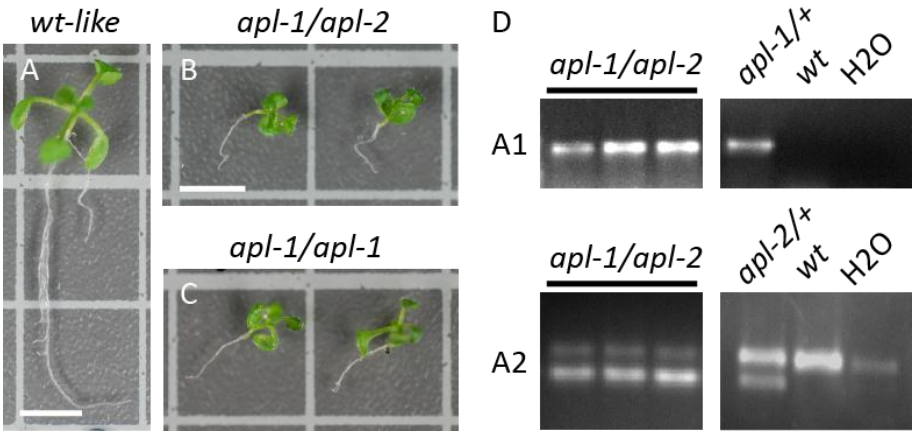

Fig. 4.18: The *apl-2* allele is not stronger than *apl-1*. A-C) In the F1 generation of a cross between *apl-1/+* and *apl-2/+* plants, seedlings resembling *apl-1* (compare B and C) were found among wild-type (wt)-like growing plants (A). **D)** Genotyping identified small plants to be positive for *apl-1* and *apl-2*. Primer combinations A1 for *apl-1* and A2 for *apl-2* (restriction of the *apl-2* derived PCR product) were used, respectively. DNA from *apl-1/+* and *apl-2/+* plants were used as positive control, from wt plants as negative control. Primer combination A2 is partially functional on *apl-1/apl-2* (or gives background due to excision of the *En-1* transposon). Scale bars: 0.5 cm; scale bar in B corresponds to C.

Among wild-type like growing plants, seedlings resembling *apl-1* homozygous plants were identified showing retarded growth and shortened roots (Fig. 4.18 A to C). PCR reactions confirmed that all *apl-1*-like plants indeed harbored both alleles, *apl-1* and *apl-2* (Fig. 4.18 D; for primer combinations see Fig. 4.6).

In conclusion, both mutations are allelic and the *apl-2* allele is not more active than *apl-1*.

4.3.8 *apl-2* embryos show altered cell division patterns

As the *apl-2* allele is not stronger than *apl-1* and *apl-2/+* plants were embryo-lethal, I wanted to gain a deeper insight into the role of APL during embryogenesis by analyzing defective *apl-2* embryos. As aborted embryos had a roundish appearance I expected to find the first defects in *apl-2* embryos before the establishment of bilateral symmetry and thus before phloem-related divisions take place which is around the bent-cotyledon stage (Bonke et al., 2003). At the dermatogen stage, the inner cells, the progenitors of the vascular and ground tissues, are formed and, subsequently, the procambium is established from early globular stage onwards (Peris et al., 2010; Scarpella and Helariutta, 2010). Thus, I focused my analysis on the time from dermatogen to transition/heart stage covering the time frame of the establishment of provascular tissues.

By DIC microscopy of cleared seeds derived from *apl-2/+* plants, one population of wild-type like embryos was detected and a second one showing defects which were assumed to represent the *apl-2* homozygous embryos.

Aberrant divisions in *apl-2* embryos were already present when sister embryos had reached the dermatogen stage (Fig. 4.19 A). At least two of the four cells visible in the *apl-2* embryo had elongated shapes and abnormal positions (Fig. 4.19 B). Assuming that the non-visible part of the embryo contains the same number of cells, eight cells should be present ('octant' stage). At the same time, embryos were visible with a symmetric altered division pattern (Fig. 4.19 C). The outer cells had already undergone a next round of division, whereas inner cells did not seem to have divided yet. Based on the shape of the cells, the outer cells were derived from elongated cells as well, resulting from a transversal division giving them a protoderm-like appearance. Protoderm is usually formed by tangential divisions at the octant stage.

At the time of globular stage when sister embryos had already formed the lens-shaped cell, the progenitor of the RAM (Fig. 4.19 D), *apl-2* embryos still appeared the same as during dermatogen stage. Thus, the developmental program might be delayed in general and divisions continue quite slowly (Fig. 4.19 E). At a different focus, additional nuclei were visible in compartments without a clear cell border (Fig. 4.19 F), at the peripheral

side of the embryo (top view). It remained unclear whether nuclei divided without cytokinesis, forming a syncytium, or if the multi nuclei appearance was transient.

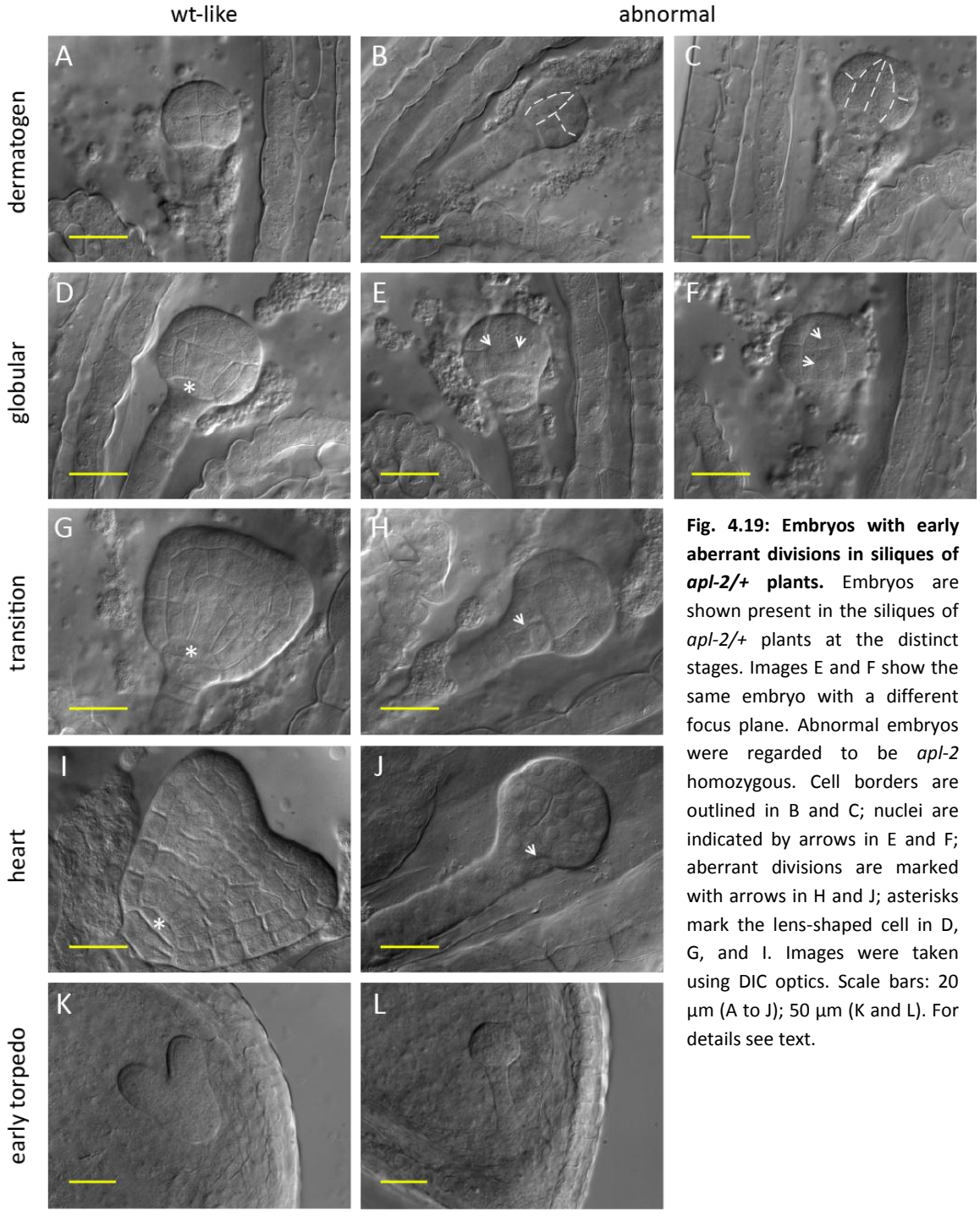

Fig. 4.19: Embryos with early aberrant divisions in siliques of *apl-2/+* plants. Embryos are shown present in the siliques of *apl-2/+* plants at the distinct stages. Images E and F show the same embryo with a different focus plane. Abnormal embryos were regarded to be *apl-2* homozygous. Cell borders are outlined in B and C; nuclei are indicated by arrows in E and F; aberrant divisions are marked with arrows in H and J; asterisks mark the lens-shaped cell in D, G, and I. Images were taken using DIC optics. Scale bars: 20 µm (A to J); 50 µm (K and L). For details see text.

During subsequent stages, when wild-type-like embryos passed through transition (Fig. 4.19 G and H), heart (Fig. 4.19 I and J), early torpedo (Fig. 4.19 K and L), cell division patterns in *apl-2* embryos got less regular and could not be clearly followed. In general, *apl-2* embryos often developed an uneven surface and a very irregular anatomy. They

often exhibited aberrant divisions (Fig. 4.19 H and J) in the place where one would expect the presence of the hypophysis and, subsequently, the lens-shaped cell (Fig. 4.19 G and I), possibly again implementing wrong division planes. These types of defects are frequently found in mutants of embryo defective genes (e.g. (Jenik et al., 2005; Johnson et al., 2008; Nodine et al., 2007)). If the division in the basal region indeed represents the hypophysis division, the embryo might still respond to a predefined developmental division program, although delayed. Aberrant divisions at this time might, of course, be just a consequence of the earlier defects which could include general altered gene expression or hormone distributions. Despite these severe defects, embryos increased in size and grew further at least until sister embryos had reached the early torpedo stage (Fig. 4.19 K and L). The suspensor developed without obvious defects.

In order to determine the position of the cells in the aberrant 'octant' stage of *apl-2* embryos more precisely, consecutive optical sections were taken. In wild-type embryos, cells at the four-cell stage divide transversally giving rise to eight cells, four in an upper and four in a lower tier (e.g. (Jenik et al., 2007)). Confirming the observations of the DIC microscopy, *apl-2* embryos showed a variable degree of altered cell patterns. In extreme cases, eight cells were arranged in an inner and an outer array of four cells each on top of the suspensor; the 3D image generated from the optical sections illustrates the cell positions based on the localizations of the nuclei more clearly (Fig. 4.20 E to G). In other cases only two cells were positioned aberrantly whereas the residual six cells showed the upper-lower tier distribution as in wild-type octant stages (Fig. 4.20 A to D). In Fig. 4.20 H a scheme for a model of aberrant divisions is depicted in comparison to wild-type development.

Taken together, *apl-2* embryos show an altered cell division pattern already at the eight-cell stage (aberrant 'octant'-stage). This might be derived from a switch of the cell plane orientation at the four-cell stage. Instead of uniform transversal divisions, cells divide along a rather longitudinal (or tangential) plane, resulting in an elongated shape. Presumably, one to all four cells might encounter this aberrant division(s). Thus, *apl-2* embryos develop partially asymmetrically exhibiting a mix of wild-type and aberrant cell

divisions. Embryos might also delay or skip ongoing divisions and further development results in roundish embryos with grossly altered cell patterns.

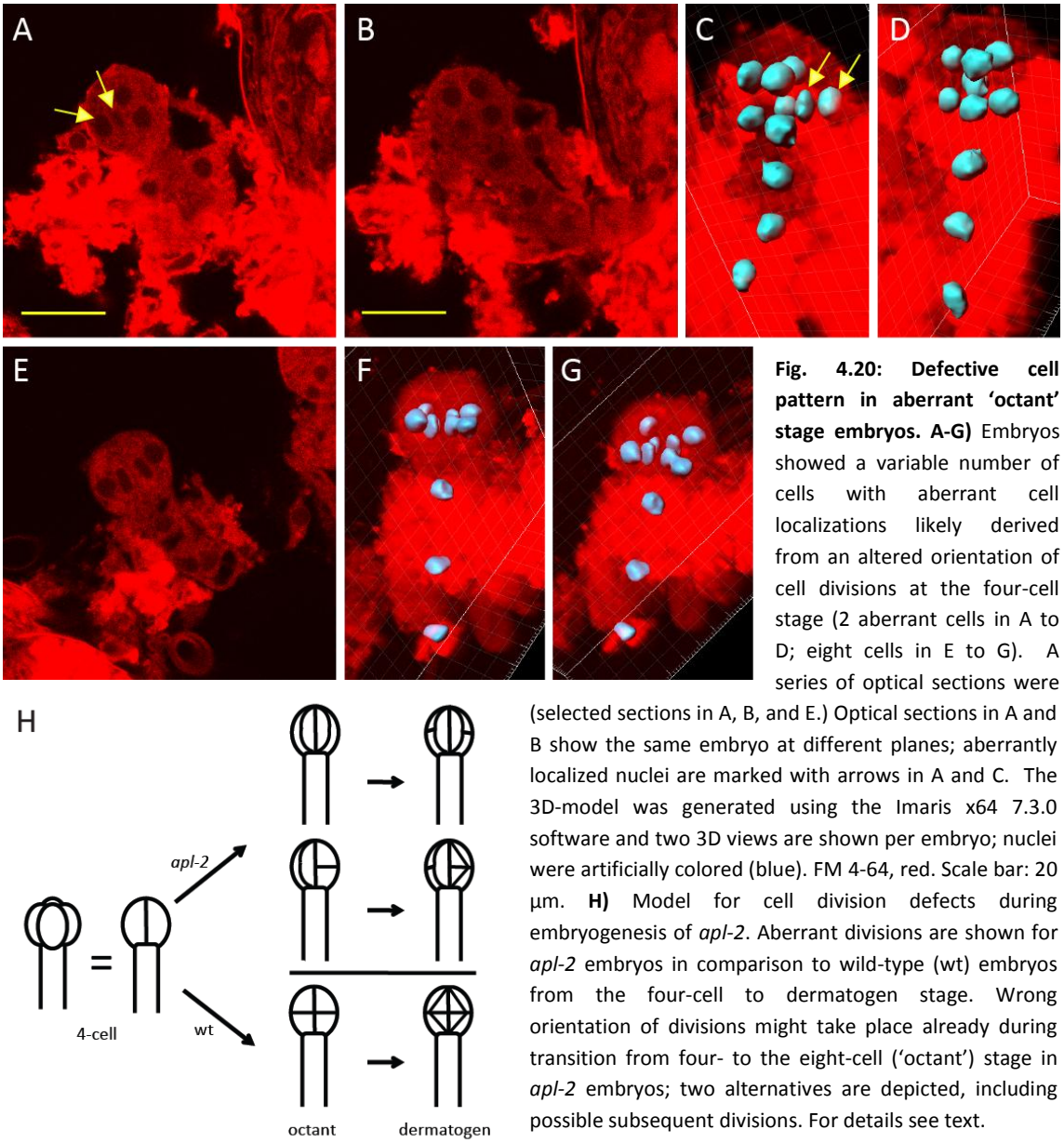

Fig. 4.20: Defective cell pattern in aberrant 'octant' stage embryos. A-G) Embryos showed a variable number of cells with aberrant cell localizations likely derived from an altered orientation of cell divisions at the four-cell stage (2 aberrant cells in A to D; eight cells in E to G). A series of optical sections were (selected sections in A, B, and E.) Optical sections in A and B show the same embryo at different planes; aberrantly localized nuclei are marked with arrows in A and C. The 3D-model was generated using the Imaris x64 7.3.0 software and two 3D views are shown per embryo; nuclei were artificially colored (blue). FM 4-64, red. Scale bar: 20 µm. **H)** Model for cell division defects during embryogenesis of *apl-2*. Aberrant divisions are shown for *apl-2* embryos in comparison to wild-type (wt) embryos from the four-cell to dermatogen stage. Wrong orientation of divisions might take place already during transition from four- to the eight-cell ('octant') stage in *apl-2* embryos; two alternatives are depicted, including possible subsequent divisions. For details see text.

4.3.9 Auxin transporter PIN1 is mislocalized in *apl-2* embryos

From early stage on, correct embryo development depends to a high degree on a dynamic gradient of the hormone auxin, established by polar distribution of different members of the transmembrane PIN auxin transport family (Friml et al., 2003; Friml et al., 2004). Among those, PIN1 is the member being expressed first in the apical part of the embryo already in the one-cell stage. PIN1 marks the newly formed inner cell

boundaries without apparent polar distribution up to the late dermatogen stage. Upon globular stage, PIN1 becomes polarly localized towards the basal membrane of the provascular cells generating an auxin maximum in the uppermost suspensor cell which becomes defined as the hypophysis (Friml et al., 2003).

To determine if auxin transport is affected in *apl-2* embryos, the PIN1-GFP marker line (Benkova et al., 2003) was crossed into the *apl-2* background and embryos of plants homozygous for the marker gene were analyzed by confocal microscopy.

Throughout all developmental stages examined, PIN1-GFP was weakly expressed in *apl-2/apl-2* in comparison to the wild-type-like embryos (Fig. 4.21). At the aberrant octant stage, when wild-type like embryos of the same silique have reached the dermatogen stage (Fig. 4.21 A), PIN1-GFP was sometimes detectable in the apical part of the *apl-2* embryos (Fig. 4. 21 B, detectable in C).

PIN1-GFP localization in *apl-2* embryos was similar at the globular stage still showing a weak apical expression (Fig. 4.21 D, and E/F). Throughout embryogenesis of wild-type embryos, PIN1 is only expressed in the apical/central part, always distally to the hypophysis and lens-shaped cell, the future RAM (Benkova et al., 2003; Friml et al., 2003). At globular stage, PIN1-GFP was partially also found in the suspensor of *apl-2* embryos (Fig. 4.21 E).

In wild-type embryos, apart from polar PIN1 expression in the (pro)vascular cells, in transition and heart stage PIN1 gets polarly localized within the protoderm to form auxin maxima at the sites of cotyledon outgrowth (Benkova et al., 2003; Friml et al., 2003).

At transition stage (Fig. 4.21 G), PIN1-GFP localization in *apl-2* varied being detectable only in e.g. the central region of the embryo (Fig. 4.21 H) or aberrantly in the basal part in the presumptive hypophysis and in the suspensor (Fig. 4.21 I). PIN1 expression did not show a specific pattern later during heart stage (Fig. 4.21 J). It was present in the protoderm-like outer layer, the suspensor as well as in inner regions (Fig. 4.21 K and L). PIN1-GFP mislocalization might reflect aberrant auxin distributions due to early misregulated embryo patterning. It will be interesting to investigate whether other especially embryonic PIN family members, PIN3, PIN4, and PIN7 (Friml et al., 2003) show aberrant or ectopic localizations, as well as if auxin distribution/maxima are altered e.g. using a transcriptional reporter fusion with the artificial auxin responsive *DR5* promoter

(Ulmasov et al., 1997). At early torpedo stage (Fig. 4.21 M), PIN1-GFP expression declined in *apl-2* embryos (Fig. 4.21 N and O), likely reflecting ongoing abort of embryos. Thus, PIN1-GFP is mislocalized in *apl-2* embryos in a highly variable manner indicating disturbed patterning processes.

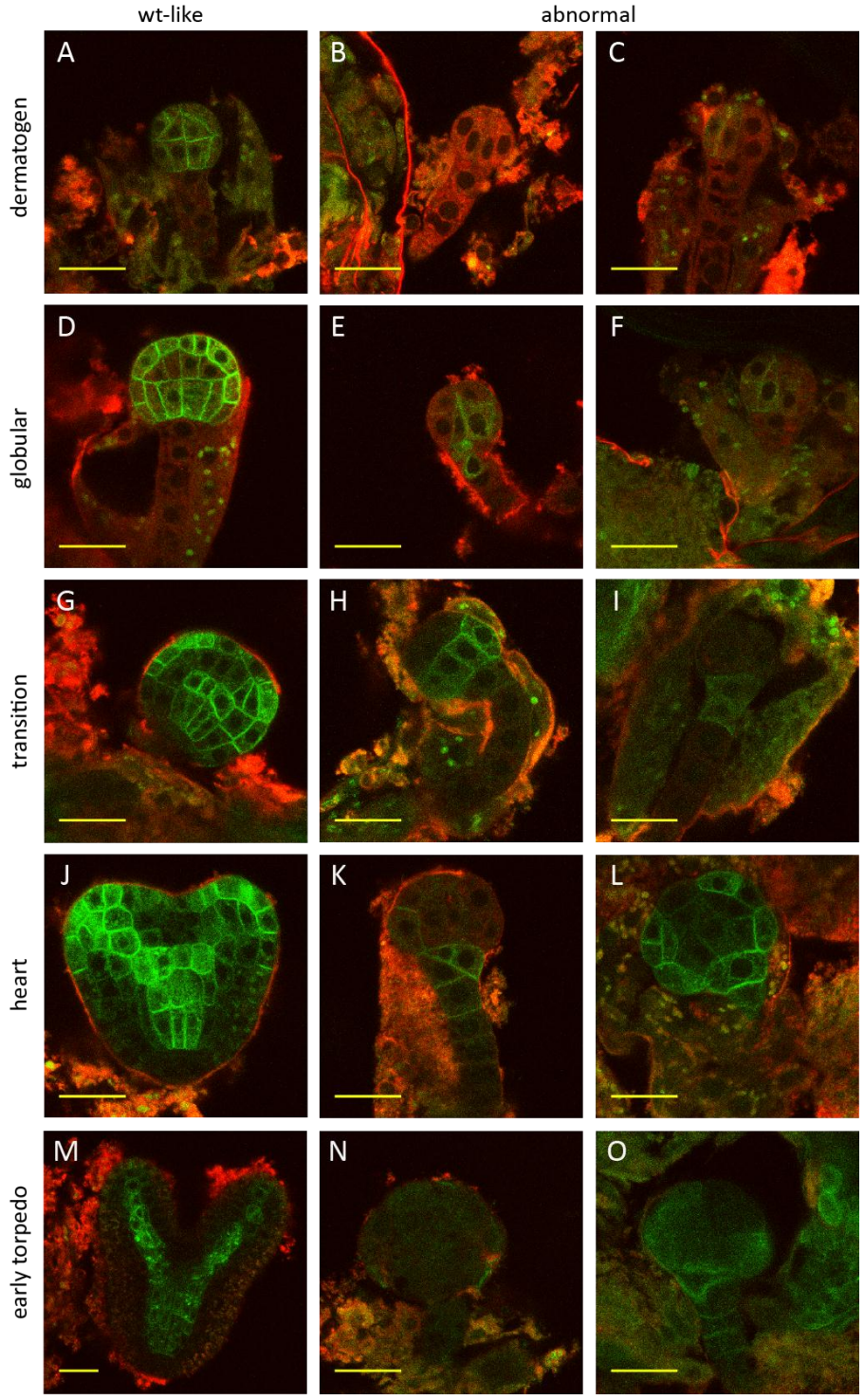

Fig. 4.21: Reduced expression and aberrant localization of PIN1-GFP in *apl-2* embryos. Embryos are shown which were found in the siliques of *apl-2/+* plants at the distinct stages. Abnormal embryos were regarded to be *apl-2* homozygous. Confocal images are shown; PIN1-GFP, green; counterstain FM4-64, red. GFP signals for *apl-2* and wt-like embryos were differentially adjusted in Photoshop. Scale bars: 20 µm. For details see text.

4.3.10 The provascular marker *ATHB8* is detectable in *apl-2* embryos

The PIN/auxin pathway seemed to be affected during *apl-2* embryogenesis. Embryo patterning is usually a very regular process with predictable clonal contributions of each cell to distinct plant body parts. Still, plant cells are flexible and also respond to positional cues thereby differentiating according to their final position (Laux et al., 2004; Poethig et al., 1986; Saulsberry et al., 2002). Thus, as *apl-2* embryos do not follow the predicted regular cell division pattern I wanted to test if or to what extent provascular tissue might be formed in *apl-2*.

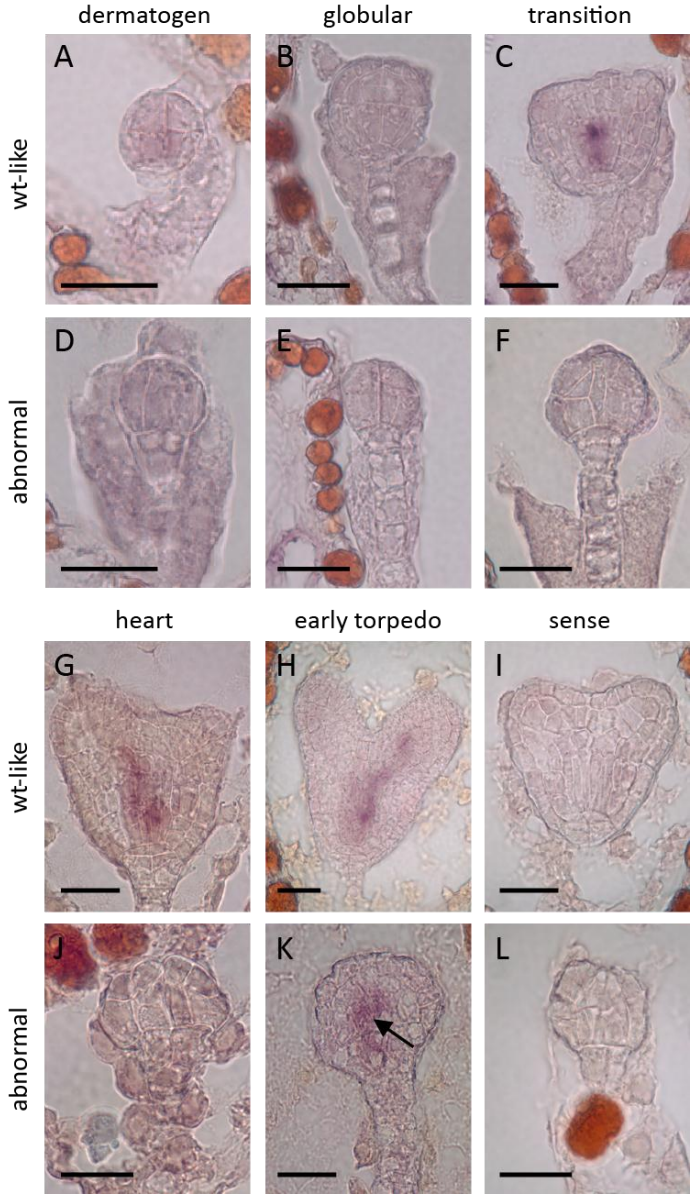

Fig. 4.22: *ATHB8* expression in late *apl-2* embryos. Detection of *ATHB8* by RNA *in situ* hybridization on sections of *apl-2/+* derived embryos at the distinct stages. *ATHB8* is detectable in *apl-2* embryos at later stages (arrow). Abnormal embryos were regarded to be *apl-2* homozygous. Sense probe control is shown in I and L. Scale bars: 100 µm. For details see text.

To this end, I analyzed the expression of the auxin-inducible HD-ZIPIII factor *ATHB8*, an early procambium marker (Baima et al., 1995), by RNA *in-situ* hybridization.

Wild-type sister embryos showed the typical pattern of *ATHB8* being detectable at the sites of procambium formation from transition stage on (Prigge et al., 2005) (Fig. 4.22 A to C, G to H; control I). In *apl-2* embryos, *ATHB8* mRNA was not detectable until sister embryos had reached the heart stage (Fig. 4.22 D to F and J). Surprisingly, *ATHB8* mRNA was detectable in central regions of some *apl-2* embryos when wild-type embryos reached early torpedo

stage (Fig. 4.22 K; control L). Thus, when *apl-2* embryos are still alive at this stage they seem to be able to establish a provascular-like inner domain as indicated by *ATHB8* transcription. The, in comparison to wild-type-like embryos, relative late onset of expression might reflect a general retarded development of *apl-2* embryos (aberrant octant stages were detected at the time when wild-type like embryos have reached dermatogen stage; see **4.3.8**/**4.3.9**).

This suggests that, despite the developmental defects, *apl-2* embryos retain the potential to establish a central provascular-like domain responding to positional cues. Detection of other tissue-specific marker genes will reveal if the basic tissue patterns (epidermis, ground and vascular tissues) are formed in *apl-2* in general.

Taken together, APL might have a role independent of vascular (phloem) development influencing the very first embryonic divisions when upper and lower domains of the embryo are defined. Although embryos continue to divide in a quite unorganized way, basic tissue patterning might take place, as shown for the provascular tissue. Defects in embryogenesis have been shown to be transient or get ameliorated in some cases (e.g. (Bayer et al., 2009; Friml et al., 2003; Ueda et al., 2011)). However, defects elicited in *apl-2* are beyond the potential of recovery and alternative mechanisms do not save the embryos. Thus, a fundamental developmental process seems to be affected in *APL*-deficient plants.

4.3.11 *APL* expression in the embryo

In order to reveal the onset and pattern of *APL* expression during early embryogenesis, different approaches were tested.

Based on publically available expression data, *APL* is expressed in the embryo at very low levels during early embryogenesis (Winter et al., 2007; Xiang et al., 2011). Very low expression levels are also listed for other genes demonstrated to function during early embryogenesis e.g. *WOX8* or *WOX9* (Breuninger et al., 2008; Wu et al., 2007; Wu et al., 2005). At the mature stage, published data for *APL* inconsistently show either a relative low (Xiang et al., 2011) or higher level (Winter et al., 2007) of expression.

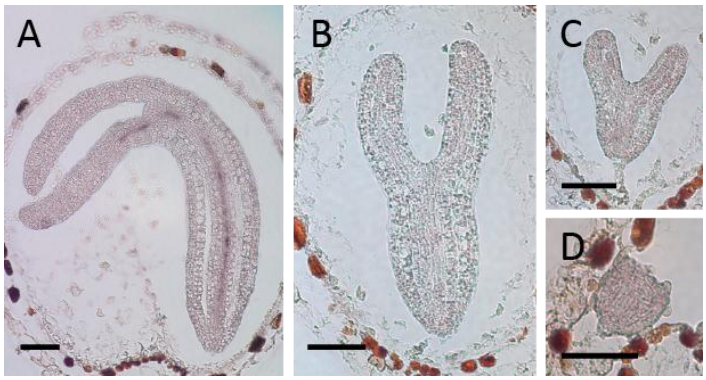

Fig. 4.23: *APL* is not detectable prior to bent-cotyledon stage embryos. Detection of *APL* by RNA *in situ* hybridization on sections of wild-type embryos. Bent-cotyledon (A), torpedo (B), early torpedo (C), and transition (D) stage embryos are shown. Scale bars: 200 nm.

Using RNA *in-situ* hybridization I could confirm the expression of *APL* in the vasculature of embryos around the bent-cotyledon stage when asymmetric phloem-related divisions take place (Bonke et al., 2003) (Fig. 4.23 A). At earlier stages, *APL* mRNA could not be detected maybe due to low sensitivity of the technique (Fig. 4.23 B to D).

Activity of a *CFP* (*CYAN FLUORESCENT PROTEIN*) reporter under the control of the *APL* promoter (provided by Pablo Sanchez, Greb lab, unpublished) was not detectable at any embryonic stage, even though activity was detectable in adult plants (phloem-specific signals were detectable; not shown).

Based on the activity of a *pAPL::GUS* reporter, an initial non-vascular specific expression of *APL* from transition stage on has been reported (Bonke, 2004); vascular specific GUS expression was shown from bent-cotyledon stage on, as described above (Bonke et al., 2003). As GUS activity was not detectable in embryos of line -2587 *pAPL::GUS*, reporter lines with very strong *GUS* expression or techniques to enhance signal intensities are required to visualize *APL* expression during early embryogenesis.

Taken together, onset and expression profile of *APL* during early embryogenesis remains to be clearly demonstrated and defined.

4.3.12 Establishment of an inducible line to down-regulate *APL* mRNA

As *apl-2* is embryo-lethal, an approach was designed which should allow monitoring and recapitulating APL deficiency during different stages of embryogenesis. To this end, inducible downregulation of *APL* was achieved by taking advantage of the two-component ethanol-switch system (Deveaux et al., 2003; Roslan et al., 2001). Posttranscriptional gene silencing is a common mechanism in many organisms for regulating gene expression at the mRNA level. For example, polymerase II-derived RNA

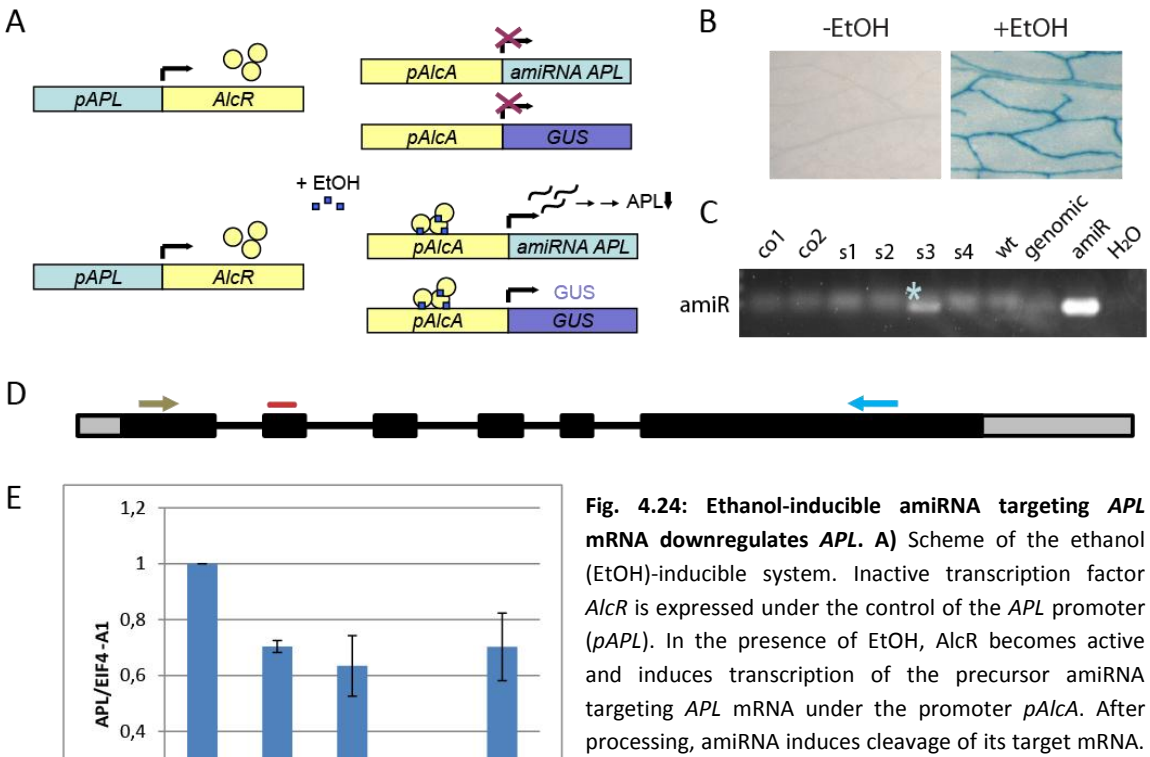

Fig. 4.24: Ethanol-inducible amiRNA targeting *APL* mRNA downregulates *APL*. A) Scheme of the ethanol (EtOH)-inducible system. Inactive transcription factor *AlcR* is expressed under the control of the *APL* promoter (*pAPL*). In the presence of EtOH, AlcR becomes active and induces transcription of the precursor amiRNA targeting *APL* mRNA under the promoter *pAlcA*. After processing, amiRNA induces cleavage of its target mRNA. Induced GUS expression from the *pAlcA::GUS* construct concomitantly transformed with *pAPL::AlcR* serves as positive control for a successful EtOH induction (GUS staining). **B)** GUS staining of leaves before (-EtOH) and after (+EtOH) induction confirms the activity of AlcR in the amiRNA lines. **C)** Precursor amiRNA is detectable by PCR on cDNA of leaves in one (s3, asterisk) out of four lines (s1 to s4) two days after EtOH induction. Controls (co1 and co2) are EtOH-treated plants lacking the *pAPL::AlcR* component; wild-type (wt) cDNA; genomic DNA (genomic); precursor amiRNA control (amiR); water control (H_2O). **D)** Arrows indicate positions of primer binding sites used for qRT-PCR of *APL* (see E) in gene model At1g79430.2; the red line indicates the amiRNA target site. **E)** *APL* transcript accumulation in line 3 (s3) is strongly reduced. *APL* transcript abundance of six (for s1 four) technical replicates was normalized to the elongation factor *EIF4-A1*. For determination of relative expression levels of single lines values for control 1 and control 2 were combined (co) and set to 1.

hairpin loops are processed into small RNAs (microRNAs), which bind to target mRNAs in an RNA-enzyme complex. Subsequently, mRNAs are usually cleaved in plants preventing translation into protein, although direct translational repression has been reported as well. This mechanism is exploited by the invention of artificial micro RNAs (amiRNAs) downregulating distinct genes for investigating their functions (for review see e.g (Mallory and Vaucheret, 2010; Sablok et al., 2011)).

Thus, a precursor for an amiRNA targeting the second exon of the mRNA of *APL* (Fig. 4.24 D) was designed (see **3.3**). The DNA encoding the precursor amiRNA was cloned under the control of the *AlcA* promoter which is activated by the transcription factor *AlcR* only in the presence of ethanol. Expression of *AlcR* was achieved by utilizing the *APL* promoter, aiming for the repression of *APL* as soon as *APL* transcription is activated (Fig.

4.24 A). Transgenic lines harboring both constructs were treated with ethanol when already several shoots with siliques and flowers had formed. The plasmid carrying the *pAPL::AlcR* component also included a *pAlcA::GUS* reporter. Therefore, *pAPL* driven expression of *AlcR* and its activity upon ethanol-treatment could be confirmed by GUS staining of leaves following the ethanol treatment (Fig. 4.24 B). As expected, vascular-specific GUS staining was observed in leaves of the transgenic plants only upon ethanol treatment. RT-PCR on cDNA from leaves harvested two days later identified one out of four independent lines with detectable amounts of amiRNA precursor (primer combination: amiRNA-APL_2-II/amiRNA_APL_2-III) (Fig. 4.24 C). Using qRT-PCR, an 80% reduction of *APL* transcript abundance was detected in the line with high pre-amiRNA levels. Here, a primer combination was used annealing up- and downstream of the amiRNA target site, thereby, not detecting cleaved mRNA fragments (primer combination: APLfor22/apl-F2gen) (Fig. 4.24 D). Other amiRNA lines showed milder alterations of mRNA levels in comparison to ethanol-treated control plants lacking the *pAPL::AlcR* component (Fig. 4.24 E).

Preliminary analyses of embryos five days after induction did not reveal defects during early embryogenesis. The analysis was complicated by toxic effects of ethanol on embryo/ovule development itself. Ethanol treatment and experimental set-up requires further optimization. In general, inducible amiRNA lines will be a valuable tool for dissecting APL's function during embryogenesis.

In summary, an inducible line was established for downregulating *APL* transcript abundance at distinct time points. Further analysis will allow getting a deeper insight into *APL*'s function at different developmental phases not only during embryogenesis but also in adult plants (Bonke et al., 2003).

4.3.13 Approaches to rescue *apl-2* embryos

To finally prove that the *apl-2* phenotype of embryos is the consequence of the mutated *APL* allele, two different approaches were performed.

The full-length *-3086 pAPL::APL* construct already successfully used to complement the *apl-1* phenotype (see **4.2.4**) was transformed into *apl-2/+* plants. The T1 generation was

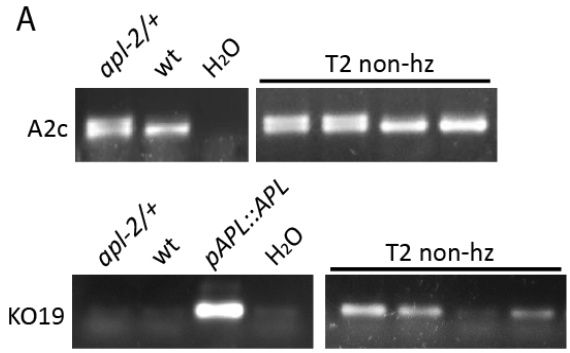

B

	no of plants (%)	*pAPL::APL pos* (%)
apl-2/+	55 (~58.5)	50 (~90.9)
wt	39 (~41.5)	33 (~84.6)
total	94 (100)	83 (~88.3)

Fig. 4.25: Genotyping potential complemented *apl-2* seedings. A) A dCAPS marker (A2c) was designed for specific amplification of the endogenous *APL* locus. The PCR product is cut in combination of the wild-type allele using *MlsI*. The presence of the complementation construct (*-3086 pAPL::APL*, KO19) was verified. All seedlings tested harboring the complementation construct were either wild-type or heterozygous for *apl-2* (T2 non-hz), thus, *apl-2* was not complemented. DNA of wild-type (wt) and *apl-2/+* plants, and plasmid *-3086 pAPL::APL* (KO19) were used as controls. **B)** T2 *apl-2/+ -3086 pAPL::APL* plants segregate into *wt* and *apl-2/+* plants at a ratio of ~1:1.4, harboring more wt plants than expected for a lethal allele *apl-2*. Almost 90% of plants are positive for the complementation construct.

selected for resistance of BASTA conferred by the construct and genotyped for the presence of the *apl-2* allele. From ten independent *apl-2*/+ *-3086 pAPL::APL* lines, siliques were analyzed. All of them displayed a seed abortion rate as determined for *apl-2/+* plants before (see Fig. 4.15) suggesting that the *-3086 pAPL::APL* construct was not sufficient for restoring *apl-2*-specific growth defects. Nevertheless, the progeny of one plant was grown on plates without BASTA selection to avoid putative stress for partially complemented plants. For detection of the *apl-2* allele, a dCAPs marker was designed. For this, a PCR product specific for the endogenous *APL* gene was generated which carried a restriction site in the case of the wild-type *APL* allele (primer pair A2c, see Fig. 4.6). Among 94 seedlings, no *apl-2* homozygous plant could be identified (Fig. 4.25 A and B); the shift towards an increased portion of wild-type plants (~41.5% instead of ~33.3%) and a reduced portion of *apl-2/+* plants (~58.5% instead of ~66.7%) might be an incidence or could argue for a slight degree of embryo-lethality of heterozygous plants. The presence of the complementing construct was verified (primer combination KO19: APLrev12/T7, see Tab. 3.2) (see example for an agarose gel in Fig. 4.25 A).

In addition, as *apl-1* homozygous plants were successfully complemented by the construct *-3086 pAPL::APL*, a complemented *apl-1* line was crossed with *apl-2/+* plants. This strategy should guarantee a functional transgene within the genome of *apl-2* mutants. The F1 generation was selected for the presence of the construct and the *apl-2* allele. In the F2 generation among 57 seedlings no *apl-2* homozygous plant could be identified (primer pair A2, see Fig. 4.6); all seedlings were positive for the *apl-1* allele

(primer pair A1, see Fig. 4.6) (Fig. 4.26 A). Seedlings were segregating into a ratio of about 1:2 as expected for a lethal allele *apl-2*; *-3086 pAPL::APL* is also segregating (primer combination KO19) (Fig. 4.26 A and B).

As the rescue of *apl-2* homozygous plants could not be achieved, it still remains open whether defects in *APL* are causative for the embryo defects on *apl-2* plants and whether *APL* is involved in the regulation of the early embryogenesis.

A

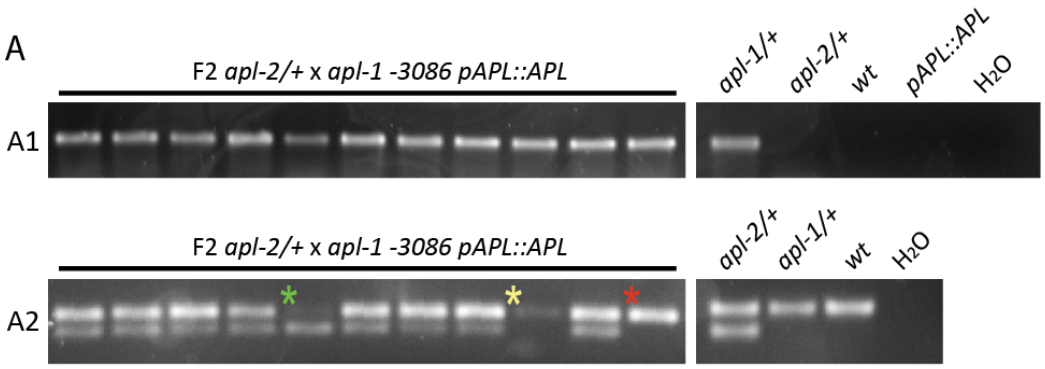

B

	no of plants (%)	*pAPL::APL* pos (%)
apl-1	20 (~35.1)	16 (~80)
apl-1/apl-2	37 (~64.9)	27 (~73)
total	57 (100)	43 (~75.4)

Fig. 4.26: No complementation of *apl-2* by *-3086 pAPL::APL* introduced by crossing. A) 57 seedlings derived from a cross between *apl-2 /+* and complemented *apl-1 -3086 pAPL::APL* plants were genotyped in the F2 generation. All seedlings were positive for *apl-1*; *pAPL::APL* is segregating. Primer combinations A1 for *apl-1* and A2 for *apl-2* (restriction of the *apl-2* derived PCR product) were used, respectively. Primer combination A2 does not produce a PCR product on the *apl-1* allele (except for alleles after *En-1* transposon excision events) but on the *pAPL::APL* construct giving rise to a wild-type like PCR product (not cut). Green asterisk marks genotype *apl-1/apl-2* lacking *pAPL::APL*, yellow *apl-1* lacking *pAPL::APL*, and red *apl-1* positive for *pAPL::APL*; *apl-1/apl-2* positive *pAPL::APL* genotypes are not labeled. DNA from *apl-1/+*, *apl-2/+,* and wild-type (wt) plants and plasmid *-3086 pAPL::APL* were used as controls. **B)** The F2 generation of *apl-2/+* x *apl-1 -3086 pAPL::APL* plants segregates into *apl-1* and *apl-1/apl-2* plants at a ratio of ~1:2, as expected for a lethal allele *apl-2*.

5. Discussion

The establishment of the vascular system is a temporally and spatially highly regulated process demanding integration of environmental and intrinsic signals. Despite the progress being made in cell-type specific transcriptional profiling and in microscopic techniques, the knowledge about the factors required for the specification and differentiation into distinct vascular tissue types, especially into phloem, is still scarce (e.g. (Cano-Delgado et al., 2010)). To date, *APL* is the only factor identified to be essential for phloem differentiation and maintenance (Bonke et al., 2003). In this study, I took advantage of the knowledge about *APL* with the aim to identify novel upstream phloem regulators.

5.1 Essential distal elements and proximal vascular-specific elements within the *APL* promoter

Distinct *cis*-regulatory motifs and combinations in a promoter sequence confer transcriptional regulatory characteristics by providing binding sites for transcription factors. The functional analysis of sub-regions of promoter sequences can reveal the prevalence of these regulatory elements. In turn, these sub-regions can be used for identifying binding factors e.g. in an Y1H screen. Applying this approach to the *APL* promoter, two distinct regions could be defined.

The largest *APL* promoter fragment used in this study comprises the region from -3086 to +356, relative to the transcriptional start site +1. Starting from that, an *APL* promoter deletion series was tested for its potential to complement *apl-1* as well as to activate the *GUS* reporter gene.

A promoter fragment -2587 bp upstream of the transcriptional start, but not -1747 or smaller was able to complement the *apl-1* phenotype (**4.2.4**). Thus, the promoter starting from -2587 was regarded as mediating wild-type like expression of *APL*. Furthermore, the region ranging from -2587 to -1747 bp upstream of the transcriptional start site harbors essential elements for wild-type like *APL* expression. A construct with an internal deletion of this promoter region could validate this function.

In addition, the gradual reduction of the *APL* promoter led to a gradual reduction in GUS activity (**4.2.2**). This suggests that additional activating elements are located at different sites along the promoter.

The promoter starting from -1761 showed reduced GUS activity in comparison to the -2587 construct. Additional reduction of the *APL* promoter down to -140 bp further reduced *GUS* activity but still preserved vascular-specificity. In contrast, complementation of *apl-1* was only achieved with a promoter starting from -2587 construct, but not from -1747 or smaller. Obviously, vascular specificity alone is not sufficient to fully restore *APL* activity but *APL* transcription might have to reach a certain level as well.

Strikingly, lines harboring T-DNA insertions even further downstream than position -1747 showed reduced *APL* expression levels but developed like wild-type (**4.2.1**). Thus, reduced *APL* expression *per se* does not affect plant development in a dramatic way. T-DNA insertions will leave most of the motifs in the promoter intact as they merely interrupt the sequence at a specific location. This suggests that some regulatory elements absent in the deletion construct used for the complementation might be still functional in the T-DNA lines. In turn, the actual distance of the (essential) motifs to the transcriptional start site seems to be less significant.

As already mentioned, vascular-specific *GUS* expression was still detectable with a promoter region starting from -140, but not from -44 or smaller. A region from -142 to +8, thereby largely excluding the 5'UTR, did not activate expression of the GUS reporter in combination with a minimal promoter (*pMin::GUS*) (**4.2.3**). In addition, GUS reporter activity or vascular-specificity was not affected by the deletion of a region from -147 to -46 from the -2587 *APL* promoter.

Thus, elements involved in enhancing gene expression and/or mediating vascular specificity are located in region -140 to -44 and, presumably, allow binding of regulatory factors. As region -140 to -44 is not essential by itself in activating vascular-specific GUS expression, elements with similar functions must be located elsewhere in the promoter. It is possible that the 5'UTR and sequences further downstream, largely excluded from the fragment tested to activate *pMin::GUS*, but present in *-140 pAPL::GUS* are required for enhanced expression.

Taken together, vascular-specific elements are located within proximal regions close to the transcriptional start site and/or further downstream.

In summary, regulatory motifs are distributed along the *APL* promoter operating in conjunction to allow wild-type like activation and expression of *APL*. Elements conferring vascular specificity which are located in a narrow region up- or downstream of the transcriptional start site are still functional in already established vasculature. Additional essential promoter elements further upstream of the transcriptional start site might regulate features like onset, timing, and/or efficiency of *APL* expression.

5.2 BPC factors are involved in transcriptional regulation of *APL*

Taking advantage of the information obtained by the promoter analysis, potential *APL* regulators were identified by performing a Y1H screen with two baits of different lengths (**4.2.5**). A long bait corresponded to the full-length *APL* promoter (-2587 to +356) and a short bait consisted of a double repeat of the region upstream of the transcriptional start site harboring vascular-specific elements (see above) (2x -140 to -1).
The candidates obtained were classified into different categories of interaction confidence, ranging from A, very high, to D, moderate. In addition to candidates from category A to C, four candidates from category D with a predicted localization in the nucleus were considered to have a high chance to act as transcriptional regulators. In total, 13 candidates were selected for future tests, three identified with both baits, and five with the long or the short bait each (see Tab. 4.1).

Among these 13 candidates, I considered the BPC proteins as the most promising ones. This was because they had been isolated by both baits and were annotated to have TF activity (Kooiker et al., 2005; Meister et al., 2004; Monfared et al., 2011). The long bait retrieved BPC1 (5 clones, cat A), the smaller bait retrieved three different BPC members, BPC1 (8 clones, cat A), BPC2 (3 clones, cat B), and BPC4 (2 clones, cat C), respectively (see Tab. 4.1). Thus, BPC factors were represented by different members belonging to either class I (BPC1 and BPC2) or class II (BPC4) (Meister et al., 2004). Their potential influence on *APL* expression was further supported by *in silico* analysis of the *APL*

promoter (**4.2.6**). GA-repeat elements known to provide BPC binding sites (Kooiker et al., 2005; Meister et al., 2004; Monfared et al., 2011; Sangwan and O'Brian, 2002; Santi et al., 2003) were clustered within the 5'UTR (of At1g79430.2, isoform 1) and up to position –66 bp. The reason why BPC factors were more often obtained with the short bait might be due to an increased binding chance because of the repetition of the 140 bp short element. Interestingly, the smaller bait excluded the 5'UTR which might enable binding of additional, maybe other, BPC factors.

Here, it is interesting to mention that the soybean Class I BPC protein (GBP) binds to a GA-repeat in the 5'UTR of the soybean glutamine semialdehyde reductase (*GSA*) gene, involved in heme and chlorophyll synthesis (Sangwan and O'Brian, 2002). In *Arabidopsis*, BPC factors bind to $(GA)_6$ and $(GA)_9$ repeats (Meister et al 2004), and $(GA)_6$ repeats were found in 7% of 3-kb promoter regions of all annotated *Arabidopsis* genes (Monfared et al., 2011). As a purine-rich consensus sequence, which is present in 80% of all *Arabidopsis* promoter regions, was identified to be bound by BPC (Kooiker et al., 2005; Monfared et al., 2011), deviations from pure GA-repeats as binding sites might be also possible in the case of other BPC factors. It was also shown that cooperative binding to multiple BPC1 binding sites induces major conformational changes within the promoter by formation of a higher-order complex (Kooiker et al., 2005). The cooperative binding of elements at large distances interacting by long range chromosome looping is particularly known in animal promoters covering distances of several thousands of base pairs (e.g. (Pan et al., 2008)). Although this mode of action is rarely present in plant promoters (Raatz et al., 2011; Riechmann, 2002) and although it was analyzed for a rather small promoter region of about 1,000 bp in the case of BPC1 (Kooiker et al., 2005), a similar regulatory mechanism could exist for the *APL* promoter as well.

Most *BPC* genes have a widespread expression pattern. In addition, mutant analysis revealed a role for BPCs in several different processes ranging from plant growth to reproduction. This lead to the assumption that BPC factors influence a variety of genes in otherwise unrelated processes, partially redundantly, and also in concert with other regulatory factors (Meister et al., 2004; Monfared et al., 2011).

To further investigate the influence of BPC factors on *APL* transcription *in vivo*, I analyzed the abundance of *APL* transcripts in higher order *bpc* mutants. Importantly, I observed a

reduction of *APL* transcript accumulation especially in the quadruple *bpc1246* mutant (**4.2.7**). The *bpc1246* phenotype is more severe than the *bpc12346*, as BPC3 has, at least partially, antagonistic functions to the other *BPC* genes (Monfared et al., 2011). The reduction in *APL* transcript levels might be less pronounced in *bpc12346* as well, although a conclusive interpretation was hampered by the high standard deviation of results of the qRT-PCR. If BPC factors had a major impact on *APL* transcription I would have expected stronger effects on down-regulating *APL* transcript levels in *bpc* mutants. Thus, BPC factors might act by fine-tuning the level of *APL* transcription. On the other hand, potential redundancy of the still expressed BPC factor BPC7 might mask a major regulatory role.

Analysis of loss and/or gain of function mutants available for other candidates obtained from the Y1H screen will provide further information on *APL* regulation. Electromobility shift assays (EMSA) or chromatin immunoprecipitation experiments could provide confirmation of direct binding of these proteins *in vitro* and *in planta*. As *APL* is known to be expressed during embryogenesis (Bonke et al., 2003), and the Y1H screen was performed using an *Arabidopsis* seedling library, additional *APL* regulators expressed during embryogenesis might be found using a cDNA library generated from embryos.

In summary, the BPC factors are the first candidates identified to have a direct regulatory influence on *APL* transcription, as shown by the Y1H results, the clustering of their binding sites in the proximal promoter region and the reduction of *APL* transcript levels in the *bpc* mutants.

5.3 APL might be involved in early embryogenesis

The second approach aiming for isolation of factors upstream of *APL* was the *in vivo* luciferase-based mutagenesis screen. The seedling-lethal *apl-1* mutant carrying the *pAPL::LUC* construct showed a strongly reduced luminescence suggesting that factors affecting phloem (vascular) development were possible to isolate (**4.3.2**). *apl-1 pAPL::GUS* seedlings also exhibited a clear, although slightly reduced and patchy pattern

of GUS staining. Thus, APL itself could affect its own expression directly, although a reduction might be an indirect consequence of the vascular defects in *apl-1*. Furthermore, the potential to isolate mutant candidates based on changes in luciferase activity was demonstrated by the isolation of four mutants with reduced signal intensities, each of them harboring a mutation in the *LUC* reporter gene (**4.3.3**). The repeated isolation of *LUC* mutants in addition to the lack of the isolation of other mutants including novel *apl* alleles led to the assumption that mutations in *APL* upstream regulators and in *APL* itself are lethal prior to the stage when plants were screened. Analysis of the novel *apl-2* allele which was available from the stock center supported this idea (**4.3.4**). *apl-2/+* plants were embryo-lethal with a ratio of about 25% of aborted seeds in siliques of heterozygous parents as expected for a lethal mutation with recessive inheritance.

5.4 What is the difference between *apl-1* and *apl-2*?

A cross between *apl-1*, the phloem-defective seedling-lethal allele (Bonke et al., 2003), and *apl-2/+* plants resulted in *apl-1/apl-2* F1 seedlings with an *apl-1*-like phenotype (**4.3.7**) showing that *apl-1* and *apl-2* are allelic and that *apl-2* is not more active than *apl-1*.

apl-1 was identified in a mutagenesis screen using the *En-1* transposon insertion system. *En-1* transposons were reported to be frequently excised in somatic and germline cells (Cardon et al., 1993; Schwarz-Sommer et al., 1985). Excision of the transposon often leaves footprints, small deletions and insertions at the site of the former transposon (Cardon et al., 1993; Haring et al., 1991; Rinehart et al., 1997; Schwarz-Sommer et al., 1985; Wessler, 1988) or restores the original sequence (Baran et al., 1992; Rinehart et al., 1997; Scott et al., 1996). In contrast, *apl-2* which is derived from an EMS-mutagenesis screen carries a stable point mutation generating a premature stop codon (Till et al., 2003). Sequencing of the *APL* locus in *apl-1* mutants demonstrated that excision events take place, as described before (Bonke et al., 2003). Furthermore, in about 50% of the excision events the *APL* wild-type sequence was restored allowing the *APL* gene to be fully functional (**4.3.5**).

At this point, the question arose whether excision events could explain the different severity of the *apl-1* and *apl-2* alleles, and allow *apl-1* plants to develop until the seedling stage. To answer this question, I tested the possibility if excision events could rescue the *apl-1* phenotype after a prolonged growth period. In addition, it was important to analyze *apl-2* embryogenesis in more detail. Hence, I will recapitulate these experiments in the following parts of the discussion.

5.5 *apl-1* mutants did not recover during prolonged growth

If transposon excisions were able to activate *APL* expression in a sufficient number of cells of *apl-1* seedlings one would expect that, at some point, the typical shortened root and the stunted growth phenotype should be ameliorated or restored. Growing *apl-1* seedlings for almost four months did not visibly alter the *apl-1* root phenotype and seedlings continued producing stunted leaves (**4.3.6**). The following aspects have to be considered concerning a possible rescue of *apl-1* plants at later stages.

One has to take into account in which cells the *APL* sequence is restored. Presumably, it has to be a meristematic, a cambium- or a phloem-related cell with the potential to either give rise to a phloem-precursor or to differentiate into phloem (SE/CC). As all these cell types include a rather small number of cells the chance of excision at the right place resulting in a restored sequence might be quite low. Furthermore, if the excision event occurs very early during embryogenesis, plants might be indistinguishable from heterozygous plants.

It is questionable whether severe vascular defects can be restored at all. With the exception of cells present in apical meristems, the sector of daughter cells which derives from a potentially *APL* expressing cell will be small, which limits the zone of potential wild-type like phloem in the *apl-1* plant. Especially, if APL's action is cell-autonomous (Bonke et al., 2003), a fully restored vasculature is unlikely. Interestingly, it was reported that seven days old *apl-1* seedlings developed sieve element-like structures (Truernit et al., 2008) being in line with potential *APL* recovery and partial restoration. Still, whereas early phloem-markers were detected in *apl-1* (Bauby et al., 2007; Truernit et al., 2008) other phloem markers for protophloem SEs and CCs were absent (Bonke et al., 2003). A possible reason might be a different developmental onset of expression of individual

phloem markers or an altered expression profile of the hybrid phloem-xylem cells in *apl-1* (Truernit et al., 2008).

In summary, lack of *apl-1* recovery during later stages is plausible despite transposon excisions.

5.6 Controversial views on APL's importance during early embryogenesis

In *apl-2/+* plants, embryo development is severely affected, showing cell division defects as early as the octant stage resulting in embryo-lethality (**4.3.8**). In addition, the abortion ratio matches with the expected value of about 25% for a recessive allele (**4.3.4**). A cross between *apl-2/+* and *apl-1/+* plants, giving rise to *apl-1*-like seedlings, demonstrated that *apl-2* is defective in APL activity and confirmed that *apl-1* and *apl*-2 are allelic (**4.3.7**). These observations strongly argue for an essential role for APL during early embryogenesis.

To prove this theory it is important to rescue the *apl-2* phenotype by expressing *APL* in the *apl-2* mutant. Still, *apl-2* rescue was not achieved with the constructs successfully used to complement the seedling-lethal *apl-1* phenotype (**4.2.4**; **4.3.13**). Neither transformation of the constructs into *apl-2/+* plants nor the cross of *apl-2/+* to complemented *apl-1* plants rescued *apl-2* embryogenesis. One reason could be that promoter motifs important for activity during the early embryogenesis are located downstream or upstream of the region cloned in the construct. Expressing *APL* from a promoter known to be active during early embryogenesis (e.g. the promoter of the ribosomal protein gene *RPS5a* (Weijers et al., 2001) could clarify the question about missing promoter motifs.

Another possible reason to explain the failed complementation is the generation of *apl-2* by EMS-mutagenesis. In order to remove background mutations I crossed *apl-2/+* plants five times back to wild-type plants. Thereby, ~97% of the EMS-mutated genomic background should have been exchanged by non-mutagenized sequences. Still, one cannot rule out that *apl-2* might harbor a second mutation tightly linked to the *APL* locus which is responsible for the embryo-lethal phenotype.

Embryo-lethality due to the production of a truncated protein from the *apl-2* locus mediating a dominant-negative effect is unlikely as *apl-2* is a recessive allele.

In contrast to *apl-2*, embryo-lethality had not been observed in *apl-1*. The *apl-1* mutation gives rise to a reproducible phenotype with short roots and retarded growth, being seedling-lethal. Within this study, transposon excision events known to take place in general (Baran et al., 1992; Cardon et al., 1993; Rinehart et al., 1997; Schwarz-Sommer et al., 1985; Scott et al., 1996) as well as in *apl-1* (Bonke et al., 2003), were confirmed (**4.3.5**). In addition, the restoration of the wild-type *APL* allele in *apl-1* was demonstrated creating potential *APL* expressing loci. This could provide an explanation for the difference between *apl-1* and *apl-2* phenotypes.
If the difference between *apl-1* and *apl-2* is indeed the unstable transposon one has to consider that the excision has to take place in a way to overcome embryo-lethality. Thus, excisions have to occur very early, during the first divisions up to the four-cell stage, prior to the defects observed in *apl-2*. Furthermore, excisions have to give rise to a functional APL protein. Both conditions need to be fulfilled to enable a normal initial development. A high frequency of both events is difficult to imagine which would, however, be required to explain normal *apl-1* embryogenesis. In addition, if the frequency of excisions is very high in early embryogenesis one might assume that embryos develop like wild-type and are not distinguishable from *apl-1/+* plants. Moreover, frequent early excision would implicate usually large parts of *apl-1* seedlings being '*apl-1/+*' which was not observed during this study. The excision events in *apl-1* would also have to explain why *apl-1* was not dependent on a rescue by expressing *APL* during early embryogenesis in contrast to *apl-2*.

Taken together, the observed defects in *apl-2* strongly support a role of APL during early embryogenesis. Due to the so far not achieved complementation of *apl-2* and some contradictory behavior of *apl-1*, *APL*'s role needs to be further defined.

5.7 How to combine transposon excisions, *apl-1* embryogenesis, and *apl-2* defects?

Here, I would like to provide a suggestion how random excision events in *apl-1* embryogenesis and, at the same time, a uniform seedling-lethal phenotype can be explained. In addition, my model will also explain the discrepancy between the lack of an embryonic defect during early *apl-1* embryogenesis and the early aberrant divisions resulting in an embryo-lethal phenotype in the case of *apl-2*.

So far, *APL* has only been considered to act cell-autonomously and in the embryo itself. Another possibility would be that APL has a function in the endosperm or that it acts non-cell-autonomously from the endosperm on the embryo. According to public expression databases, *APL* is expressed at very low levels in the endosperm, similarly as in the early embryo itself (Winter et al., 2007). There is no conclusive evidence for a role of the endosperm in embryo patterning (Peris et al., 2010). Still, embryo and endosperm develop simultaneously, and based on mutant studies their growth might be interdependent (Berger et al., 2006).

In *Arabidopsis*, the initial endosperm nucleus divides repeatedly without cell wall formation, resulting in a coenocytic endosperm (comparable to a syncytium), thus, lacking cell borders. The nuclei are located at the periphery of a giant single cell (Dumas and Rogowsky, 2008). Subsequent divisions result in about 200 nuclei before cellularization of the endosperm takes place which is initiated after the globular stage of the embryo. At the two/four cell stage about 44 to 48 nuclei are present in the endosperm (Boisnard-Lorig et al., 2001).

Thus, there is a large amount of nuclei and, in particular, haplotypes as the endosperm is triploid. This creates a large repertoire of possible locations for excision events in *apl-1* (the endosperm is homozygous for *apl-1* in case of *apl-1* homozygous embryos), and the chance of a successful restoration of *APL* expression is highly increased. As the initial endosperm lacks cell borders the localization of restored *APL* expression would not be crucial. Restored *APL* expression in the endosperm could therefore rescue *apl-1* embryogenesis during early stages. If APL's function during early embryogenesis in the endosperm is independent of its requirement for phloem-development later, it also

provides an explanation why *apl-1* would finally develop a seedling-defect but was able to survive early embryogenesis. If *RPS5a* driven *APL* expression is able to rescue *apl-2* embryogenesis, one could further differentiate between APL's location of function using promoters specific for the endosperm and the early embryo, respectively. The gene *MINISEED3* is expressed in the endosperm immediately after fertilization and then in the globular stage embryo, leaving a temporal gap to monitor *apl-2* embryos for a potential rescue by endosperm-specific *APL* expression (Luo et al., 2005). The *PIN1* promoter could be used for embryo-specific expression (Friml et al., 2003). Diverse functions of APL could be explained by differential interactions with other proteins via its coiled-coil domain e.g. resulting in endosperm/embryo- and seedling-specific heterodimers, respectively. A yeast two-hybrid screen could reveal potential APL interacting proteins.

Thus, if *APL* is functional in the endosperm, transposon excisions in *apl-1* explain both: the reproducibility of the seedling-lethal phenotype of *apl-1* as well as normal *apl-1* embryogenesis in contrast to embryo-lethality in *apl-2*.
A detailed analysis of onset and pattern of embryonic *APL* expression, including the endosperm, is a prerequisite for further investigations.

5.8 Is APL involved in regulation of cell division planes?

Initially, I expected APL to be involved only in phloem development (Bonke et al., 2003). Still, already the first dissections of aborted embryos within *apl-2/+* derived siliques suggested an earlier role of APL because bilateral symmetry was not established and aborted *apl-2* embryos appeared roundish (**4.3.4**). At the dermatogen stage, the inner cells, the progenitors of the vascular and ground tissues, are formed and subsequently the procambium is established from early globular stage onwards (Peris et al., 2010; Scarpella and Helariutta, 2010). Expecting a role for APL during vascular development, I concentrated my analysis from the dermatogen stage on.

Siliques from *apl-2/+* plants harbored embryos with aberrant phenotypes in comparison to wild-type like embryos within the same silique. Thus, I assumed that these are *apl-2* homozygous embryos. *apl-2* embryos tended to divide and grow more slowly than wild-type like embryos (**4.3.8**). For instance, *apl-2* embryos consisted of eight cells when wild-

type like embryos had reached dermatogen stage. Their appearance was very similar during the dermatogen to globular stage of corresponding wild-type like embryos. Based on these observations, I conclude that in *apl-2* embryos cell divisions are delayed or omitted.

The most unexpected observation was that the defects in *apl-2* embryos were already observed in the 'octant' stage where at least two out of eight cells showed an altered cell division pattern. In wild-type four-cell stage embryos, cells divide transversally giving rise to eight cells, four in an upper and four in a lower tier (e.g. (Jenik et al., 2007; Peris et al., 2010). The aberrant cell pattern in *apl-2* embryos likely derives from an altered cell plane orientation at the four-cell stage. Instead of uniform transversal divisions, cells divide along a rather longitudinal (or tangential) plane, perpendicular in reference to the division plane of suspensor cells (see Fig. 4.20).

Interestingly, the asymmetric divisions giving rise to SEs (tangential) and CC files (periclinal) (see Fig. 1.6) were partially delayed in roots of *apl-1* seedlings and it was suggested that APL might be required for phloem-specific asymmetric cell divisions (Bonke et al., 2003). Thus, it is tempting to speculate that APL is involved in determining cell division planes during early embryogenesis as well. However, neither the *apl-2* phenotype was completely penetrant in terms of that not always all four cells encountered these aberrant divisions, nor is APL itself sufficient for phloem differentiation (Bonke et al., 2003). Therefore, I assume that APL operates in conjunction with other factors.

Correct positioning of cell division planes also involves auxin flow and PIN polarity in a so far not completely understood interaction with cytoskeletal rearrangements (Dhonukshe et al., 2005a). Cell division plane defects were observed in mutants defective in polar auxin transport or signaling like *gnom, bdl*, *pin*, or *mp*, (Berleth and Jurgens, 1993; Friml et al., 2003; Friml et al., 2004; Hamann et al., 2002; Hamann et al., 1999; Mayer et al., 1993; Shevell et al., 2000; Shevell et al., 1994) as well as in tobacco cells treated with auxin efflux inhibitors (Dhonukshe et al., 2005b; Petrasek et al., 2002). For instance, *gnom* zygotes do not undergo the typical asymmetric division producing a small apical and a larger basal cell but produce two rather symmetric cells (Mayer et al., 1993) and, *mp* and *bdl* embryos both display altered division planes in the apical daughter of the zygote (Berleth and Jurgens, 1993; Hamann et al., 2002; Hamann et al., 1999).

Subsequently, divisions of the presumptive hypophysis are defective as well (Berleth and Jurgens, 1993; Hamann et al., 2002; Hamann et al., 1999; Mayer et al., 1993). I observed aberrant initial divisions of the embryo proper with subsequent defects at the site of the presumptive hypophysis in *apl-2* embryos (Fig. 4.19 and Fig. 4.21). Expression of the PIN1-GFP reporter was reduced in *apl-2* embryos throughout all developmental stages examined and was localized in a varying pattern also ectopically from globular stage on (**4.3.9**, Fig. 4.21). This suggests that auxin flow and, in turn, the establishment of the distribution/maxima required for normal patterning might be altered in *apl-2*. It remains open whether defects in auxin signaling are causative for the division defects in *apl-2*. It will be interesting to visualize auxin maxima in *apl-2* by auxin responsive *DR5* reporters (Ulmasov et al., 1997) as well as to visualize localization of other PIN proteins like embryonically expressed PIN4 or PIN7 (Friml et al., 2003).

Investigation of cytoskeletal and cell division-related components might provide further insight into *apl-2* derived defects. It would be very exciting if APL is involved in decisions about cell division orientation already in early embryogenesis. APL might be involved in the integration of intrinsic and external signals, affecting one of the players in the cell division system during different stages of development.

5.9 *APL* and tissue patterning

Auxin signaling has an important role in embryo pattern formation (e.g. (Jenik et al., 2007; Moller and Weijers, 2009)). Although there are indications for defects in the distribution and levels of the PIN1 auxin exporter during *apl-2* embryogenesis, basic tissue patterning seems to take place. Transcripts of the procambium expressed gene *ATHB8* (Baima et al., 1995) were detectable within the presumptive provascular cells of *apl-2* embryos around the time they were usually aborted (**4.3.10**). Thus, despite the aberrant divisions, *apl-2* embryos retain the potential to establish a provascular-like domain and detection of other tissue-specific marker genes will reveal whether basic tissues (epidermis, ground and vascular tissues) are formed in *apl-2* in general. This is in line with the assumption that the highly organized divisions in embryos are not essential for cell fate specification in general (Moller and Weijers, 2009; Torres-Ruiz and Jurgens,

1994). For example, embryos of mutants defective in the *FASS* gene show severely altered cell divisions but are still able to produce a basic body plan (Torres-Ruiz and Jurgens, 1994).

Thus, positional cues still serve as patterning determinants in *apl-2* which argues against a major role of *APL* in cell fate specification during early embryogenesis. On the other hand, PIN1-GFP was aberrantly localized e.g. in presumptive basal embryo domains usually not expressing *PIN1* (Fig. 4.21) which might lead to defects in apical-basal polarity. Although defects during embryogenesis of some mutants have been shown to be transient or get ameliorated (e.g. (Bayer et al., 2009; Friml et al., 2003; Ueda et al., 2011)), defects elicited in *apl-2* are not restored. As alternative mechanisms obviously do not save the embryos, a fundamental developmental process, possibly connected to cell division (see **5.8**), seems to be affected in *APL*-deficient plants.

5.10 Conclusions

APL has been identified to be crucial for phloem differentiation and maintenance (Bonke et al., 2003). So far, no information concerning *APL* regulation has been available, and information regarding phloem differentiation is scarce in general. The identification of *APL* upstream regulators is, thus, informative in both respects.

Within this study, members of the BPC TF family were identified as the first candidates for having a direct regulatory effect on *APL* transcription. This view is supported by the prevalence of different members of BPC factors isolated by the Y1H screen (**4.2.5**), the clustering of their binding sites in the proximal promoter region (**4.2.6**) and the reduction of *APL* transcript levels in the *bpc* mutants (**4.2.7**).

The widespread distribution of regulatory elements along the *APL* promoter (**4.2.6**), including the identification of essential and vascular-specific elements (**4.2.2**, **4.2.4**), suggests a combinatorial action of several TFs in regulating *APL* expression. So far unknown regulatory modules might be present and might be revealed by exploiting additional bioinformatics tools. Further evaluation of potential *APL* regulators identified by the Y1H screen in combination with proceeding examination of *APL* promoter regions will allow gaining more insight into *APL* regulation and, in turn, phloem development.

Based on the characterization of the novel *apl-2* allele, a function for *APL* during early embryogenesis not related to vascular development is possible. Due to parallels between the defects described for the *apl-1* mutant, showing APL to be involved in asymmetric cell divisions during phloem differentiation (Bonke et al., 2003), and the defects in the orientation of cell division planes in *apl-2* embryos (**4.3.8**), it is tempting to speculate that APL functions in general in orienting the cell division plane. A link between cell plane orientation and the PIN/auxin machinery has been described (e.g. (Berleth and Jurgens, 1993; Dhonukshe et al., 2005a; Friml et al., 2003; Friml et al., 2004; Hamann et al., 2002; Hamann et al., 1999; Mayer et al., 1993; Shevell et al., 2000; Shevell et al., 1994)). An involvement for PIN/auxin in the defects observed in *apl-2* is in line with the observed mislocalization of PIN1 from globular stage on (**4.3.9**). Interpretation of *apl-2* defects also requires a detailed analysis of early embryonic *APL* expression pattern, especially considering the speculations on APL's function in the endosperm. Future experiments can address APL's function in phloem development/maintenance and asymmetric cell divisions also by induced down-regulation of *APL*, taking advantage of the amiRNA line generated in this study (**4.3.12**). The demonstration of a role of *APL* in endosperm-embryo communication would open up a fascinating avenue.

Thus, this work provides several directions for future research to investigate specifically *APL* regulation and function and phloem development in general.

6. References

Abe, M., Katsumata, H., Komeda, Y. and Takahashi, T. (2003). Regulation of shoot epidermal cell differentiation by a pair of homeodomain proteins in Arabidopsis. *Development* **130**, 635-43.
Agusti, J., Lichtenberger, R., Schwarz, M., Nehlin, L. and Greb, T. (2011). Characterization of Transcriptome Remodeling during Cambium Formation Identifies MOL1 and RUL1 as Opposing Regulators of Secondary Growth. *PLoS Genet* **7**, e1001312.
Aida, M., Ishida, T., Fukaki, H., Fujisawa, H. and Tasaka, M. (1997). Genes involved in organ separation in Arabidopsis: an analysis of the cup-shaped cotyledon mutant. *Plant Cell* **9**, 841-57.
Aida, M., Ishida, T. and Tasaka, M. (1999). Shoot apical meristem and cotyledon formation during Arabidopsis embryogenesis: interaction among the CUP-SHAPED COTYLEDON and SHOOT MERISTEMLESS genes. *Development* **126**, 1563-70.
Aloni, R. (2001). Foliar and Axial Aspects of Vascular Differentiation: Hypotheses and Evidence. 22-34.
Aloni, R., Aloni, E., Langhans, M. and Ullrich, C. I. (2006). Role of cytokinin and auxin in shaping root architecture: regulating vascular differentiation, lateral root initiation, root apical dominance and root gravitropism. *Ann Bot* **97**, 883-93.
Alonso, J. M., Stepanova, A. N., Leisse, T. J., Kim, C. J., Chen, H., Shinn, P., Stevenson, D. K., Zimmerman, J., Barajas, P., Cheuk, R. et al. (2003). Genome-wide insertional mutagenesis of Arabidopsis thaliana. *Science* **301**, 653-7.
Baima, S., Nobili, F., Sessa, G., Lucchetti, S., Ruberti, I. and Morelli, G. (1995). The expression of the Athb-8 homeobox gene is restricted to provascular cells in Arabidopsis thaliana. *Development* **121**, 4171-4182.
Baran, G., Echt, C., Bureau, T. and Wessler, S. (1992). Molecular analysis of the maize wx-B3 allele indicates that precise excision of the transposable Ac element is rare. *Genetics* **130**, 377-84.
Barton, M. K. and Poethig, R. S. (1993). Formation of the shoot apical meristem in Arabidopsis thaliana: an analysis of development in the wild type and in the shoot meristemless mutant. *Development* **119**, 823-831.
Bauby, H., Divol, F., Truernit, E., Grandjean, O. and Palauqui, J. C. (2007). Protophloem differentiation in early Arabidopsis thaliana development. *Plant Cell Physiol* **48**, 97-109.
Baucher, M., El Jaziri, M. and Vandeputte, O. (2007). From primary to secondary growth: origin and development of the vascular system. *J Exp Bot*.
Bayer, M., Nawy, T., Giglione, C., Galli, M., Meinnel, T. and Lukowitz, W. (2009). Paternal control of embryonic patterning in Arabidopsis thaliana. *Science* **323**, 1485-8.
Benfey, P. N. and Chua, N. H. (1990). The Cauliflower Mosaic Virus 35S Promoter: Combinatorial Regulation of Transcription in Plants. *Science* **250**, 959-66.
Benfey, P. N., Ren, L. and Chua, N. H. (1990). Tissue-specific expression from CaMV 35S enhancer subdomains in early stages of plant development. *EMBO J* **9**, 1677-84.
Benkova, E., Michniewicz, M., Sauer, M., Teichmann, T., Seifertova, D., Jürgens, G. and Friml, J. (2003). Local, efflux-dependent auxin gradients as a common module for plant organ formation. *Cell* **115**, 591-602.
Berger, F., Grini, P. E. and Schnittger, A. (2006). Endosperm: an integrator of seed growth and development. *Curr Opin Plant Biol* **9**, 664-70.
Berleth, T. and Jurgens, G. (1993). The role of the monopteros gene in organising the basal body region of the Arabidopsis embryo. *Development* **118**, 575-587.
Birnbaum, K., Shasha, D. E., Wang, J. Y., Jung, J. W., Lambert, G. M., Galbraith, D. W. and Benfey, P. N. (2003). A gene expression map of the Arabidopsis root. *Science* **302**, 1956-60.
Bishopp, A., Help, H., El-Showk, S., Weijers, D., Scheres, B., Friml, J., Benkova, E., Mahonen, A. P. and Helariutta, Y. (2011a). A mutually inhibitory interaction between auxin and cytokinin specifies vascular pattern in roots. *Curr Biol* **21**, 917-26.

Bishopp, A., Lehesranta, S., Vaten, A., Help, H., El-Showk, S., Scheres, B., Helariutta, K., Mahonen, A. P., Sakakibara, H. and Helariutta, Y. (2011b). Phloem-transported cytokinin regulates polar auxin transport and maintains vascular pattern in the root meristem. *Curr Biol* **21**, 927-32.

Boisnard-Lorig, C., Colon-Carmona, A., Bauch, M., Hodge, S., Doerner, P., Bancharel, E., Dumas, C., Haseloff, J. and Berger, F. (2001). Dynamic analyses of the expression of the HISTONE::YFP fusion protein in arabidopsis show that syncytial endosperm is divided in mitotic domains. *Plant Cell* **13**, 495-509.

Bonke, M. (2004). PhD thesis: The Roles of WOL and APL in phloem development in Arabidopsis thaliana roots. Institute of Biotechnology and Department of Biological and Environmental Sciences, Division of Genetics, Faculty of Biosciences, and Viikki Graduate School in Biosciences, University of Helsinki.

Bonke, M., Thitamadee, S., Mähönen, A. P., Hauser, M. T. and Helariutta, Y. (2003). APL regulates vascular tissue identity in Arabidopsis. *Nature* **426**, 181-186.

Bougourd, S., Marrison, J. and Haseloff, J. (2000). Technical advance: an aniline blue staining procedure for confocal microscopy and 3D imaging of normal and perturbed cellular phenotypes in mature Arabidopsis embryos. *Plant J* **24**, 543-50.

Bowman, J. L., Alvarez, J., Weigel, D., Meyerowitz, E. M. and Smyth, D. R. (1993). Control of flower development in Arabidopsis thaliana by APETALA1 and interacting genes. *Development* **119**, 721-743.

Brady, S. M., Orlando, D. A., Lee, J. Y., Wang, J. Y., Koch, J., Dinneny, J. R., Mace, D., Ohler, U. and Benfey, P. N. (2007). A high-resolution root spatiotemporal map reveals dominant expression patterns. *Science* **318**, 801-6.

Brady, S. M., Zhang, L., Megraw, M., Martinez, N. J., Jiang, E., Yi, C. S., Liu, W., Zeng, A., Taylor-Teeples, M., Kim, D. et al. (2011). A stele-enriched gene regulatory network in the Arabidopsis root. *Mol Syst Biol* **7**, 459.

Breuninger, H., Rikirsch, E., Hermann, M., Ueda, M. and Laux, T. (2008). Differential expression of WOX genes mediates apical-basal axis formation in the Arabidopsis embryo. *Dev Cell* **14**, 867-76.

Busse, J. S. and Evert, R. F. (1999). Vascular differentiation and transition in the seedling of Arabidopsis thaliana (Brassicaceae). *International Journal of Plant Sciences* **160**, 241-251.

Cano-Delgado, A., Lee, J. Y. and Demura, T. (2010). Regulatory Mechanisms for Specification and Patterning of Plant Vascular Tissues. *Annu Rev Cell Dev Biol*.

Cano-Delgado, A., Yin, Y., Yu, C., Vafeados, D., Mora-Garcia, S., Cheng, J. C., Nam, K. H., Li, J. and Chory, J. (2004). BRL1 and BRL3 are novel brassinosteroid receptors that function in vascular differentiation in Arabidopsis. *Development* **131**, 5341-5351.

Capron, A., Chatfield, S., Provart, N. and Berleth, T. (2009). Embryogenesis: Pattern Formation from a Single Cell. *The Arabidopsis Book*, 1-28.

Cardon, G. H., Frey, M., Saedler, H. and Gierl, A. (1993). Mobility of the maize transposable element En/Spm in Arabidopsis thaliana. *Plant J* **3**, 773-84.

Carlsbecker, A., Lee, J. Y., Roberts, C. J., Dettmer, J., Lehesranta, S., Zhou, J., Lindgren, O., Moreno-Risueno, M. A., Vaten, A., Thitamadee, S. et al. (2010). Cell signalling by microRNA165/6 directs gene dose-dependent root cell fate. *Nature* **465**, 316-21.

Chattopadhyay, S., Puente, P., Deng, X. W. and Wei, N. (1998). Combinatorial interaction of light-responsive elements plays a critical role in determining the response characteristics of light-regulated promoters in Arabidopsis. *Plant J* **15**, 69-77.

Chinnusamy, V., Stevenson, B., Lee, B. H. and Zhu, J. K. (2002). Screening for gene regulation mutants by bioluminescence imaging. *Sci STKE* **2002**, pl10.

Clay, N. K. and Nelson, T. (2002). VH1, a provascular cell-specific receptor kinase that influences leaf cell patterns in Arabidopsis. *Plant Cell* **14**, 2707-22.

Clough, S. J. and Bent, A. F. (1998). Floral dip: a simplified method for Agrobacterium-mediated transformation of Arabidopsis thaliana. *Plant J* **16**, 735-43.
De Smet, I., Lau, S., Mayer, U. and Jurgens, G. (2010). Embryogenesis - the humble beginnings of plant life. *Plant J* **61**, 959-70.
Deplancke, B., Dupuy, D., Vidal, M. and Walhout, A. J. (2004). A gateway-compatible yeast one-hybrid system. *Genome Res* **14**, 2093-101.
Deveaux, Y., Peaucelle, A., Roberts, G. R., Coen, E., Simon, R., Mizukami, Y., Traas, J., Murray, J. A., Doonan, J. H. and Laufs, P. (2003). The ethanol switch: a tool for tissue-specific gene induction during plant development. *Plant J* **36**, 918-30.
Dhonukshe, P., Kleine-Vehn, J. and Friml, J. (2005a). Cell polarity, auxin transport, and cytoskeleton-mediated division planes: who comes first? *Protoplasma* **226**, 67-73.
Dhonukshe, P., Mathur, J., Hulskamp, M. and Gadella, T. W., Jr. (2005b). Microtubule plus-ends reveal essential links between intracellular polarization and localized modulation of endocytosis during division-plane establishment in plant cells. *BMC Biol* **3**, 11.
Dinneny, J. R. and Yanofsky, M. F. (2004). Vascular patterning: xylem or phloem? *Curr Biol* **14**, R112-4.
Donner, T. J., Sherr, I. and Scarpella, E. (2009). Regulation of preprocambial cell state acquisition by auxin signaling in Arabidopsis leaves. *Development* **136**, 3235-46.
Dubos, C., Stracke, R., Grotewold, E., Weisshaar, B., Martin, C. and Lepiniec, L. (2010). MYB transcription factors in Arabidopsis. *Trends Plant Sci* **15**, 573-81.
Dumas, C. and Rogowsky, P. (2008). Fertilization and early seed formation. *C R Biol* **331**, 715-25.
Elge, S., Brearley, C., Xia, H. J., Kehr, J., Xue, H. W. and Mueller-Roeber, B. (2001). An Arabidopsis inositol phospholipid kinase strongly expressed in procambial cells: synthesis of PtdIns(4,5)P2 and PtdIns(3,4,5)P3 in insect cells by 5-phosphorylation of precursors. *Plant J* **26**, 561-571.
Emery, J. F., Floyd, S. K., Alvarez, J., Eshed, Y., Hawker, N. P., Izhaki, A., Baum, S. F. and Bowman, J. L. (2003). Radial patterning of Arabidopsis shoots by class III HD-ZIP and KANADI genes. *Curr Biol* **13**, 1768-74.
Eshed, Y., Baum, S. F., Perea, J. V. and Bowman, J. L. (2001). Establishment of polarity in lateral organs of plants. *Curr Biol* **11**, 1251-60.
Etchells, J. P. and Turner, S. R. (2010). The PXY-CLE41 receptor ligand pair defines a multifunctional pathway that controls the rate and orientation of vascular cell division. *Development* **137**, 767-774.
Ferrandiz, C., Gu, Q., Martienssen, R. and Yanofsky, M. F. (2000). Redundant regulation of meristem identity and plant architecture by FRUITFULL, APETALA1 and CAULIFLOWER. *Development* **127**, 725-34.
Filichkin, S. A., Priest, H. D., Givan, S. A., Shen, R., Bryant, D. W., Fox, S. E., Wong, W. K. and Mockler, T. C. (2010). Genome-wide mapping of alternative splicing in Arabidopsis thaliana. *Genome Res* **20**, 45-58.
Fisher, K. and Turner, S. (2007). PXY, a Receptor-like Kinase Essential for Maintaining Polarity during Plant Vascular-Tissue Development. *Curr Biol* **17**, 1061-6.
Friml, J., Vieten, A., Sauer, M., Weijers, D., Schwarz, H., Hamann, T., Offringa, R. and Jürgens, G. (2003). Efflux-dependent auxin gradients establish the apical-basal axis of Arabidopsis. *Nature* **426**, 147-153.
Friml, J., Yang, X., Michniewicz, M., Weijers, D., Quint, A., Tietz, O., Benjamins, R., Ouwerkerk, P. B., Ljung, K., Sandberg, G. et al. (2004). A PINOID-dependent binary switch in apical-basal PIN polar targeting directs auxin efflux. *Science* **306**, 862-5.
Fukuda, H. (2004). Signals that control plant vascular cell differentiation. *Nat Rev Mol Cell Biol* **5**, 379-91.
Gao, X., Nagawa, S., Wang, G. and Yang, Z. (2008). Cell polarity signaling: focus on polar auxin transport. *Mol Plant* **1**, 899-909.

Gardiner, J., Sherr, I. and Scarpella, E. (2010). Expression of DOF genes identifies early stages of vascular development in Arabidopsis leaves. *Int J Dev Biol* **54**, 1389-96.
Greb, T., Clarenz, O., Schafer, E., Muller, D., Herrero, R., Schmitz, G. and Theres, K. (2003). Molecular analysis of the LATERAL SUPPRESSOR gene in Arabidopsis reveals a conserved control mechanism for axillary meristem formation. *Genes Dev* **17**, 1175-87.
Greb, T., Mylne, J. S., Crevillen, P., Geraldo, N., An, H., Gendall, A. R. and Dean, C. (2007). The PHD Finger Protein VRN5 Functions in the Epigenetic Silencing of Arabidopsis FLC. *Curr Biol* **17**, 73-8.
Haecker, A., Gross-Hardt, R., Geiges, B., Sarkar, A., Breuninger, H., Herrmann, M. and Laux, T. (2004). Expression dynamics of WOX genes mark cell fate decisions during early embryonic patterning in Arabidopsis thaliana. *Development* **131**, 657-68.
Hamann, T., Benkova, E., Baurle, I., Kientz, M. and Jurgens, G. (2002). The Arabidopsis BODENLOS gene encodes an auxin response protein inhibiting MONOPTEROS-mediated embryo patterning. *Genes Dev* **16**, 1610-5.
Hamann, T., Mayer, U. and Jurgens, G. (1999). The auxin-insensitive bodenlos mutation affects primary root formation and apical-basal patterning in the Arabidopsis embryo. *Development* **126**, 1387-95.
Hames, C., Ptchelkine, D., Grimm, C., Thevenon, E., Moyroud, E., Gerard, F., Martiel, J. L., Benlloch, R., Parcy, F. and Muller, C. W. (2008). Structural basis for LEAFY floral switch function and similarity with helix-turn-helix proteins. *EMBO J* **27**, 2628-37.
Hardtke, C. S. and Berleth, T. (1998). The Arabidopsis gene MONOPTEROS encodes a transcription factor mediating embryo axis formation and vascular development. *EMBO J* **17**, 1405-11.
Haring, M. A., Rommens, C. M., Nijkamp, H. J. and Hille, J. (1991). The use of transgenic plants to understand transposition mechanisms and to develop transposon tagging strategies. *Plant Mol Biol* **16**, 449-61.
Hellens, R. P., Edwards, E. A., Leyland, N. R., Bean, S. and Mullineaux, P. M. (2000). pGreen: a versatile and flexible binary Ti vector for Agrobacterium-mediated plant transformation. *Plant Mol Biol* **42**, 819-32.
Hirakawa, Y., Kondo, Y. and Fukuda, H. (2010). TDIF peptide signaling regulates vascular stem cell proliferation via the WOX4 homeobox gene in Arabidopsis. *Plant Cell* **22**, 2618-29.
Hirakawa, Y., Shinohara, H., Kondo, Y., Inoue, A., Nakanomyo, I., Ogawa, M., Sawa, S., Ohashi-Ito, K., Matsubayashi, Y. and Fukuda, H. (2008). Non-cell-autonomous control of vascular stem cell fate by a CLE peptide/receptor system. *Proc Natl Acad Sci U S A* **105**, 15208-13.
Hofgen, R. and Willmitzer, L. (1988). Storage of competent cells for Agrobacterium transformation. *Nucleic Acids Res* **16**, 9877.
Ilegems, M., Douet, V., Meylan-Bettex, M., Uyttewaal, M., Brand, L., Bowman, J. L. and Stieger, P. A. (2010). Interplay of auxin, KANADI and Class III HD-ZIP transcription factors in vascular tissue formation. *Development* **137**, 975-84.
Izhaki, A. and Bowman, J. L. (2007). KANADI and class III HD-Zip gene families regulate embryo patterning and modulate auxin flow during embryogenesis in Arabidopsis. *Plant Cell* **19**, 495-508.
Jenik, P. D., Gillmor, C. S. and Lukowitz, W. (2007). Embryonic patterning in Arabidopsis thaliana. *Annu Rev Cell Dev Biol* **23**, 207-36.
Jenik, P. D., Jurkuta, R. E. and Barton, M. K. (2005). Interactions between the cell cycle and embryonic patterning in Arabidopsis uncovered by a mutation in DNA polymerase epsilon. *Plant Cell* **17**, 3362-77.
Jeong, S., Palmer, T. M. and Lukowitz, W. (2011). The RWP-RK Factor GROUNDED Promotes Embryonic Polarity by Facilitating YODA MAP Kinase Signaling. *Curr Biol* **21**, 1268-76.
Jin, H. and Martin, C. (1999). Multifunctionality and diversity within the plant MYB-gene family. *Plant Mol Biol* **41**, 577-85.

Johannesson, H., Wang, Y. and Engstrom, P. (2001). DNA-binding and dimerization preferences of Arabidopsis homeodomain-leucine zipper transcription factors in vitro. *Plant Mol Biol* **45**, 63-73.

Johnson, K. L., Degnan, K. A., Ross Walker, J. and Ingram, G. C. (2005). AtDEK1 is essential for specification of embryonic epidermal cell fate. *Plant J* **44**, 114-27.

Johnson, K. L., Faulkner, C., Jeffree, C. E. and Ingram, G. C. (2008). The phytocalpain defective kernel 1 is a novel Arabidopsis growth regulator whose activity is regulated by proteolytic processing. *Plant Cell* **20**, 2619-30.

Kempin, S. A., Savidge, B. and Yanofsky, M. F. (1995). Molecular basis of the cauliflower phenotype in Arabidopsis. *Science* **267**, 522-5.

Kim, H. S., Kim, S. J., Abbasi, N., Bressan, R. A., Yun, D. J., Yoo, S. D., Kwon, S. Y. and Choi, S. B. (2010). The DOF transcription factor Dof5.1 influences leaf axial patterning by promoting Revoluta transcription in Arabidopsis. *Plant J* **64**, 524-35.

Kim, Y., Schumaker, K. S. and Zhu, J. K. (2006). EMS mutagenesis of Arabidopsis. *Methods Mol Biol* **323**, 101-3.

Konieczny, A. and Ausubel, F. M. (1993). A procedure for mapping Arabidopsis mutations using co-dominant ecotype-specific PCR-based markers. *Plant J* **4**, 403-10.

Konishi, M. and Yanagisawa, S. (2007). Sequential activation of two Dof transcription factor gene promoters during vascular development in Arabidopsis thaliana. *Plant Physiol Biochem* **45**, 623-9.

Kooiker, M., Airoldi, C. A., Losa, A., Manzotti, P. S., Finzi, L., Kater, M. M. and Colombo, L. (2005). BASIC PENTACYSTEINE1, a GA binding protein that induces conformational changes in the regulatory region of the homeotic Arabidopsis gene SEEDSTICK. *Plant Cell* **17**, 722-9.

Kubo, M., Udagawa, M., Nishikubo, N., Horiguchi, G., Yamaguchi, M., Ito, J., Mimura, T., Fukuda, H. and Demura, T. (2005). Transcription switches for protoxylem and metaxylem vessel formation. *Genes Dev* **19**, 1855-60.

Lareau, L. F., Brooks, A. N., Soergel, D. A., Meng, Q. and Brenner, S. E. (2007). The coupling of alternative splicing and nonsense-mediated mRNA decay. *Adv Exp Med Biol* **623**, 190-211.

Laux, T., Mayer, K. F., Berger, J. and Jurgens, G. (1996). The WUSCHEL gene is required for shoot and floral meristem integrity in Arabidopsis. *Development* **122**, 87-96.

Laux, T., Wurschum, T. and Breuninger, H. (2004). Genetic regulation of embryonic pattern formation. *Plant Cell* **16 Suppl**, S190-202.

Le Hir, R., Beneteau, J., Bellini, C., Vilaine, F. and Dinant, S. (2008). Gene expression profiling: keys for investigating phloem functions. *Trends Plant Sci* **13**, 273-80.

Lee, J. Y., Colinas, J., Wang, J. Y., Mace, D., Ohler, U. and Benfey, P. N. (2006). Transcriptional and posttranscriptional regulation of transcription factor expression in Arabidopsis roots. *Proc Natl Acad Sci U S A* **103**, 6055-60.

Long, J. A., Moan, E. I., Medford, J. I. and Barton, M. K. (1996). A member of the KNOTTED class of homeodomain proteins encoded by the STM gene of Arabidopsis. *Nature* **379**, 66-69.

Lukowitz, W., Roeder, A., Parmenter, D. and Somerville, C. (2004). A MAPKK kinase gene regulates extra-embryonic cell fate in Arabidopsis. *Cell* **116**, 109-19.

Luo, M., Dennis, E. S., Berger, F., Peacock, W. J. and Chaudhury, A. (2005). MINISEED3 (MINI3), a WRKY family gene, and HAIKU2 (IKU2), a leucine-rich repeat (LRR) KINASE gene, are regulators of seed size in Arabidopsis. *Proc Natl Acad Sci U S A* **102**, 17531-6.

Lupas, A., Van Dyke, M. and Stock, J. (1991). Predicting coiled coils from protein sequences. *Science* **252**, 1162-4.

Luscombe, N. M., Austin, S. E., Berman, H. M. and Thornton, J. M. (2000). An overview of the structures of protein-DNA complexes. *Genome Biol* **1**, REVIEWS001.

Maeo, K., Tokuda, T., Ayame, A., Mitsui, N., Kawai, T., Tsukagoshi, H., Ishiguro, S. and Nakamura, K. (2009). An AP2-type transcription factor, WRINKLED1, of Arabidopsis thaliana

binds to the AW-box sequence conserved among proximal upstream regions of genes involved in fatty acid synthesis. *Plant J* **60**, 476-87.
Mallory, A. and Vaucheret, H. (2010). Form, function, and regulation of ARGONAUTE proteins. *Plant Cell* **22**, 3879-89.
Mason, J. M. and Arndt, K. M. (2004). Coiled coil domains: stability, specificity, and biological implications. *Chembiochem* **5**, 170-6.
Mayer, U., Buttner, G. and Jurgens, G. (1993). Apical-basal pattern formation in the Arabidopsis embryo: studies on the role of the gnom gene. *Development* **117**, 149-162.
McKillup, S. (2006). "Statistics Explained: An Introductory Guide for Life Scientists", Cambridge University Press.
Meister, R. J., Williams, L. A., Monfared, M. M., Gallagher, T. L., Kraft, E. A., Nelson, C. G. and Gasser, C. S. (2004). Definition and interactions of a positive regulatory element of the Arabidopsis INNER NO OUTER promoter. *Plant J* **37**, 426-38.
Metz, A. M., Timmer, R. T. and Browning, K. S. (1992). Sequences for two cDNAs encoding Arabidopsis thaliana eukaryotic protein synthesis initiation factor 4A. *Gene* **120**, 313-4.
Mittelsten Scheid, O., Afsar, K. and Paszkowski, J. (1998). Release of epigenetic gene silencing by trans-acting mutations in Arabidopsis. *Proc Natl Acad Sci USA* **95** 632-637.
Moller, B. and Weijers, D. (2009). Auxin control of embryo patterning. *Cold Spring Harb Perspect Biol* **1**, a001545.
Monfared, M. M., Simon, M. K., Meister, R. J., Roig-Villanova, I., Kooiker, M., Colombo, L., Fletcher, J. C. and Gasser, C. S. (2011). Overlapping and antagonistic activities of BASIC PENTACYSTEINE genes affect a range of developmental processes in Arabidopsis. *Plant J* **66**, 1020-31.
Mouchel, C. F., Osmont, K. S. and Hardtke, C. S. (2006). BRX mediates feedback between brassinosteroid levels and auxin signalling in root growth. *Nature* **443**, 458-61.
Neff, M. M., Turk, E. and Kalishman, M. (2002). Web-based primer design for single nucleotide polymorphism analysis. *Trends Genet* **18**, 613-5.
Nishikawa, T., Nagadoi, A., Yoshimura, S., Aimoto, S. and Nishimura, Y. (1998). Solution structure of the DNA-binding domain of human telomeric protein, hTRF1. *Structure* **6**, 1057-65.
Nodine, M. D., Yadegari, R. and Tax, F. E. (2007). RPK1 and TOAD2 are two receptor-like kinases redundantly required for arabidopsis embryonic pattern formation. *Dev Cell* **12**, 943-56.
Nolan, T., Hands, R. E. and Bustin, S. A. (2006). Quantification of mRNA using real-time RT-PCR. *Nat Protoc* **1**, 1559-82.
Odell, J. T., Nagy, F. and Chua, N. H. (1985). Identification of DNA sequences required for activity of the cauliflower mosaic virus 35S promoter. *Nature* **313**, 810-2.
Ohashi-Ito, K. and Fukuda, H. (2010). Transcriptional regulation of vascular cell fates. *Curr Opin Plant Biol* **13**, 670-6.
Olsen, A. N., Ernst, H. A., Leggio, L. L. and Skriver, K. (2005). NAC transcription factors: structurally distinct, functionally diverse. *Trends Plant Sci* **10**, 79-87.
Oparka, K. J. and Turgeon, R. (1999). Sieve elements and companion cells-traffic control centers of the phloem. *Plant Cell* **11**, 739-50.
Pan, Y. F., Wansa, K. D., Liu, M. H., Zhao, B., Hong, S. Z., Tan, P. Y., Lim, K. S., Bourque, G., Liu, E. T. and Cheung, E. (2008). Regulation of estrogen receptor-mediated long range transcription via evolutionarily conserved distal response elements. *J Biol Chem* **283**, 32977-88.
Peris, C. I., Rademacher, E. H. and Weijers, D. (2010). Green beginnings - pattern formation in the early plant embryo. *Curr Top Dev Biol* **91**, 1-27.
Petrasek, J., Elckner, M., Morris, D. A. and Zazimalova, E. (2002). Auxin efflux carrier activity and auxin accumulation regulate cell division and polarity in tobacco cells. *Planta* **216**, 302-8.
Poethig, R. S., Coe, E. H. and Johri, M. M. (1986). Cell lineage patterns in maize embryogenesis: A clonal analysis. *Developmental Biology* **117**, 392-404.

Prigge, M. J., Otsuga, D., Alonso, J. M., Ecker, J. R., Drews, G. N. and Clark, S. E. (2005). Class III homeodomain-leucine zipper gene family members have overlapping, antagonistic, and distinct roles in Arabidopsis development. *Plant Cell* **17**, 61-76.

Puente, P., Wei, N. and Deng, X. W. (1996). Combinatorial interplay of promoter elements constitutes the minimal determinants for light and developmental control of gene expression in Arabidopsis. *EMBO J* **15**, 3732-43.

Pyo, H., Demura, T. and Fukuda, H. (2004). Spatial and temporal tracing of vessel differentiation in young Arabidopsis seedlings by the expression of an immature tracheary element-specific promoter. *Plant Cell Physiol* **45**, 1529-1536.

Qu, L. J. and Zhu, Y. X. (2006). Transcription factor families in Arabidopsis: major progress and outstanding issues for future research. *Curr Opin Plant Biol* **9**, 544-9.

Raatz, B., Eicker, A., Schmitz, G., Fuss, E., Muller, D., Rossmann, S. and Theres, K. (2011). Specific expression of LATERAL SUPPRESSOR is controlled by an evolutionarily conserved 3' enhancer. *Plant J*.

Ramsay, N. A. and Glover, B. J. (2005). MYB-bHLH-WD40 protein complex and the evolution of cellular diversity. *Trends Plant Sci* **10**, 63-70.

Riechmann, J. L. (2002). Transcriptional Regulation: a Genomic Overview. *The Arabidopsis Book*, e0085.

Riechmann, J. L., Heard, J., Martin, G., Reuber, L., Jiang, C., Keddie, J., Adam, L., Pineda, O., Ratcliffe, O. J., Samaha, R. R. et al. (2000). Arabidopsis transcription factors: genome-wide comparative analysis among eukaryotes. *Science* **290**, 2105-10.

Rinehart, T. A., Dean, C. and Weil, C. F. (1997). Comparative analysis of non-random DNA repair following Ac transposon excision in maize and Arabidopsis. *Plant J* **12**, 1419-27.

Roslan, H. A., Salter, M. G., Wood, C. D., White, M. R., Croft, K. P., Robson, F., Coupland, G., Doonan, J., Laufs, P., Tomsett, A. B. et al. (2001). Characterization of the ethanol-inducible alc gene-expression system in Arabidopsis thaliana. *Plant J* **28**, 225-35.

Ruiz-Medrano, R., Xoconostle-Cazares, B. and Lucas, W. J. (2001). The phloem as a conduit for inter-organ communication. *Curr Opin Plant Biol* **4**, 202-9.

Sablok, G., Perez-Quintero, A. L., Hassan, M., Tatarinova, T. V. and Lopez, C. (2011). Artificial microRNAs (amiRNAs) engineering - On how microRNA-based silencing methods have affected current plant silencing research. *Biochem Biophys Res Commun* **406**, 315-9.

Sambrook, J. and Russell D. (2001)." Molecular Cloning: A Laboratory Manual", Cold Spring Harbor Laboratory Press, Cold Spring Harbor, New York, Third Edition.

Sanchez, R. and Zhou, M. M. (2011). The PHD finger: a versatile epigenome reader. *Trends Biochem Sci* **36**, 364-72.

Sangwan, I. and O'Brian, M. R. (2002). Identification of a soybean protein that interacts with GAGA element dinucleotide repeat DNA. *Plant Physiol* **129**, 1788-94.

Santi, L., Wang, Y., Stile, M. R., Berendzen, K., Wanke, D., Roig, C., Pozzi, C., Muller, K., Muller, J., Rohde, W. et al. (2003). The GA octodinucleotide repeat binding factor BBR participates in the transcriptional regulation of the homeobox gene Bkn3. *Plant J* **34**, 813-26.

Saulsberry, A., Martin, P. R., O'Brien, T., Sieburth, L. E. and Pickett, F. B. (2002). The induced sector Arabidopsis apical embryonic fate map. *Development* **129**, 3403-10.

Scacchi, E., Osmont, K. S., Beuchat, J., Salinas, P., Navarrete-Gomez, M., Trigueros, M., Ferrandiz, C. and Hardtke, C. S. (2009). Dynamic, auxin-responsive plasma membrane-to-nucleus movement of Arabidopsis BRX. *Development* **136**, 2059-67.

Scarpella, E. and Helariutta, Y. (2010). Vascular pattern formation in plants. *Curr Top Dev Biol* **91**, 221-65.

Scheres, B., Di Laurenzio, L., Willemsen, V., Hauser, M. T., Janmaat, K., Weisbeek, P. and Benfey, P. N. (1995). Mutations affecting the radial organisation of the Arabidopsis root display specific defects throughout the embryonic axis. *Development* **121**, 53-62.

Scheres, B., Wolkenfelt, H., Willemsen, V., Terlouw, M., Lawson, E., Dean, C. and Weisbeek, P. (1994). Embryonic origin of the Arabidopsis primary root and root meristem initials. *Development* **120**, 2475-2487.

Schlereth, A., Moller, B., Liu, W., Kientz, M., Flipse, J., Rademacher, E. H., Schmid, M., Jurgens, G. and Weijers, D. (2010). MONOPTEROS controls embryonic root initiation by regulating a mobile transcription factor. *Nature* **464**, 913-6.

Schrick, K., Mayer, U., Horrichs, A., Kuhnt, C., Bellini, C., Dangl, J., Schmidt, J. and Jurgens, G. (2000). FACKEL is a sterol C-14 reductase required for organized cell division and expansion in Arabidopsis embryogenesis. *Genes Dev* **14**, 1471-84.

Schrick, K., Mayer, U., Martin, G., Bellini, C., Kuhnt, C., Schmidt, J. and Jurgens, G. (2002). Interactions between sterol biosynthesis genes in embryonic development of Arabidopsis. *Plant J* **31**, 61-73.

Schwarz-Sommer, Z., Gierl, A., Cuypers, H., Peterson, P. A. and Saedler, H. (1985). Plant transposable elements generate the DNA sequence diversity needed in evolution. *EMBO J* **4**, 591-7.

Scott, L., LaFoe, D. and Weil, C. F. (1996). Adjacent sequences influence DNA repair accompanying transposon excision in maize. *Genetics* **142**, 237-46.

Sehr, E. M., Agusti, J., Lehner, R., Farmer, E. E., Schwarz, M. and Greb, T. (2010). Analysis of secondary growth in the Arabidopsis shoot reveals a positive role of jasmonate signalling in cambium formation. *Plant J* **63**, 811-22.

Seo, P. J., Hong, S. Y., Kim, S. G. and Park, C. M. (2011). Competitive inhibition of transcription factors by small interfering peptides. *Trends Plant Sci*.

Shevell, D. E., Kunkel, T. and Chua, N. H. (2000). Cell wall alterations in the arabidopsis emb30 mutant. *Plant Cell* **12**, 2047-60.

Shevell, D. E., Leu, W. M., Gillmor, C. S., Xia, G., Feldmann, K. A. and Chua, N. H. (1994). EMB30 is essential for normal cell division, cell expansion, and cell adhesion in Arabidopsis and encodes a protein that has similarity to Sec7. *Cell* **77**, 1051-62.

Sieburth, L. E. and Deyholos, M. K. (2006). Vascular development: the long and winding road. *Curr Opin Plant Biol* **9**, 48-54.

Sieburth, L. E. and Meyerowitz, E. M. (1997). Molecular dissection of the AGAMOUS control region shows that cis elements for spatial regulation are located intragenically. *Plant Cell* **9**, 355-65.

Simpson, C. G., Manthri, S., Raczynska, K. D., Kalyna, M., Lewandowska, D., Kusenda, B., Maronova, M., Szweykowska-Kulinska, Z., Jarmolowski, A., Barta, A. et al. (2010). Regulation of plant gene expression by alternative splicing. *Biochem Soc Trans* **38**, 667-71.

Sjolund, R. D. (1997). The Phloem Sieve Element: A River Runs through It. *Plant Cell* **9**, 1137-1146.

Souer, E., van Houwelingen, A., Kloos, D., Mol, J. and Koes, R. (1996). The no apical meristem gene of Petunia is required for pattern formation in embryos and flowers and is expressed at meristem and primordia boundaries. *Cell* **85**, 159-70.

Southern, E. M. (1975). Detection of specific sequences among DNA fragments separated by gel electrophoresis. *J Mol Biol* **98**, 503-17.

Steinmann, T., Geldner, N., Grebe, M., Mangold, S., Jackson, C. L., Paris, S., Galweiler, L., Palme, K. and Jurgens, G. (1999). Coordinated polar localization of auxin efflux carrier PIN1 by GNOM ARF GEF. *Science* **286**, 316-8.

Takada, S. and Jurgens, G. (2007). Transcriptional regulation of epidermal cell fate in the Arabidopsis embryo. *Development* **134**, 1141-50.

Ten Hove, C. A. and Heidstra, R. (2008). Who begets whom? Plant cell fate determination by asymmetric cell division. *Curr Opin Plant Biol* **11**, 34-41.

Till, B. J., Reynolds, S. H., Greene, E. A., Codomo, C. A., Enns, L. C., Johnson, J. E., Burtner, C., Odden, A. R., Young, K., Taylor, N. E. et al. (2003). Large-scale discovery of induced point mutations with high-throughput TILLING. *Genome Res* **13**, 524-30.

Torii, K. U., Mitsukawa N., Oosumi T., Matsuura Y., Yokoyama R., Whittier R. F. and Komeda, Y. (1996). The Arabidopsis ERECTA gene encodes a putative receptor protein kinase with extracellular leucine-rich repeats. *Plant Cell* **8**, 735-46.

Torres-Ruiz, R. A. and Jurgens, G. (1994). Mutations in the FASS gene uncouple pattern formation and morphogenesis in Arabidopsis development. *Development* **120**, 2967-78.

Truernit, E., Bauby, H., Dubreucq, B., Grandjean, O., Runions, J., Barthelemy, J. and Palauqui, J. C. (2008). High-resolution whole-mount imaging of three-dimensional tissue organization and gene expression enables the study of Phloem development and structure in Arabidopsis. *Plant Cell* **20**, 1494-503.

Ueda, M., Zhang, Z. and Laux, T. (2011). Transcriptional activation of Arabidopsis axis patterning genes WOX8/9 links zygote polarity to embryo development. *Dev Cell* **20**, 264-70.

Ulker, B., Peiter, E., Dixon, D. P., Moffat, C., Capper, R., Bouche, N., Edwards, R., Sanders, D., Knight, H. and Knight, M. R. (2008). Getting the most out of publicly available T-DNA insertion lines. *Plant J* **56**, 665-77.

Ulmasov, T., Murfett, J., Hagen, G. and Guilfoyle, T. J. (1997). Aux/IAA proteins repress expression of reporter genes containing natural and highly active synthetic auxin response elements. *Plant Cell* **9**, 1963-1971.

Vroemen, C. W., Mordhorst, A. P., Albrecht, C., Kwaaitaal, M. A. and de Vries, S. C. (2003). The CUP-SHAPED COTYLEDON3 gene is required for boundary and shoot meristem formation in Arabidopsis. *Plant Cell* **15**, 1563-77.

Weigel, D. and Glazebrook, J. (2002). "Arabidopsis: A laboratory manual." Arabidopsis: A laboratory manual: i-xii, 1-354.

Weijers, D., Franke-van Dijk, M., Vencken, R. J., Quint, A., Hooykaas, P. and Offringa, R. (2001). An Arabidopsis Minute-like phenotype caused by a semi-dominant mutation in a RIBOSOMAL PROTEIN S5 gene. *Development* **128**, 4289-99.

Weijers, D., Schlereth, A., Ehrismann, J. S., Schwank, G., Kientz, M. and Jurgens, G. (2006). Auxin triggers transient local signaling for cell specification in Arabidopsis embryogenesis. *Dev Cell* **10**, 265-70.

Wessler, S. R. (1988). Phenotypic diversity mediated by the maize transposable elements Ac and Spm. *Science* **242**, 399-405.

Winter, D., Vinegar, B., Nahal, H., Ammar, R., Wilson, G. V. and Provart, N. J. (2007). An "Electronic Fluorescent Pictograph" browser for exploring and analyzing large-scale biological data sets. *PLoS One* **2**, e718.

Wu, X., Chory, J. and Weigel, D. (2007). Combinations of WOX activities regulate tissue proliferation during Arabidopsis embryonic development. *Dev Biol* **309**, 306-16.

Wu, X., Dabi, T. and Weigel, D. (2005). Requirement of homeobox gene STIMPY/WOX9 for Arabidopsis meristem growth and maintenance. *Curr Biol* **15**, 436-40.

Xiang, D., Venglat, P., Tibiche, C., Yang, H., Risseeuw, E., Cao, Y., Babic, V., Cloutier, M., Keller, W., Wang, E. et al. (2011). Genome-wide analysis reveals gene expression and metabolic network dynamics during embryo development in Arabidopsis. *Plant Physiol* **156**, 346-56.

Xie, B., Wang, X., Zhu, M., Zhang, Z. and Hong, Z. (2011). CalS7 encodes a callose synthase responsible for callose deposition in the phloem. *Plant J* **65**, 1-14.

Yamaguchi-Shinozaki, K. and Shinozaki, K. (2005). Organization of cis-acting regulatory elements in osmotic- and cold-stress-responsive promoters. *Trends Plant Sci* **10**, 88-94.

Yamaguchi, M., Kubo, M., Fukuda, H. and Demura, T. (2008). Vascular-related NAC-DOMAIN7 is involved in the differentiation of all types of xylem vessels in Arabidopsis roots and shoots. *Plant J* **55**, 652-64.

Yanagisawa, S. (2004). Dof domain proteins: plant-specific transcription factors associated with diverse phenomena unique to plants. *Plant Cell Physiol* **45**, 386-91.
Zhang, C., Barthelson, R. A., Lambert, G. M. and Galbraith, D. W. (2008). Global characterization of cell-specific gene expression through fluorescence-activated sorting of nuclei. *Plant Physiol* **147**, 30-40.

Curriculum Vitae

Name	Katrin OLLRAM, Mag.
Date of birth	6th April 1981
Place of birth	Vienna
Nationality	Austrian

Education:

October 2007- present:	PhD studies in Molecular Biology at the University of Vienna; focus on vascular development in the model species *Arabidopsis thaliana*.
August 2007 – August 2011:	PhD thesis within the International PhD program of the Vienna Biocenter (VBC) at the GMI- Gregor Mendel Institute of Molecular Plant Biology GmbH, Dr. Bohrgasse 3, A-1030 Vienna. Group: Dr. Thomas Greb. Title: The Identification of Potential Factors Involved in the Transcriptional Regulation of the Phloem-Specific Gene *ALTERED PHLOEM DEVELOPMENT* (*APL*) and the Analysis of its Role during Embryogenesis in *Arabidopsis thaliana.*
October 2001- June 2007:	Undergraduate studies in Molecular Biology at the University of Vienna; focus on cell biology, immunology, and molecular medicine; Graduation: 12th June 2007.
November 2005 – November 2006:	Diploma thesis at the Department of Medical Biochemistry, Division of Molecular Cell Biology, Medical University of Vienna, Dr. Bohrgasse 9/3, A-1030 Vienna. Group: Univ. Prof. Dr. Roland Foisner. Title: Properties and Interactions of Disease-linked Lamin A Variants and their Potential Influence on the Cell Cycle.
October 1999 – February 2002:	Undergraduate studies in Nutritional Sciences at the University of Vienna (1st Diploma exam: 7th February 2002).
June 1999:	Graduation from secondary school BGVIII ('Piaristengymnasium'), Jodok Fink Platz, Vienna.